In presenting the dissertation as a partial fulfillment of the requirements for an advanced degree from the Georgia Institute of Technology, I agree that the Library of the Institute shall make it available for inspection and circulation in accordance with its regulations governing materials of this type. I agree that permission to copy from, or to publish from, this dissertation may be granted by the professor under whose direction it was written, or, in his absence, by the Dean of the Graduate Division when such copying or publication is solely for scholarly purposes and does not involve potential financial gain. It is understood that any copying from, or publication of, this dissertation which involves potential financial gain will not be allowed without written permission.

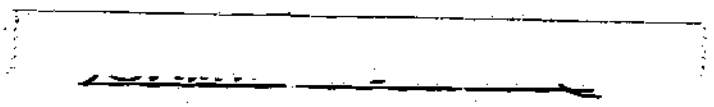

3/17/65
b

OPTIMIZATION OF LINEAR ARRAYS

A THESIS

Presented to

The Faculty of the Graduate Division

by

Gordon Worley Breland

In Partial Fulfillment

of the Requirements for the Degree

Doctor of Philosophy in the

School of Electrical Engineering

Georgia Institute of Technology

September, 1966

OPTIMIZATION OF LINEAR ARRAYS

Approved:

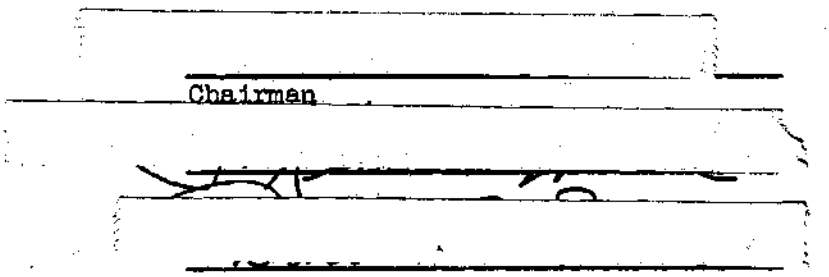

Chairman

Date approved by Chairman: 9-12-66

ACKNOWLEDGEMENTS

The research reported in this dissertation could not have been accomplished without the active assistance, cooperation, and encouragement of many individuals. It is a distinct pleasure to acknowledge the support which I have received during the course of this work.

My sincere thanks are extended to my thesis advisor, Dr. Demetrius T. Paris, for his suggestions, constructive criticism, and continuing encouragement during this investigation. The discussions held with Dr. Paris during the latter phases of the research were particularly helpful. I also express my sincere appreciation to Dr. F. Kenneth Hurd and Dr. Daniel C. Fielder for their valuable suggestions during the preparation of the manuscript. Special thanks are also due Dr. R. D. Hayes for his assistance.

Special gratitude is owed to the Lockheed-Georgia Company for financial support during the early phases of the research effort. I particularly wish to thank Mr. M. D. Prince and Mr. W. B. Wrigley of the Systems Sciences Laboratory for their encouragement. My discussions with Mr. Wrigley were especially helpful.

Finally, my heartfelt gratitude goes out to my wife Marie without whose faithful support during the long effort, I could not have hoped for success.

TABLE OF CONTENTS

LIST OF TABLES

LIST OF ILLUSTRATIONS

SUMMARY

The objective of this research is the synthesis of linear arrays of isotropic radiators whose performance is optimum when evaluated by either of two optimality criteria. The specific optimality criteria investigated are listed below.

1. Pattern Synthesis for Minimum Error

The basic problem of radiation pattern synthesis may be concisely stated in the following manner. Given a desired far field radiation pattern, determine the excitation of an array such that the radiation pattern of the synthesized array provides the best approximation to the desired pattern. The best or optimum array in this research is defined as the array whose parameters are such that the mean squared error between the desired pattern and the synthesized pattern is minimum.

2. Synthesis for Maximum Signal-to-Noise Ratio

The index of performance to be maximized in this case is the ratio of received signal power to received noise power. The noise or interference environment is specified as a spatial distribution of power at a single frequency coinciding with the signal frequency. The signal is assumed to be incident from a distant source at a known angle.

In the synthesis of arrays whose pattern represents the optimum approximation to a desired pattern, there are basically two sets of independent variables which may be used to optimize array performance. These are the complex radiator excitations and the positions of the radiators along the array axis. There are several well known methods

for synthesizing arrays using only the complex excitations as variables. The most widely applied of these methods is the Fourier synthesis technique. Until the recent emphasis on the use of arrays rather than the more conventional single element radiating systems, these procedures for designing equally spaced arrays were adequate. The prospect of improving antenna system performance by using both the complex excitations and radiator positions as independent variables in array design has resulted in considerable effort being expended toward the development of the necessary synthesis procedures. This effort has been handicapped by mathematical complexity introduced by the inclusion of variable spacings, with the result that the use of digital computers has become mandatory. A second feature of this effort toward the synthesis of unequally spaced arrays has been the apparent emphasis on sidelobe reduction using the additional flexibility provided by variable interelement spacings.

The approach taken in this research differs considerably from that of previous work, and recognizes the requirement of the use of the digital computer from the outset. Rather than continuing the attempts at sidelobe reduction, this work has emphasized the study of the role of the spacing parameter as an independent variable in the approximation of radiation patterns. To overcome mathematical complexity, the techniques of nonlinear programming are applied. It is shown that use of spacings as independent variables results in substantial reduction of the mean squared error between a desired pattern and the synthesized approximate pattern. This reduction, however, appeared to be the result of more efficient use of total aperture rather than from wide variations in

interelement spacings. In the specific cases examined, unequal spacings were apparent, but the interelement spacings did not depart radically from an average value.

A second feature of a synthesis procedure based on nonlinear programming is the ease with which inequality constraints relating the independent variables may be incorporated into the design process. In this work, this is accomplished by application of the created response surface technique. None of the previous synthesis methods allow the specification of such inequality constraints.

The design of linear arrays for maximum signal-to-noise ratio is a subject of contemporary research interest. Prior to this work, there had been little reported in the current literature. Initial attention was therefore directed toward the optimization of equally spaced arrays. It is shown that when the constraint of equal spacings is imposed, the maximization of the signal-to-noise ratio results in a generalized characteristic value problem. The use of two linear transformations reduces the generalized eigenvalue problem to a conventional eigenvalue problem, the solution of which is obtainable by well documented methods.

The inclusion of unequal spacings in the signal-to-noise optimization procedure is accomplished using the methods of nonlinear programming. Indications from the examples considered are that unequal spacings play a secondary role in improving the signal-to-noise ratio, with the amplitude distribution across the aperture being of primary importance.

In the discussion of each optimum synthesis procedure, numerous examples are included to illustrate application of the developed techniques.

CHAPTER I

INTRODUCTION

The central theme of the research summarized in this dissertation is the optimization of the performance of linear arrays consisting of isotropic radiators. Optimization of some characteristic of a physical system such as an antenna array requires precise definition of a criterion with which to evaluate system performance. Optimization then becomes the extremization of the mathematical statement of this criterion. The specific optimality criteria considered in this research are described below.

1. Pattern Synthesis for Minimum Error

The basic problem of radiation pattern synthesis may be concisely stated in the following manner. Given a desired far field radiation pattern, determine the excitation of an array such that the radiation pattern of the synthesized array provides the best approximation to the desired pattern. The best or optimum array in this research is defined as the array whose parameters are such that the mean squared error between the desired pattern and the synthesized pattern is minimum.

2. Maximum Signal-to-Noise Ratio

The index of performance to be maximized in this case is the ratio of received signal power to received noise (or undesired signal) power. The noise or interference environment is specified as a spatial distribution of power at a single frequency coinciding with the signal frequency. The signal is assumed to be incident from a distant source at a

known angle.

For each of the two criteria, the development of mathematical optimization procedures which incorporate as many as possible of the adjustable parameters (or degrees of freedom) of the antenna system is required. In the design of arrays, the possible degrees of freedom include the complex excitations of the radiators and the positions of the radiators on the array axis. The inclusion of the radiator positions as independent variables complicates the optimization problem to such a degree that conventional mathematics may not be readily employed. The powerful iterative techniques of nonlinear mathematical programming relieve this difficulty, in addition to providing other benefits such as the means for the incorporation of inequality constraints relating the array parameters.

It is instructive to review the background of the optimum array synthesis and the related work which has been accomplished before proceeding to the approach taken in this research.

The theory and design of linear arrays of radiating elements has been the object of a considerable amount of intensive research over the past three decades. While the primary objective of this work has been the synthesis of illumination functions required for a given far field pattern, other problems such as design for optimum directivity and optimum array performance in a specific noise environment have also been examined. In the review of these past efforts which follows, the reader is assumed familiar with the standard texts on antenna and array (1)-(3).

The theory of linear arrays was first extensively studied by Schelkunoff (4). Limiting his considerations to arrays of N equally

spaced isotropic point sources, he found that the array factor could be expressed as a complex polynomial of the form

$$f(z) = A_0 + A_1 z + A_2 z^2 + \ldots + A_{N-1} z^{N-1} \qquad (1)$$

where $z = \exp(j\beta d \sin\theta)$, $\beta = 2\pi/\lambda$, λ is the operating wavelength, d is the interelement spacing, and θ is the angle measured from broadside to the array. Schelkunoff then imposed the additional constraint that the array be composed of an odd number of elements, symmetrical about the center element, and assumed that corresponding element pairs had complex conjugate excitations. With these restrictions, the pattern factor (1) becomes

$$f(\psi) = a_o + 2 \sum_{m=1}^{M} a_m \cos m\psi + b_m \sin m\psi \qquad (2)$$

where $\psi = \arg(z) = \beta d \sin\theta$, and the complex excitation coefficients have been separated into real and imaginary components in accordance with $A_i = a_i + jb_i$. Equation (2) is a finite Fourier expansion for the array factor, and well known techniques may be applied to evaluate the excitation coefficients.

Hoffman (5) elaborated on array synthesis by matrix inversion, and showed that for a set of properly chosen sample points z_k, the set of linear equations in the A_i resulting from the application of equation (1) at these sample points could be solved without resorting to direct inversion of a high order matrix with complex elements. This technique is equivalent to Fourier synthesis, and requires equally spaced elements

in the array.

Woodward (6) used component $\frac{\sin x}{x}$ patterns with adjustable amplitude and phase displacement to synthesize illumination functions for a continuous line source. This particular technique is quite useful as is the direct matrix inversion scheme in that it provides for precise control of the pattern at selected points.

The design of optimum arrays was studied by Dolph (7) for the case of broadside arrays, and the analysis was later extended by DuHamel (8) to include endfire arrays of equally spaced sources. The optimality criterion employed was that of minimizing beamwidth for a given sidelobe level. This optimization technique involved the use of Tchebyscheff polynomials in the selection of the array excitation coefficients, and has become one of the most widely used methods of array design. It is readily adaptable to computer implementation, and extensive computer compiled design data are available in the literature (9). It should be noted, however, that Dolph-Tchebyscheff synthesis is, strictly speaking, an optimization technique rather than a synthesis method in that the array designer controls only the beamwidth and sidelobe level.

Taylor (10)-(11) optimized beamwidth for a specified sidelobe level for continuously illuminated line sources and circular aperture distributions using a result derived by Van der Maas (12) on the pattern of a Dolph-Tchebyscheff array as the number of radiators increased indefinitely.

All of the synthesis and optimum synthesis techniques mentioned above are based on the assumption of an array of equally spaced sources and on some characteristic of the polynomial which describes the radiation

characteristics of the array. As pointed out very effectively by Von Aulock (13), the use of equal spacings, in addition to reducing the number of design variables available, imposes certain other limitations, the most serious being the secondary maxima which may occur. One may see immediately from equation (2) that use of constant interelement spacings results in a periodic pattern factor with the appearance of secondary maxima, or grating lobes, with amplitudes equal to that of the main lobe when the interelement spacing, d, exceeds one wavelength. This restriction becomes considerably more serious if the array is to be steered over a wide angular sector.

Both the availability of an additional degree of freedom in varying the element locations and the desirability of suppressing the secondary beams by breaking up the periodicity of the pattern factor stimulated interest in the design of unequally spaced arrays. Unz (14) discussed the general aspects of such an array and formulated a figure of merit with which to compare the performance of unequally spaced arrays with other arrays. Using a specific set of arrays, King et al. (15) illustrated some of the advantageous features of unequally spaced arrays, but no synthesis was undertaken.

Since the pattern factor for an unequally spaced array is non-periodic, representative of the radiation pattern by a conventional polynomial as in equation (1) is not possible, and straightforward mathematical synthesis is discouraged because of the large numbers of variables involved for arrays of moderate size. Perturbational and statistical techniques have proved useful because of this low degree of tractability. Harrington (16) used a perturbational analysis to minimize

the sidelobe levels for uniformly excited but non-uniformly spaced arrays of isotropic elements, and was able to reduce the sidelobes to approximately 1/2N times the amplitude of the main beam (where N is the total number of elements) without increasing the beamwidth of the main lobe. Maffett (17) applied statistical techniques to the study of the general behavior of arrays having variable spacings, but did not undertake the problem of synthesizing such an array. Andreasen (18) designed arrays with very wide interelement spacings using an interative procedure to adjust the element positions and examined the steerability of such arrays.

Using a clever mathematical substitution, Ishimaru (19) showed that the radiation pattern of an unequally spaced array could be expressed as a series of integrals, each of which represented the pattern of a continuously illuminated line source. This was accomplished by the use of Poisson's sum formula and the subsequent definition of "source position" and "source number" functions. Taylor's (10) method was then applied to the synthesis of the component patterns. While Ishimaru's technique is a true synthesis procedure as opposed to a perturbational or successive approximation method, the inversion of the source number function may be a very complicated process, as pointed out in his paper.

Tang (20) outlined a novel procedure for synthesizing an unequally spaced array whereby the desired pattern is first realized using an equally spaced array after which the element positions are adjusted slightly. The resulting array is a uniformly excited array whose pattern best approximates the desired pattern in the immediate region of the main beam. However, the approximation becomes worse as the angle from broadside increases.

The synthesis of linear arrays and aperture antennas for optimum directivity is of considerable practical importance, and has been widely discussed in the literature, although not to the extent that pattern synthesis has been covered. Synthesis for optimum directivity is not quite as straightforward as ordinary pattern synthesis because of the fact that, unless some constraint is imposed, there is no theoretical limit to the attainable directivity. This situation, where unlimited directivity is obtainable from a source of finite size, is referred to as the supergain phenomenon and is adequately covered in the literature, early discussions being undertaken by Schelkunoff (4), Uzkov (21), and Woodward and Lawson (22). Bouwkamp and deBruijn (23) showed that the directivity of a finite linear source was not limited by the source size, and their analysis was later extended by Riblet (24) to include two dimensional sources and the infinite current strip. Taylor (25) discussed the maximum practical directivity of continuous sources and arrays of discrete radiating elements. Tai (26) optimized the directivity of arrays of uniformly spaced dipoles, while Solymar (27) determined the maximum directivity of a line source whose illumination function could be expressed as a finite Fourier series.

Optimization of antenna arrays for maximum performance in a given noise environment is a problem of increasing practical importance, particularly when the antenna is part of a precision signal processing system, such as a radio astronomy installation. Little has been reported in the present literature on this topic, one notable exception being the work of Kritikos (28). The signal-to-noise ratio of an array of equally spaced isotropic sources was maximized, subject to a particular set of

constraints on the element excitations.

The approach taken in this research departs considerably from the more conventional approaches of the related work reviewed in the preceding paragraphs. It will be recalled that in these efforts the common characteristic of all was the use of relatively complicated mathematical methods including perturbational techniques, methods of successive approximation, and even statistical studies in attempts to circumvent the mathematical complexities introduced by the spacing parameter. In every case, the use of a digital computer was dictated for implementation of the developed techniques, although the number of variables involved contributed to this factor as much as mathematical complexity.

Recognition of these problems led in this research to the application of the techniques of nonlinear mathematical programming in the development of optimum synthesis procedures. The nonlinear programming problem, sometimes called the general mathematical programming problem, is concerned with the extremization of an objective function subject to a set of inequality constraints. This subject is well developed in the literature of applied mathematics, with excellent summaries appearing in texts by Saaty and Bram (29), Hadley (30), and Leitmann (31). These methods have been widely applied in other fields such as automatic control, operations research, systems engineering, and economic studies. They have not, however, found extensive utilization in electromagnetic problems.

It is shown in this research that in the area of pattern synthesis for minimum mean squared error, the methods of nonlinear programming provide an excellent synthesis procedure at no sacrifice in complexity

with respect to current methods. The results of several case studies in array synthesis are given to illustrate the improvement in pattern approximation when spacings are included as independent variables.

In the case of synthesis of arrays for maximum signal-to-noise performance, the design of equally spaced arrays is treated initially because there has been little previous work in this area. Following this treatment, the steepest descent procedure is utilized to investigate the effects of variable spacings. Three examples are included to illustrate the developed optimization procedures.

CHAPTER II

OPTIMUM SYNTHESIS OF ARRAYS

The problem of designing an aperture and its associated illumination function has been the object of considerable research over the past three decades. Despite the considerable effort expended, the mathematical complexity of array and aperture design has resulted in only a few techniques which are extensively employed. In this chapter the methods which have been developed for pattern synthesis are reviewed so that the present work may be evaluated in proper perspective. It should be noted at the outset that the following discussions deal only with arrays of discrete radiating elements as opposed to a continuously illuminated aperture.

The radiation pattern of a linear array of isotropic radiators of the form illustrated in Figure 2.1 may be easily shown to be given by

$$\bar{E}(\theta) = \bar{I}_o + \sum_{n=1}^{N} \bar{I}_n e^{j\beta x_n \cos\theta} \qquad (2.1)$$

where $\bar{I}_i$ denotes the complex excitation of the i-th element, $\beta = \frac{2\pi}{\lambda}$, λ is the operating wavelength, and θ is the angle off the array axis. Note that in (2.1) no restrictions are placed on the location of the radiators along the array axis. If the radiator excitations are complex, then in general $\bar{E}(\theta)$ will be complex. It is important to note the specific parameters in expression (2.1) which affect the value of the

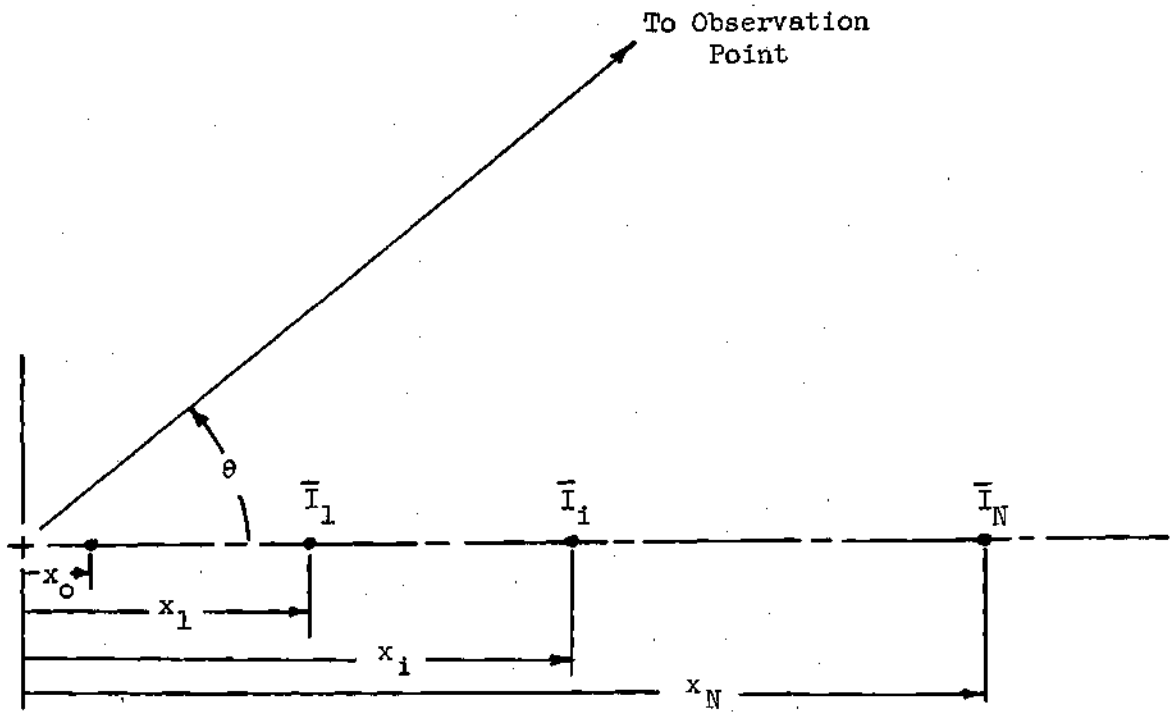

Fig. 2.1 General Linear Array.

radiation pattern for any given value of θ. Clearly, the excitations and element positions for any fixed N determine the magnitude and phase of the complex $\overline{E}(\theta)$; hence, a more meaningful notation would be

$$\overline{E}(\overline{I}, \overline{x}, \theta) = \overline{I}_o + \sum_{n=1}^{N} \overline{I}_n e^{j\beta x_n \cos\theta} \tag{2.2}$$

where

$$\overline{I} = [I_o \quad I_1 \quad I_2 \cdots I_N] \tag{2.3}$$

denotes the current excitation vector, and $\overline{x}$ denotes the vector whose components are the element positions.

$$\overline{x} = [x_1 \quad x_2 \quad x_3 \cdots x_N] \tag{2.4}$$

In most practical situations, the phase of a radiation pattern is of much less importance than the magnitude of the pattern. In such a case, the array designer is confronted with the problem of either disregarding the phase information, or attempting to realize a pattern whose values are purely real for any value of θ. That this second alternative is preferable will be illustrated in the following discussion.

Let the array be composed of (2M + 1) radiators, where M is an integer, and let the radiators be arranged in symmetrical pairs about the center element as illustrated in Figure 2.2. If the further constraint that element pairs have excitations which are complex conjugates is imposed, then the excitation vector is simplified after substitution of

$$\overline{I}_i = \overline{I}_{-i}^{*} \tag{2.5a}$$

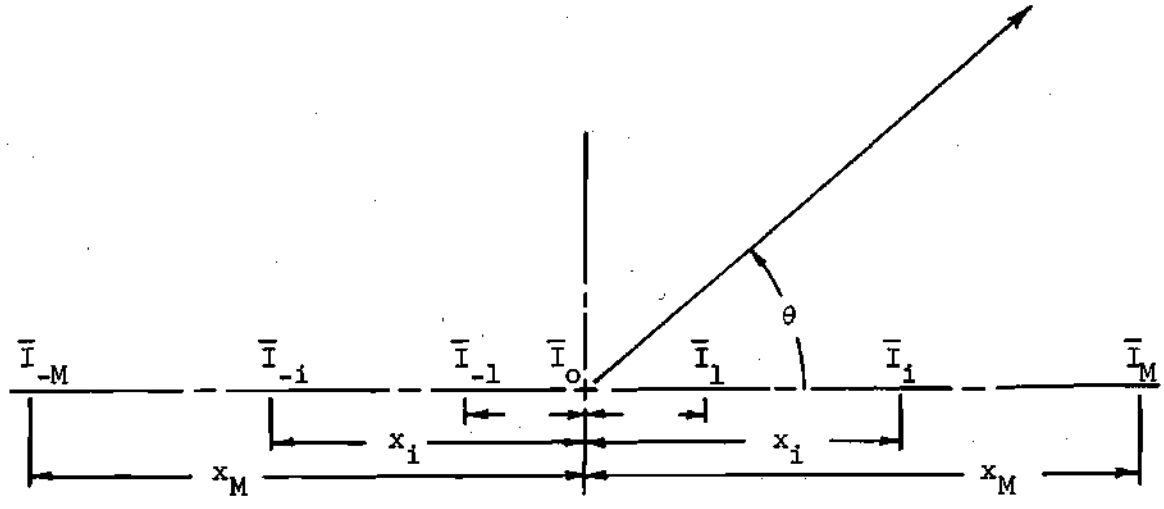

Fig. 2.2 Symmetrically Excited Array.

where

$$\bar{I}_i = a_i + jb_i \tag{2.5b}$$

and

$$\bar{I}_{-i} = a_i - jb_i \,. \tag{2.5c}$$

The expression (2.2) representing the radiation pattern becomes

$$\bar{E}\,(\bar{a},\bar{b},\bar{x},\theta) = a_o + 2\sum_{m=1}^{M} a_m \cos\,(\beta x_m \cos\,\theta) + b_m \sin\,(\beta x_m \cos\theta) \tag{2.6}$$

which is purely real expression. In addition to this latter factor, it is further important to note that for (N + 1) radiators, where N is an even integer, the vectors (2.3) and (2.4) have a cumulative total of (3N + 1) components including the components of the complex $\bar{I}$, whereas the vectors

$$\bar{a} = [a_o \;\; a_1 \;\; a_2 \cdots a_M]$$

$$\bar{b} = [b_1 \;\; b_2 \;\; b_3 \cdots b_M] \tag{2.7}$$

and $$\bar{x} = [x_1 \;\; x_2 \;\; x_3 \cdots x_M]$$

have (3M + 1) components, a difference of 3M components for the same number of radiators in each case. This reduction in the order of vectors is particularly valuable when the number of radiators is large.

Having justified the selection of an array whose radiation pattern is given by (2.6), it is instructive to consider the general characteristics

of the overall pattern synthesis problem. Schelkunoff (4) proposed the first pattern synthesis method when he recognized that when the substitution

$$\psi = \beta d \cos \theta \tag{2.8}$$

was introduced into the expression for an equally spaced array, for which

$$x_m = md \qquad m = 1,2,\cdots,M \tag{2.9}$$

expression (2.6) becomes

$$E(\psi) = a_o + 2 \sum_{m=1}^{M} a_m \cos m\psi + b_m \sin m\psi \tag{2.10}$$

This is recognized immediately as the finite Fourier series; consequently, given a desired radiation pattern $F(\theta)$, it is only necessary to make the change of variables (2.8), thus obtaining $F(\psi)$, after which it is a simple matter to compute the Fourier coefficients $a_o \cdots a_M$, $b_1 \cdots b_M$. While this particular synthesis procedure and related ones by Woodward (6), Hoffman (5), and others are straightforward and have proved invaluable in array design, there are, however, several serious limitations which must be examined.

The first of the limitations is clearly the requirement that the radiators be equally spaced along the array axis, a restriction which in itself reduces the amount of flexibility available to the array designer. Furthermore, it is easily established that the set of excitation coefficients derived from applying the Fourier method are unique only for one-half wavelength interelement spacings. To illustrate this last

assertation, consider the range of the variable ψ in (2.8) and (2.10). For $d = \frac{\lambda}{2}$, the range of ψ is the closed interval $[-\pi,\pi]$ for θ in the interval $[0,\pi]$. Consider the pattern $F(\theta)$ illustrated in Figure 2.3(a). A change of horizontal axis results in $F(\psi)$ shown in Figure 2.3(b). Note that the domain of $F(\psi)$ is the entire interval $[-\pi,\pi]$. Since the functions cos $m\psi$ and sin $n\psi$ are orthogonal over $[-\pi,\pi]$, the coefficients a_i and b_i are uniquely determined. Furthermore, the resultant Fourier series approximation to the given $F(\psi)$ is in this case optimum in the mean square sense for any given number of terms. Figure 2.3(c), however, illustrates $F(\psi)$ for a spacing of one-quarter wavelength, in which case the domain of the given $F(\psi)$ is the closed interval $[-\pi/2, \pi/2]$. Since the functions sin $m\psi$ and cos $n\psi$ are not orthogonal over this interval, then a "fill-in" function will be required over the intervals $[-\pi,-\pi/2]$ and $[\pi/2,\pi]$ if the Fourier technique is to be applied. Clearly, the form of this fill-in function will affect the quality of the approximation of the resulting series. There are, however, no straightforward methods for specification of this auxiliary function, the designer's intuition playing the major role in its selection. Similar remarks apply for spacings greater than one-half wavelength. It is clear then that even the synthesis of "optimum" equally spaced arrays, in the sense that optimum is used in this research, has major restrictions and difficulties in implementation.

These and similar limitations apply to the other widely used pattern synthesis methods as summarized by Walter (36). To alleviate these restrictions, there have been a number of attempts in recent years to incorporate the radiator positions as independent variables in

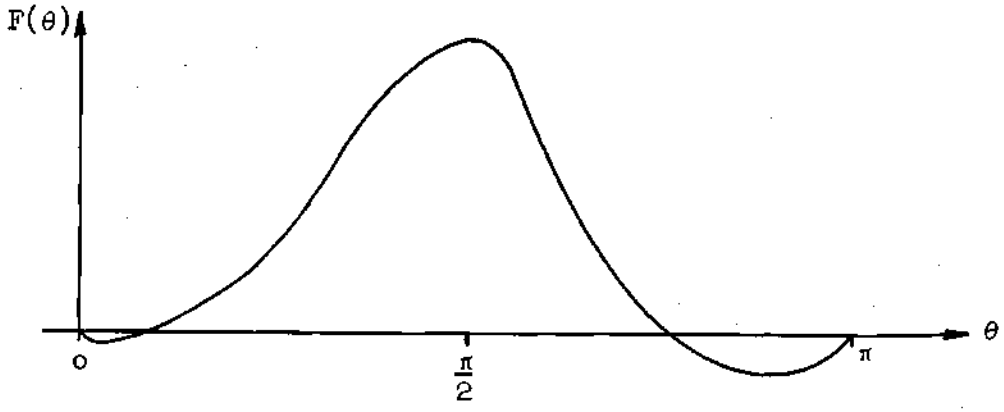

(a) Desired Radiation Pattern $F(\theta)$

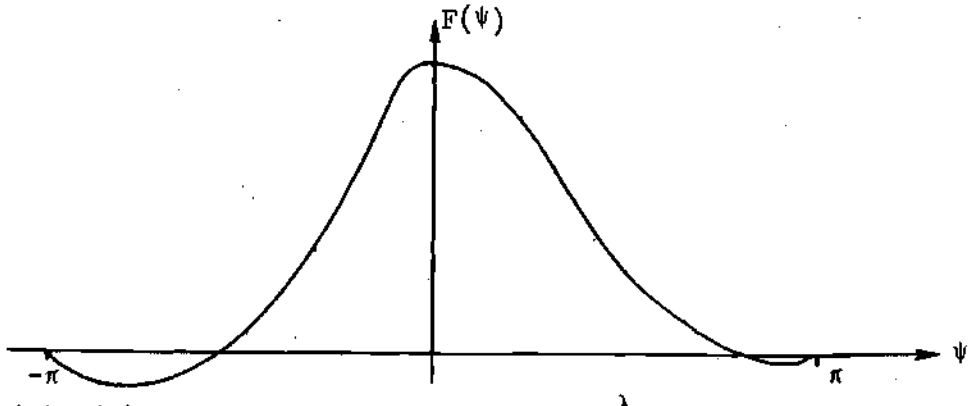

(b) $F(\psi)$ for Interelement Spacing of $\frac{\lambda}{2}$

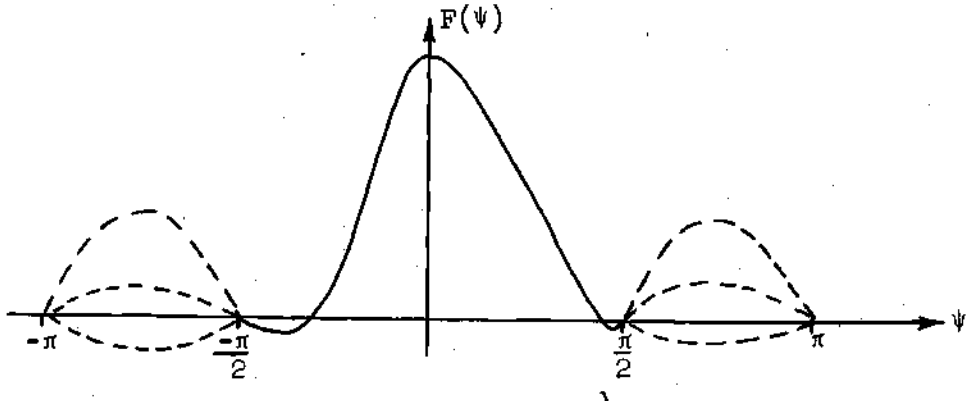

(c) $F(\psi)$ for Interelement Spacing of $\frac{\lambda}{4}$

Fig. 2.3 Illustration of Spacing Limitation in Fourier Synthesis.

synthesis procedures. Unz (14) was among the first to suggest the use of unequally spaced arrays, and since his initial paper, a variety or proposed methods have appeared. Almost without exception, these methods have been of an iterative nature because of the mathematical complexities introduced by allowing unequally spaced elements. A review of these efforts was included in the introduction to this dissertation and will not be repeated here.

The specific approach taken to the synthesis problem in this research is outlined in the following discussions.

The central problem in radiation pattern synthesis is to determine a radiation pattern of an actual array, say $E(\theta)$, such that $E(\theta)$ is the best approximation in some prescribed sense to a given or desired pattern, say $F(\theta)$. There a variety of criteria for evaluating the quality of the approximation for a particular $E(\theta)$. The most practical optimality criterion is that of best approximation in the mean square sense. In mathematical terms, the optimum synthesis problem is that of finding a realizable function $E(\theta)$ which minimizes the functional

$$\mathcal{E}[E(\theta)] = \frac{1}{\pi} \int_0^{\pi} [F(\theta) - E(\theta)]^2 \, d\theta \qquad (2.11)$$

There exists only the trivial solution to the conventional variational approach to the minimization of (2.11). The direct methods of optimization must therefore be employed since no single extremal exists. This is to be expected since the allowed comparison functions $E(\theta)$ are not unrestricted but are limited to linear combinations of the component

functions

$$u_i(\theta) = \cos(\beta x_i \cos\theta)$$
$$v_i(\theta) = \sin(\beta x_i \cos\theta) \tag{2.12}$$

The application of the Ritz Procedure for direct optimization is then required, with the set of comparison functions restricted to the set

$$E_M(\theta) = a_o + 2\sum_{m=1}^{M} a_m \cos(\beta x_m \cos\theta) + b_m \sin(\beta x_m \cos\theta) \tag{2.13}$$

which is precisely equation (2.6). Upon substitution of a particular comparison function into functional (2.11), the optimization problem is transformed to the minimization of a conventional function of the adjustable parameters $\underline{a}$, $\underline{b}$, and $\underline{x}$.

$$\mathcal{E}(\bar{a},\bar{b},\bar{x}) = \frac{1}{\pi}\int_0^{\pi}\Big[F(\theta) - \Big(a_o + 2\sum_{m=1}^{M} a_m \cos(\beta x_m \cos\theta) + b_m \sin(\beta x_m \cos\theta)\Big)\Big]^2 d\theta \tag{2.14}$$

The optimum array is then completely described by the vectors $\hat{\underline{a}}$, $\hat{\underline{b}}$, and $\hat{\underline{x}}$ which minimize this mean squared error expression. In principle, these vectors may be determined by solving the following set of equations:

$$\frac{\partial \mathcal{E}}{\partial a_i} = 0 \qquad i = 0,1,\cdots,M$$

$$\frac{\partial \mathcal{E}}{\partial b_i} = 0 \qquad i = 1,\cdots,M \tag{2.15}$$

$$\frac{\partial \mathcal{E}}{\partial x_i} = 0 \qquad i = 1,\cdots,M$$

While this approach to pattern synthesis may appear straightforward, it is instructive to consider the mathematical character of the equations (2.15). As an illustration, the partial derivatives with respect to the position vector components yield nonlinear equations of the form

$$\int_0^{\pi} \left[F(\theta) - E_M(\bar{a},\bar{b},\bar{x},\theta) \right] \tag{2.16}$$

$$\{ \cos(\beta x_i \cos\theta) - \sin(\beta x_i \cos\theta) \} \cos\theta \, d\theta = 0$$

The solution of equations (2.16) in conjunction with the other nonlinear equations resulting from differentiation with respect to the excitation coefficients is clearly a nontrivial undertaking. The solution is, however, required if the synthesis procedure is to yield an optimum array.

It is illuminating to discuss the mathematical characteristics of equation (2.14) in order to motivate the proposed means of arriving at the solution of equations (2.15). Geometrically, expression (2.14) represents a surface in $(3M + 2)$ dimensions, each dimension or axis corresponding to a single component of the independent variables $\underline{a}$, $\underline{b}$, and $\underline{x}$, in addition to the axis corresponding to $\epsilon(\bar{a},\bar{b},\bar{x})$. The general optimization problem is to find the vectors $\hat{\underline{a}}$, $\hat{\underline{b}}$, and $\hat{\underline{x}}$ for which $\epsilon(\underline{a},\underline{b},\underline{x})$

assumes its global minimum value. This solution is, of course, the solution to equations (2.15). The nonlinear nature of these equations suggests that instead of a single solution, the surface described by (2.14) may have a number of relative minima with various values for the mean-squared error. Such a surface is described by the adjective multimodal, while a surface with a single minimum is called a unimodal surface. Figure 2.4 illustrates the contours of a typical multimodal error surface which were calculated on the digital computer. In this example, the desired pattern has been deliberately chosen to be the pattern of the array illustrated in Figure 2.4, so that exact solutions exist. These solutions are indicated at points $(\pi,3\pi)$ and $(3\pi,\pi)$. Note, however, that stationary points which are relative minima exist at (π,π) and approximately $(3\pi,3\pi)$. Thus, in the limited region shown in Figure 2.4, there are four mimina whose coordinates represent solutions to equations (2.15).

The preceding discussions have presented the fact that the nonlinear objective function representing the mean squared error in a typical pattern synthesis example will in many cases geometrically describe a multimodal surface. Because several relative minima may exist on such a surface, the question arises concerning the identification of the global minimum among the several relative minima. There are, unfortunately, no convenient mathematical procedures for identifying a global minimum. The physical characteristics of the radiation pattern synthesis problem are, however, such that this difficulty may be circumvented with relative ease. The error response surface does not undergo violent undulations within small regions, and other qualitative considerations

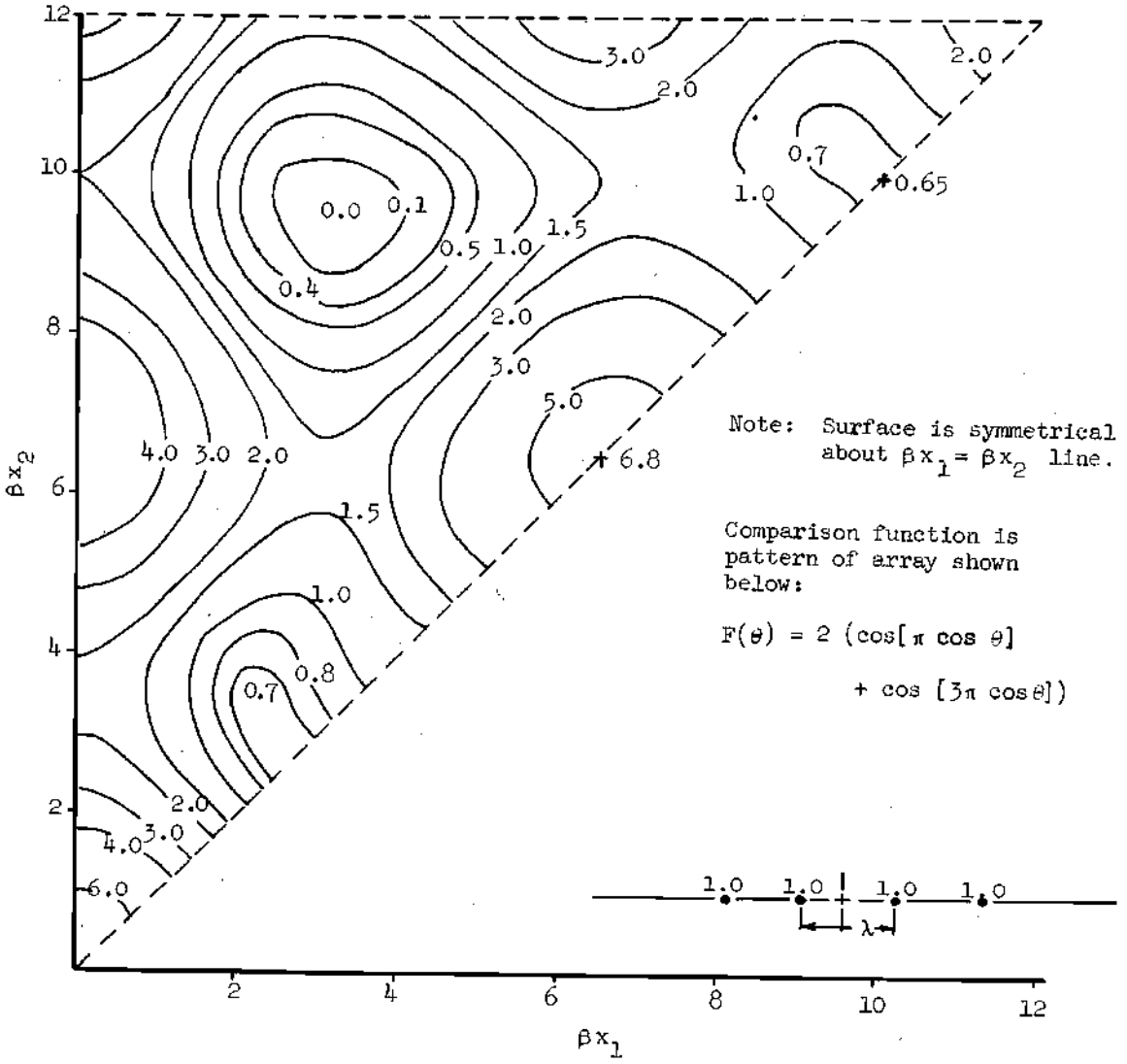

Fig. 2.4 Typical Error Surface

of secondary beam formation and high sidelobe levels which are consequences of widely varying interelement spacings narrow the region where the global minimum should be located. The contours of Figure 2.4 will confirm this last statement. It will be noted in this illustration that the relative minima shown do not, in fact, correspond to practical solutions because in two cases they represent elements which occupy the same positions along the array axis. The effective number of radiators in the synthesized array would be reduced if either of these relative minima were chosen as the global minimum. This clearly would not represent a desirable solution, and one would know immediately that the global minimum lay elsewhere. While such qualitative arguments are far from providing an error free method for assuring the determination of the optimum array, their application in this research has been quite successful. The synthesis examples reported herein did not result in error surfaces where the minimum located did not appear to be a strong minimum with a decreased mean squared error when compared with the error of an array synthesized by the Fourier method.

The Method of Steepest Descent

It is apparent from the previous discussions that the synthesis of the optimum array requires the location of the global minimum on the error response surface. While the location of all stationary points may be determined, in principle at least, by the solutions to equations (2.15), the complexity of these nonlinear equations rules out any attempt at a direct solution. Because of this complexity, the techniques of nonlinear programming are applied in this research as the specific means of

determining the location of the global minimum. Most of the iterative procedures which fall under the general heading of nonlinear programming are modifications of the method of steepest descent, and excellent summaries appear in texts by Saaty and Bram (29), Hadley (30), and Leitmann (31). These techniques have been widely applied in other areas such as automatic control, operations research, and economics, but little effort has been devoted to their application to electromagnetic problems. One notable exception is an effort reported by Michelson and Schomer (32) where synthesis of arrays using element amplitude, phase, and position as variables was undertaken. Their work was done independently and concurrently with the early work done on the proposed research and was largely concerned with the design of arrays on irregular curves. However, it was assumed that the mathematical expression for the curve was known. This approach, coupled with the fact that the effects of constraints upon the array variables were not examined, serves to separate substantially their work from that of the present research.

The mathematical procedure involved in the minimization of a nonlinear function of several variables, say $f(\bar{x})$ where $\bar{x} = (x_1, x_2, \cdots, x_N)$ should be considered. Note that while the minimization of $f(\bar{x})$ is specifically considered, the same techniques would apply to the problem of maximization, since the minima of $-f(\bar{x})$ correspond exactly to the maxima of $f(\bar{x})$. It is well known that the direction of maximum rate of decrease of a function is that direction described by the negative gradient of the function. That is, if $\bar{x}_0$ is chosen as the initial point in a steepest descent procedure, and $\nabla f(\bar{x}_0) \neq 0$ there will exist a $\lambda < 0$ such that if

$$\bar{x}_1 = \bar{x}_0 + \lambda \nabla f(\bar{x}_0) \tag{2.17}$$

then $f(\bar{x}_1) \leq f(\bar{x}_0)$. Subsequent application of the above results in an iterative process which will ideally terminate arbitrarily closely to a point $\bar{x}_m$ at which $\nabla f(\bar{x}_m) = 0$, a necessary condition for $\bar{x}_m$ to be the location of an extremum of $f(\bar{x})$.

To further illustrate the basic workings of the method of steepest descent, consider the hypothetical surface in these dimensions specified by the function $f(\bar{x}) = f(x_1,x_2)$ shown in the contour map of Figure 2.5. The minimum of this unimodal surface is assumed to be located at the origin. A typical steepest descent trajectory is illustrated, with the starting point $\bar{x}_0$ as shown on the figure. Since $\nabla f(\bar{x}_0) \neq 0$, moving in the direction specified by the negative of the gradient will allow a step to point $\bar{x}_1$. Since $\nabla f(\bar{x}_1) \neq 0$, subsequent iteration to $\bar{x}_2$ is possible, until one may approach arbitrarily close to the minimum at the origin as illustrated by the trajectory shown.

Clearly, the selection of λ at each iteration will affect the rate of convergence of the procedure. The conventional approach in this selection is to expand the objective function in a Taylor's series about the current iteration point, say x, retaining only the first three terms.

$$f(\bar{x} + \lambda\bar{u}) - f(x) = \lambda \sum_{i=1}^{N} \frac{\partial f(\bar{x})}{\partial x_i} u_i + \frac{\lambda^2}{2} \sum_{i=1}^{N} \sum_{j=1}^{N} \frac{\partial^2 f(\bar{x})}{\partial x_i \partial x_j} u_i u_j \qquad (2.18)$$

where $u_i = \frac{\partial f}{\partial x_i}$, and $\bar{u} = \nabla f(\bar{x})$.

λ should be selected so that the decrease in the value of the objective function is maximized; consequently, application of ordinary calculus yields

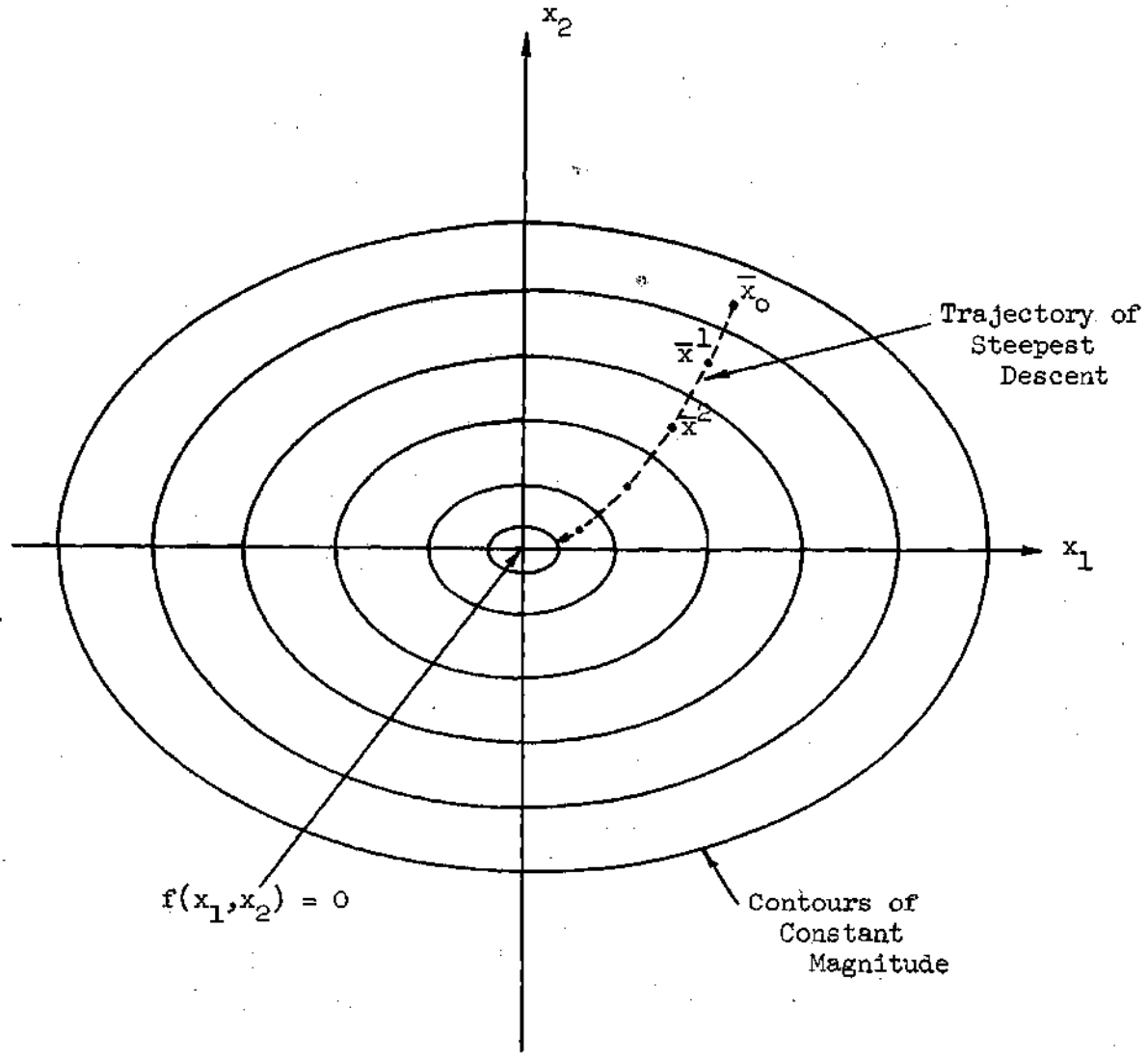

Fig. 2.5 Contour Plot of Hypothetical Surface $f(x_1,x_2)$ Illustrating a Typical Steepest Descent Trajectory.

$$\lambda = - \frac{\sum_{i=1}^{N} \frac{\partial f(\bar{x})}{\partial x_i} u_i}{\sum_{i=1}^{N} \sum_{j=1}^{N} \left[\frac{\partial^2 f(\bar{x})}{\partial x_i \partial x_j} \right] u_i u_j} \tag{2.19}$$

Since $u_i = \frac{\partial f(\bar{x})}{\partial x_i}$

$$\lambda = - \frac{\sum_{i=1}^{N} \left[\frac{\partial f(\bar{x})}{\partial x_i} \right]^2}{\sum_{i=1}^{N} \sum_{j=1}^{N} \left[\frac{\partial^2 f(\bar{x})}{\partial x_i \partial x_j} \right] \frac{\partial f}{\partial x_i} \frac{\partial f}{\partial x_j}} \tag{2.20}$$

If the objective function $f(\bar{x})$ is quadratic, then selection of step size by this method will result in convergence to the minimum of $f(\bar{x})$ in the direction of the gradient $\nabla f(\bar{x})$ in a single step. If $f(\bar{x})$ is not quadratic as is generally the case, then the expression (2.20) does not guarantee that this step size is optimum. In some cases the value of the function after the step is taken will even be greater than that at the initial point. This latter difficulty may be avoided in application of the technique by simply checking the value of the function at each point, comparing values between successive iterations, and interpolating along the line segment between points to determine a new point where the value of the function decreases. In spite of these drawbacks, it is conventional to apply (2.20) to obtain the initial step size in a steepest descent procedure.

Another feature of interest in the determination of step size is the fact that the NxN matrix of mixed second order partial derivatives of the function at each iteration must be evaluated. If N is large or if the second partial derivatives are given by complicated mathematical expressions, then a severe computational restriction may be experienced. Expressions involving integrals such as those encountered in pattern synthesis for minimum mean squared error are particularly troublesome. Considerable effort has been devoted to the development of methods which do not require evaluation of the Hessian at each iteration, but rather use an estimate of this matrix which is corrected based on actual information or the behavior of the function at each iteration. Davidon (33) was the first to implement a procedure of this type and his work was extended somewhat by Powell and Fletcher (37). In this research, a modified version of Davidon's procedure is used to implement the steepest descent technique.

There is, finally, the question of the mathematical establishment of the convergence of the steepest descent procedure. Proofs of convergence are available in many standard texts on nonlinear programming, and for completeness in this presentation, a convergence proof is included in Appendix A of this report.

Implementation of the Procedure

The method of steepest descent for the synthesis of optimum arrays was implemented on the B-5500 digital computer using a modification of the variable metric minimization technique due to Davidon (33). The significant difference between this method and conventional steepest

descent procedures is the lack of necessity for evaluation of the matrix of second order mixed partial derivatives at each iteration. Results of this implementation are shown in the following examples.

Examples on Synthesis by the Method of Steepest Descent

An illustration of the synthesis of arrays by an appropriate set of examples is complicated by the fact that no single example has all of the necessary characteristics required. Consequently, a series of case studies is dictated, with due care being devoted to the selection of the cases to be examined. The following two examples represent respectively the cases of pattern synthesis for an array with complex excitations and pattern synthesis for a broadside array, in which case excitations are real.

Example I. Synthesis of Cosecant pattern.

The pattern selected for this example is given by the set of expressions

$$F(\theta) = \begin{cases} 0 & 0 \leq \theta < \pi/2 \\ 1 & \frac{\pi}{2} \leq \theta \leq \theta_o \\ \frac{\sec \theta}{\sec \theta_o} & \theta_o < \theta \leq \pi \end{cases} \tag{2.21}$$

where θ is measured from the array axis.

Such a radiation pattern has considerable practical significance, being widely used in ground based search radars. This pattern is illustrated graphically in Figure 2.6, which illustrates both the desired pattern (dashed line) and its approximation (solid line) by an array of

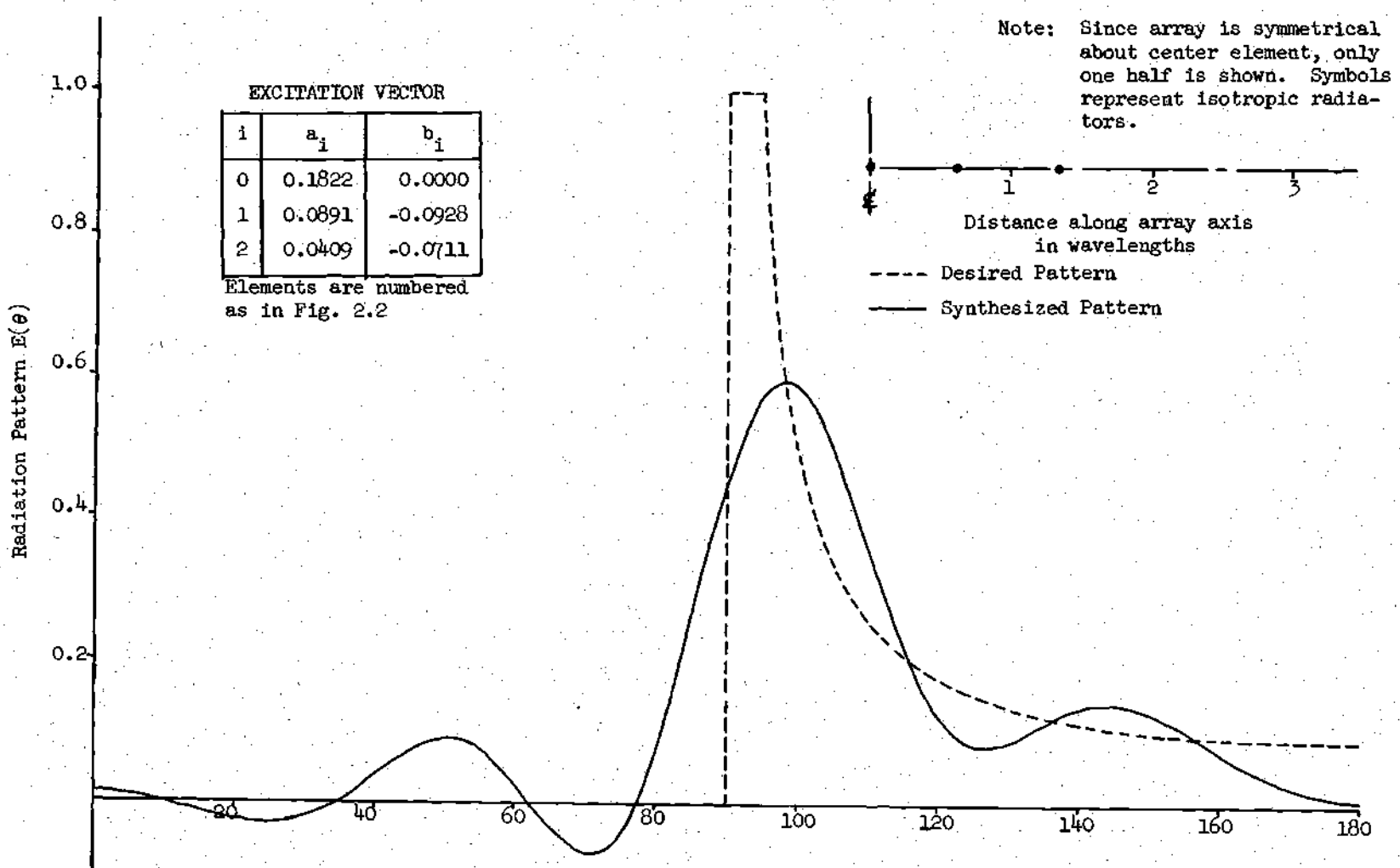

Fig. 2.6 Synthesis of CSC Pattern with Five Element Array - Example I.

five elements. Figures 2.7 and 2.8 illustrate the patterns of nine and thirteen element arrays respectively.

The physical arrangements of these arrays are illustrated in the respective figures. An important feature to be noted is the variation in element spacings along the array axis. While these variations are noticeable in every case in the illustration, they are not marked by a large fluctuation about some average value, as indicated in Table I. The average value of spacing in this table was obtained by dividing the total aperture width by the number of interelement intervals.

A final characteristic of this example which is of primary interest is a comparison of this synthesis procedure with the Fourier method of pattern synthesis, since the Fourier technique is the most widely employed technique for synthesis of equally spaced arrays. This comparison of mean squared error is shown in Figure 2.9. Note that a substantial improvement in array performance is realized by using the steepest descent technique where element locations are employed as independent variables.

Example II. Synthesis of an Exponential Pattern

The second case to be examined involves the approximation of the pattern given mathematically by

$$F(\theta) = \exp\left[-50 \cos^2 \theta\right] \qquad (2.22)$$

This pattern is similar to the familiar Gaussian function. Figure 2.10 provides a graphical illustration of its characteristics. Note that because the pattern $F(\theta)$ is symmetrical about the broadside direction, the pattern will be approximated by

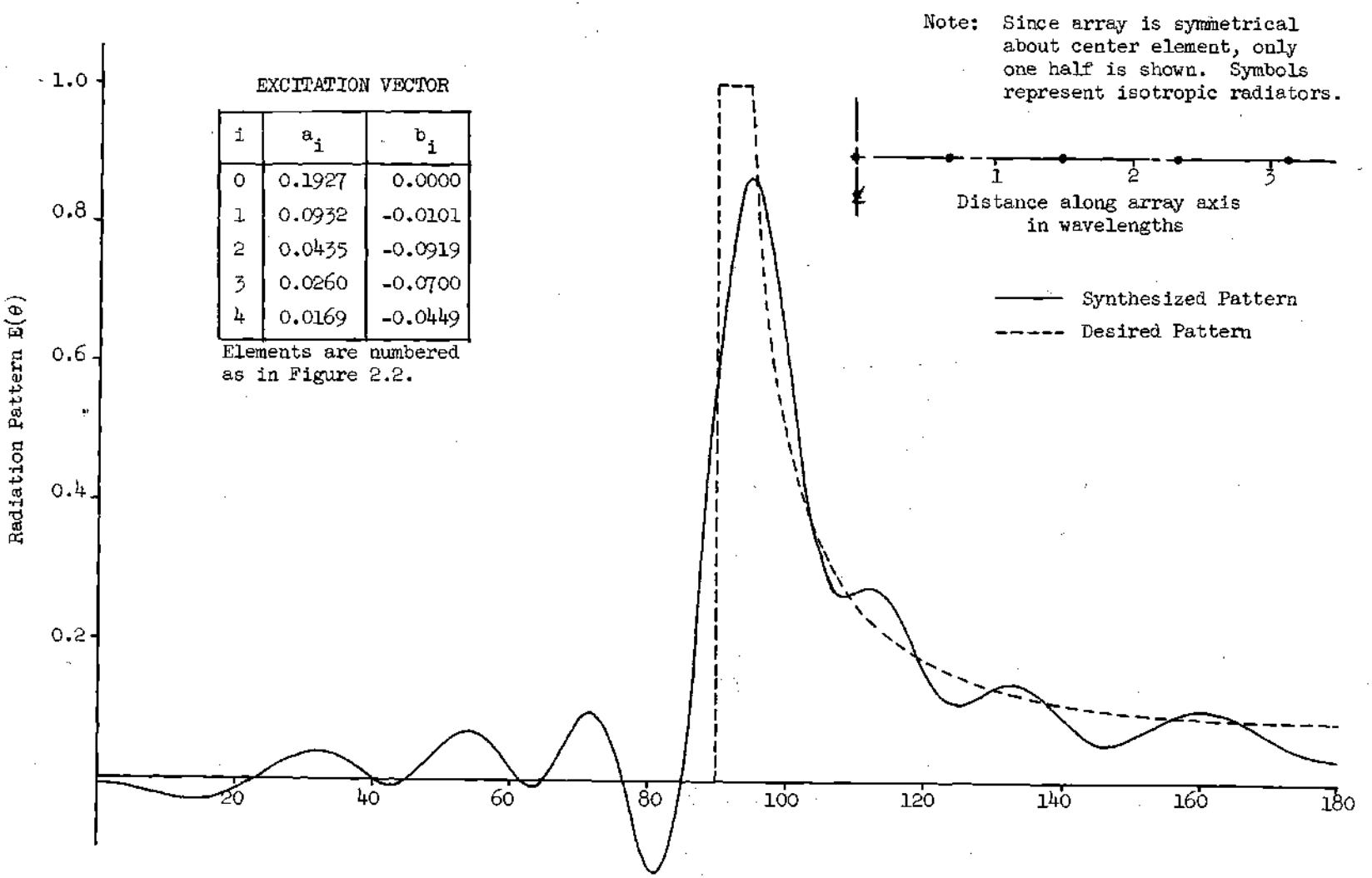

Fig. 2.7 Synthesis of CSC Pattern with Nine Element Array - Example I.

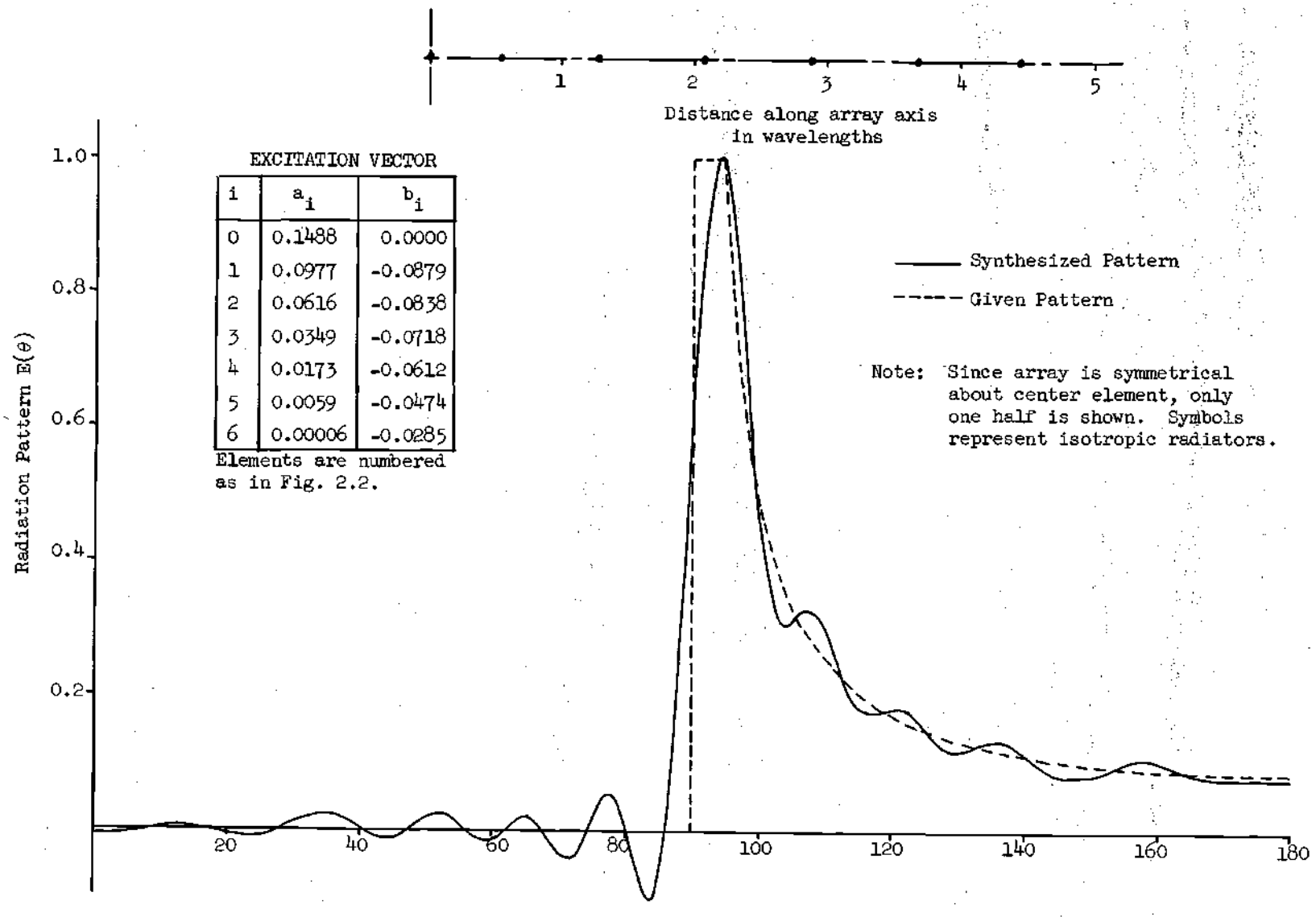

Fig. 2.8 Comparison of CSC θ Pattern and Pattern of 13 Element Array-Example I.

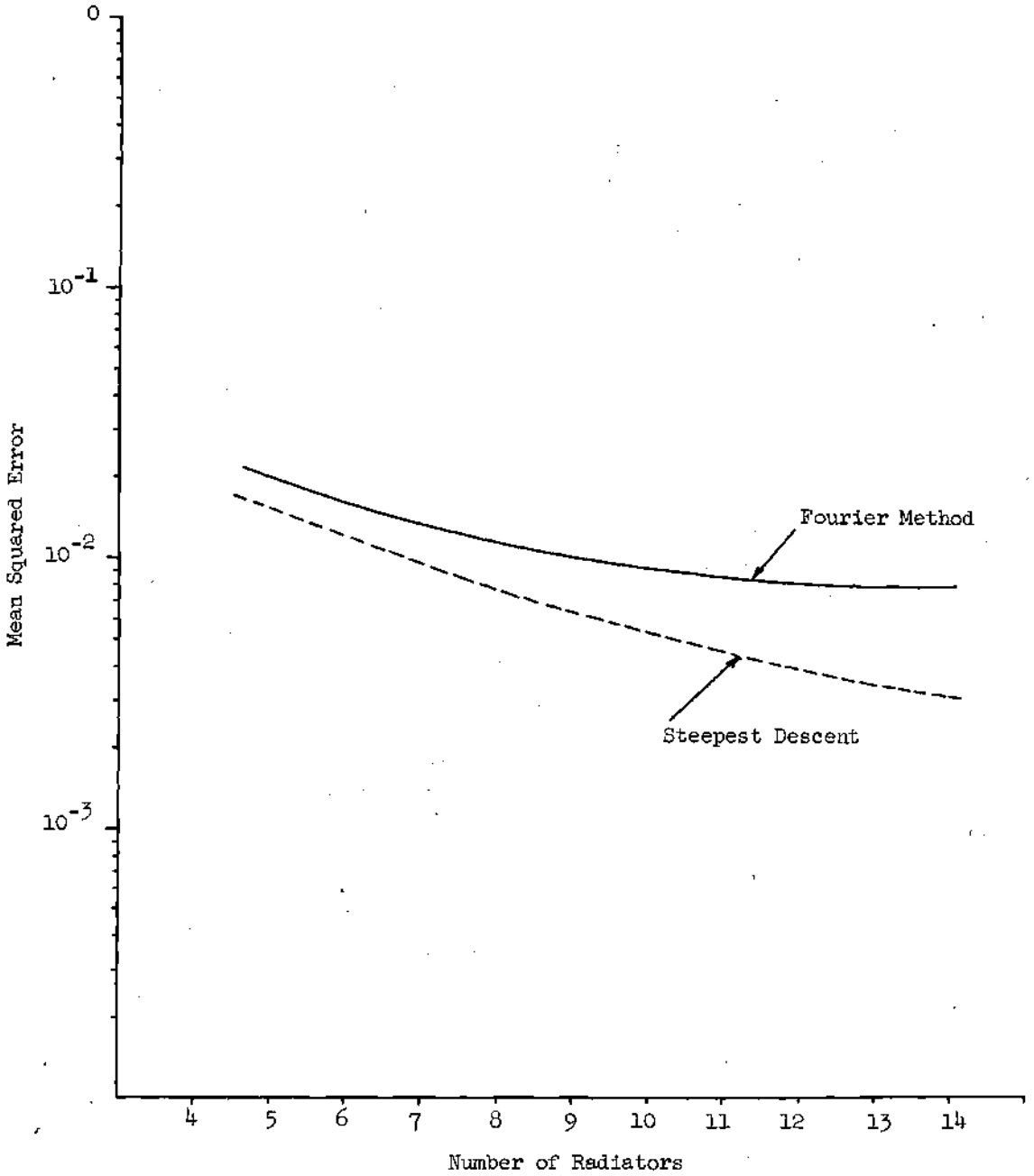

Fig. 2.9 Comparison of Mean Squared Error for CSC θ Synthesis - Example I.

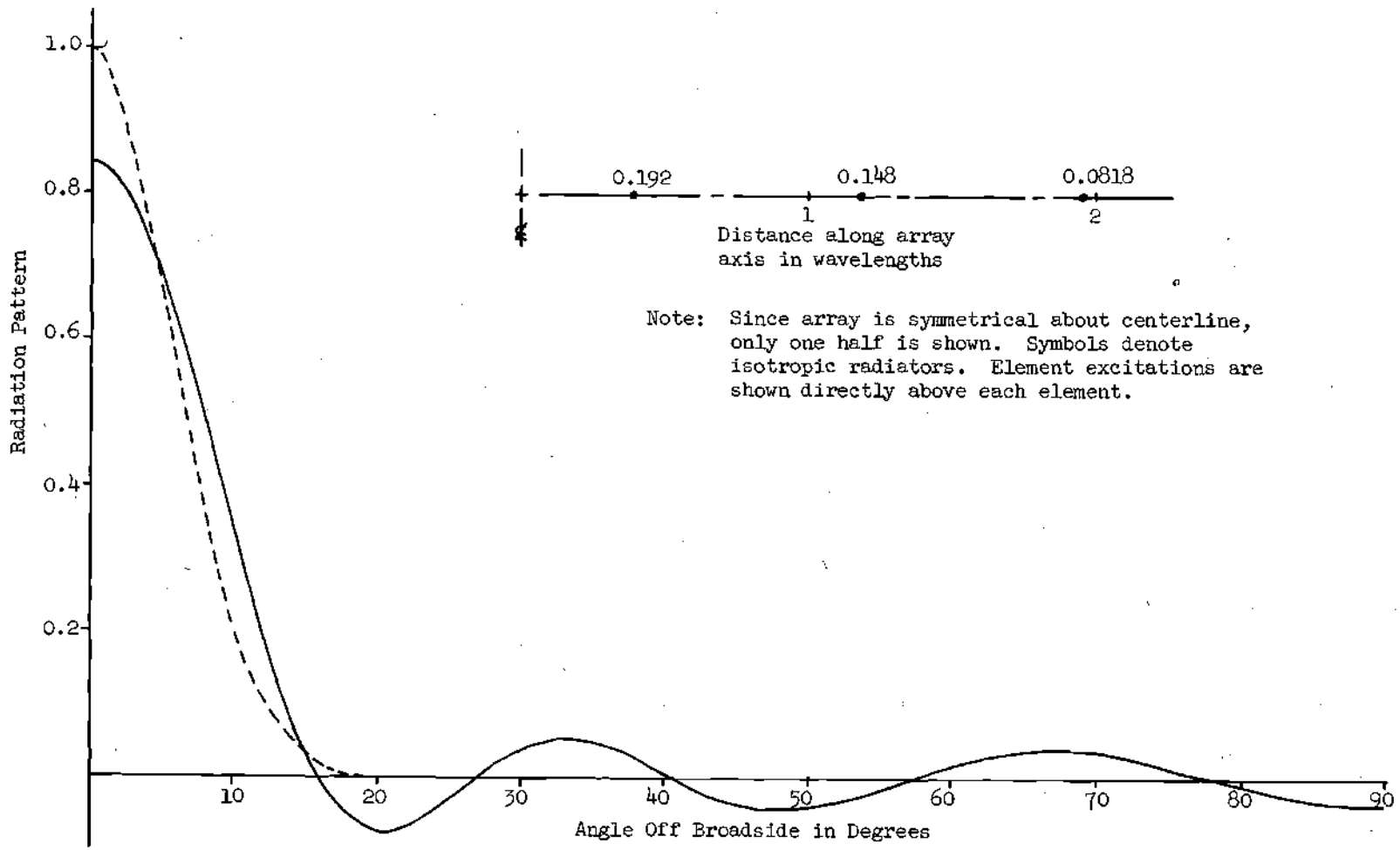

Fig. 2.10 Synthesis of Gaussian Pattern with Six Element Array - Example II.

Number of Elements	Total Aperture in Wavelengths	Average Spacing in Wavelengths	Separation Between Elements in Wavelengths*					
			d_{10}	d_{21}	d_{32}	d_{43}	d_{54}	d_{65}
5	2.6667	0.665	0.6184	0.7149				
7	4.442	9.7403	0.6504	0.7926	0.778			
9	6.258	0.7822	0.6693	0.8207	0.844	0.795		
11	7.3732	0.7373	0.5225	0.7395	0.8118	0.8284	0.7844	
13	9.916	0.8263	0.5307	0.7313	0.805	0.831	0.800	0.762

* $d_{ij} = d_i - d_j$, i.e. d_{21} is spacing between first and second radiators.

TABLE I TABULATION OF ELEMENT SPACINGS — EXAMPLE I

$$E_M(\theta) = a_o + 2 \sum_{m=1}^{M} a_m \cos (\beta x_m \cos \theta) \qquad (2.23)$$

where the excitation coefficients a_i are purely real numbers.

Figure 2.10 illustrates the approximation to the desired pattern which is realized with a six element array, while Figure 2.11 shows the improvement in the approximation when ten elements are employed in the array. Note that the spacings of the radiators in the illustration of the physical arrangement of each array are noticeably nonuniform, but that there are no radical variations in spacing along the arrays.

A comparison of the mean squared error for the Fourier synthesis method and the steepest descent method is given in Figure 2.12. A substantial improvement is to be noted for the array synthesized using steepest descent procedures.

Synthesis Incorporating Linear Inequality Constraints

The preceding discussions and examples have demonstrated the advantages of using the powerful techniques of nonlinear mathematical programming in the design of radiating systems. One of the most useful features of this approach to the pattern synthesis problem is the ease with which inequality constraints may be incorporated into the design procedures. None of the present synthesis techniques provide for the specification of such constraints. In fact, the mathematical techniques of the methods in wide use do not allow this additional flexibility.

In the preceding development on pattern synthesis, an optimum

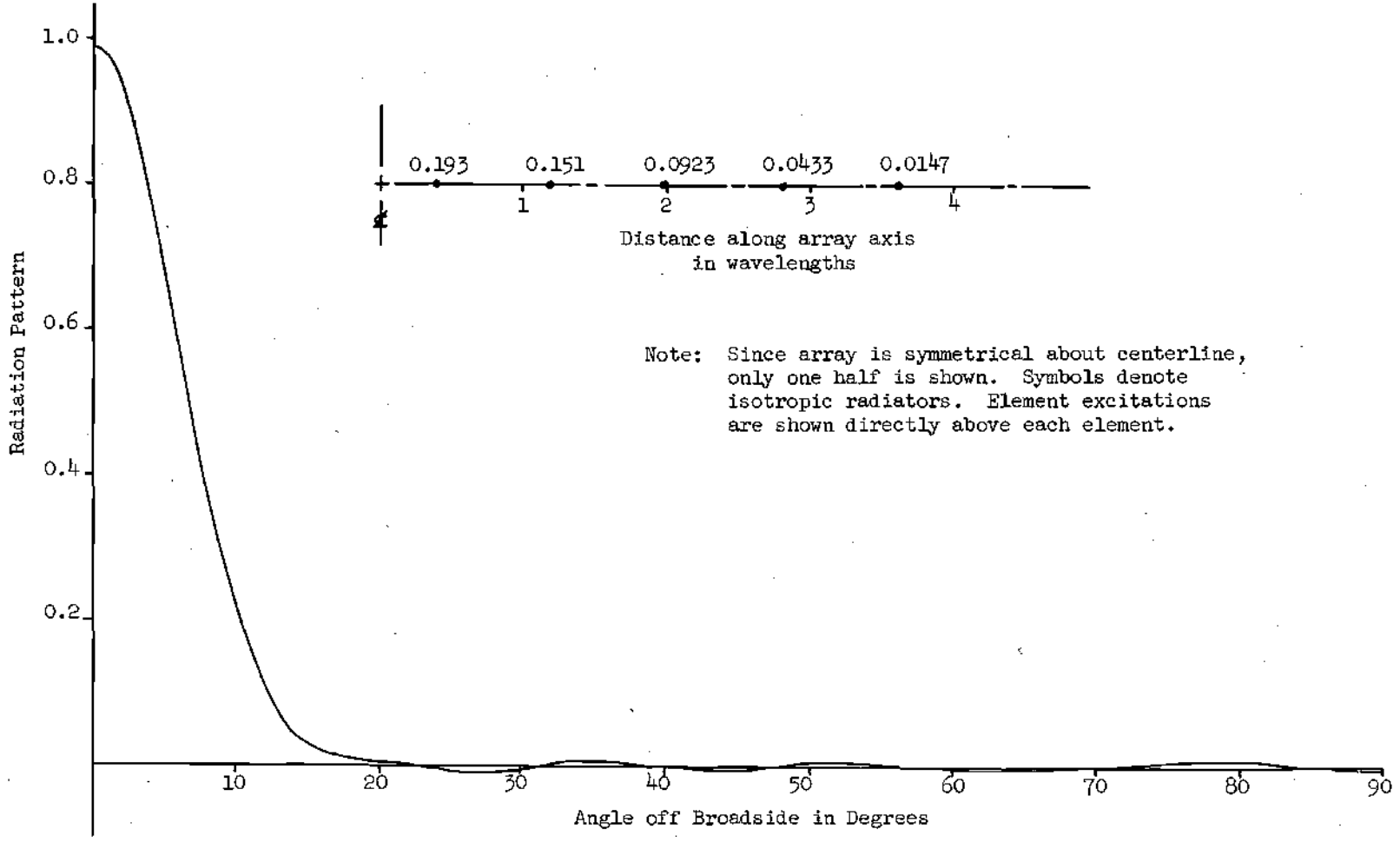

Fig. 2.11 Synthesis of Gaussian Pattern with Ten Element Array - Example II.

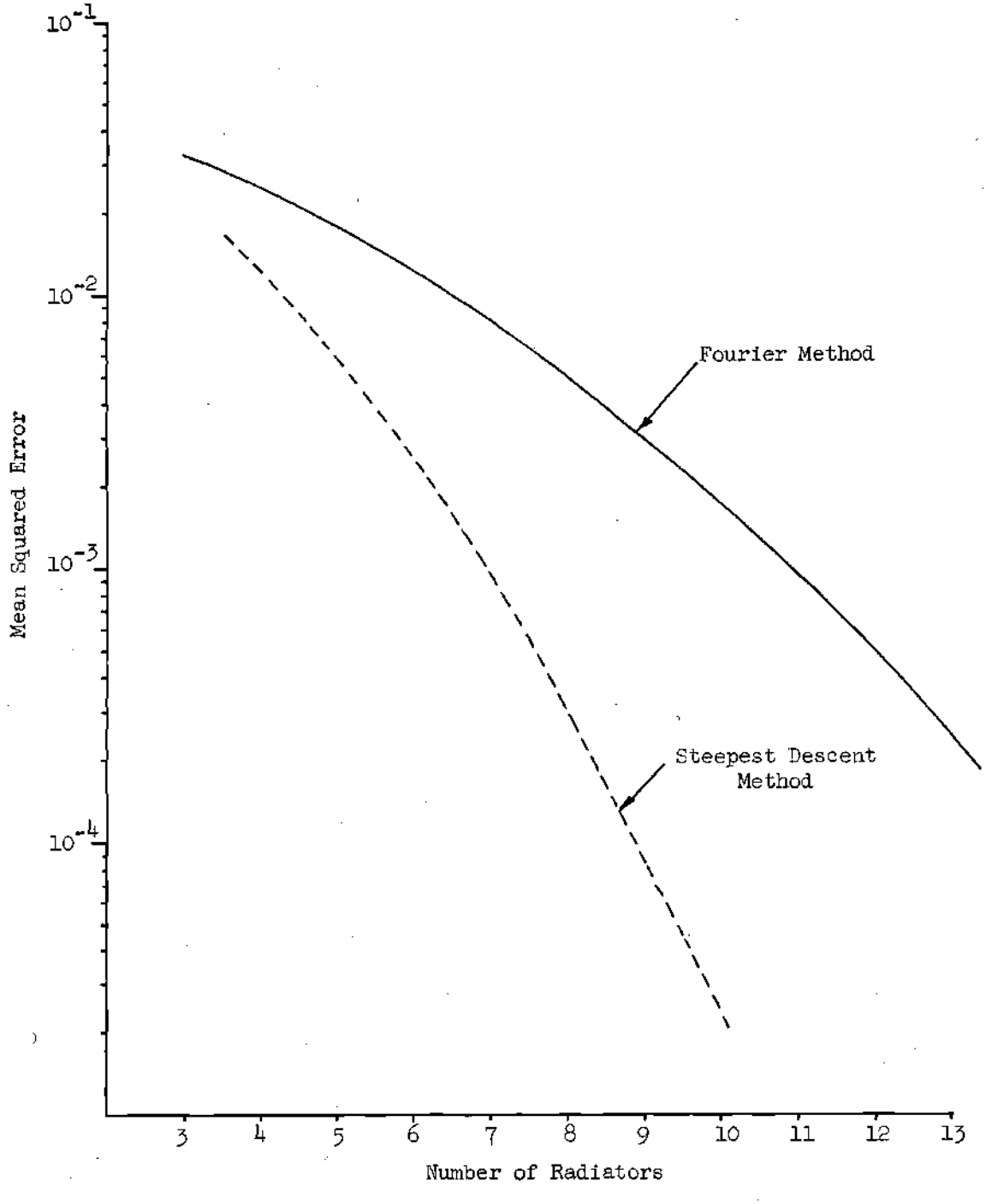

Fig. 2.12 Comparison of Mean Squared Error - Example II.

array was sought in which the system variables included both the complex excitation coefficients and the positions of the radiators along the array axis. The values of these parameters which resulted in minimum mean squared error between a given pattern and the pattern of the synthesized array completely described the optimum array. There were, however, no limitations imposed on the values which these parameters could assume. In many practical instances, the array designer may not have complete flexibility in selection of parameters due to space limitations and other factors. Electrical restrictions, such as the mutual coupling problems which exist in multielement antennas, also impose certain limitations.

There might be constraints on the ranges of the excitation coefficients themselves, such as a specification of maximum allowable amplitude taper. The important characteristic of these types of design constraints is that they will in general be inequality constraints, and thus they could not be accommodated using the Lagrange multiplier method or by the elimination of variables by direct substitution.

The specific mathematical form of these constraints is restricted to linear inequalities of the form

$$g(\bar{a},\bar{b},\bar{x}) \geq 0 \qquad (2.24)$$

where $\bar{a}$, $\bar{b}$, and $\bar{x}$ are the vectors of array parameters previously defined. This limitation is not a serious restriction because each of the constraints mentioned above is linear as the following illustrations will show. A constraint of the maximum allowable aperture would be specified as

$$x_i - d_{max} \geq 0 \quad , \quad i = 1,\cdots,M \tag{2.25}$$

while the minimum allowable spacing constraint would be written as

$$x_{i+1} - x_i - d_{min} \geq 0 \quad , \quad i = 1,\cdots,M-1 \tag{2.26}$$

where $2d_{max}$ and d_{min} represent maximum allowable aperture and minimum allowable interelement spacing, respectively. Similarly, if a_o were taken as reference, the specification of maximum allowable amplitude taper would be expressed as

$$a_i - k\,a_o \geq 0 \quad , \quad i = 1,\cdots,M \tag{2.27}$$

for some prescribed k. Constraints relating components of vector $\bar{b}$ could be similarly constructed.

It is worthwhile to discuss briefly the geometrical significance of inequality constraints to further illustrate the complications caused by the inequality sign. Consider the problem of locating the minimum on a unimodal three dimensional surface given mathematically by

$$f(\bar{x}) = f(x_1,x_2) \tag{2.28}$$

which satisfies linear inequality constraints

$$\begin{aligned} g_1(\bar{x}) &\geq 0 \\ g_2(\bar{x}) &\geq 0 \end{aligned} \tag{2.29}$$

On the (x_1,x_2) plane, these constraints define a region of two dimensions

in which feasible solutions may exist. If these constraints were equality constraints, however, each equality would reduce the space of feasible solutions by one dimension; consequently, the minimization of $f(\bar{x})$ subject to $g_1(\bar{x}) = 0$ and $g_2(\bar{x}) = 0$ is trivial. The solution is the point of intersection of the boundary planes described by the two equalities. Inequality constraints, because they do not reduce the dimension of the region of feasible solutions, do not allow any such simplification of the minimization problem.

These points are further illuminated by the hypothetical surface shown in Figure 2.13. This illustration shows a contour plot of a unimodal three dimensional surface on which is superimposed two constraint boundaries representing two linear constraints.

$$\begin{aligned} g_1(\bar{x}) &= 3 - x_1 \\ g_2(\bar{x}) &= 9 - 3x_2 + x_1 \end{aligned} \tag{2.30}$$

For $g_1(\bar{x}) \geq 0$ and $g_2(\bar{x}) \geq 0$, the region of feasible solutions is labeled R, where it is further assumed that $x_1 \geq 0$, $x_2 \geq 0$. Note the locations of the global minimum, the constrained minimum, and the intersection of the constraint boundaries. The fact that for this simple example these points are separate and distinct illustrates the difficulties encountered when inequality constraints are added to the overall minimization problem. The minimization might also be further complicated by the fact that the surface described by the objective function could be multimodal with a relative minimum located inside the feasible region. The remarks on multimodal surfaces of the preceding section would apply, but the

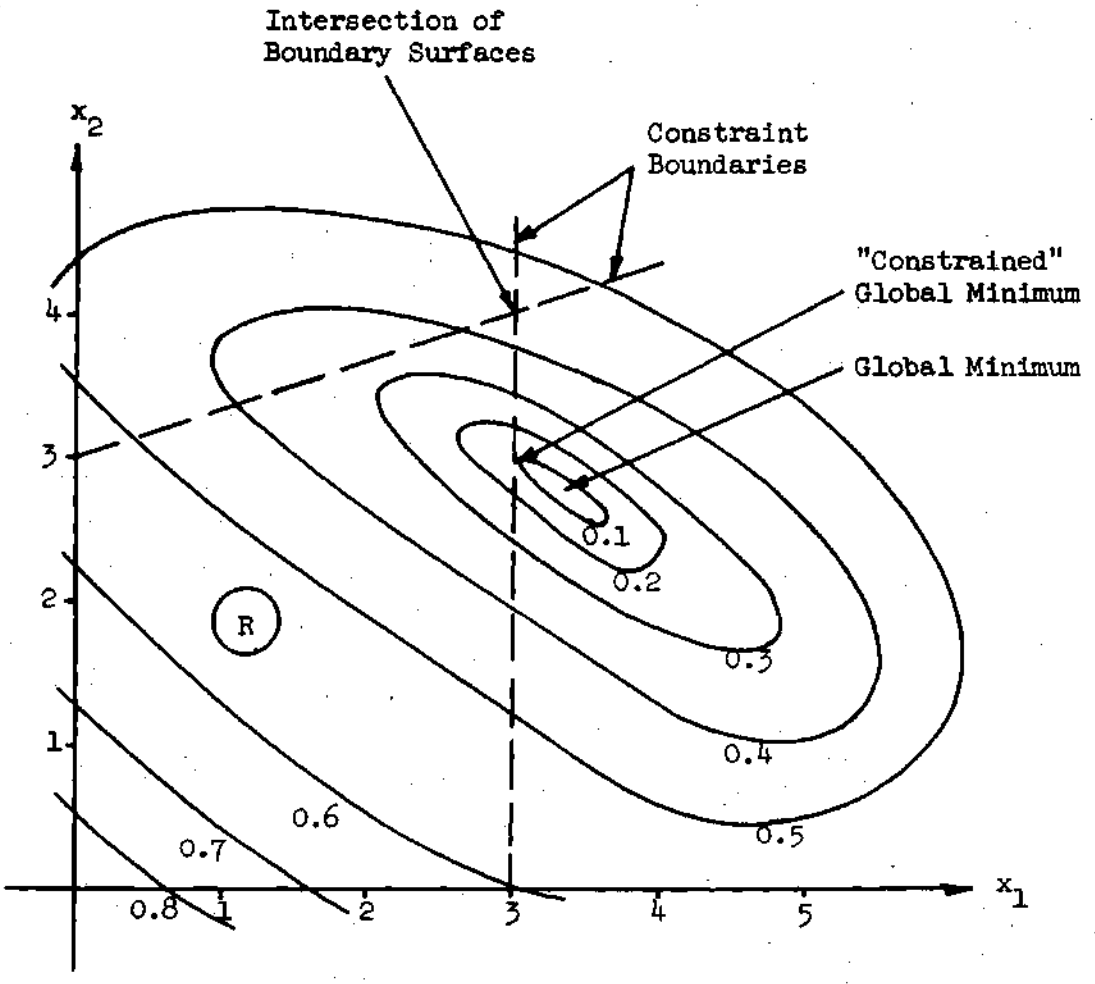

Fig. 2.13 Contour Plot of Hypothetical Three Dimensional Surface.

conclusion is that again physical considerations are the major factors in identifying and rejecting these minima. Extension of these remakrs to spaces of higher dimension is straightforward.

Despite these difficulties, there are procedures for incorporating linear constraints in direct optimization techniques. A variety of these are reported in the literature (34)-(35). The created response surface technique is originally due to Carroll and is particularly well suited to the optimization problem of this research.

Consider the minimization of a nonlinear objective function, say $f(\bar{x})$, where $\bar{x}$ is an n-vector subject to the (m+n) linear inequality constraints

$$\begin{aligned} g_i(\bar{x}) &= x_i \geq 0 \quad , \quad i = 1,\cdots,n \\ g_i(\bar{x}) &\geq 0 \quad , \quad i = n+1,\cdots,m+n \end{aligned} \tag{2.31}$$

An auxiliary function is formed as indicated below.

$$F(\bar{x},r) = f(\bar{x}) + r \sum_{i=1}^{m+n} \frac{1}{g_i(\bar{x})} \tag{2.32}$$

The basis of this procedure is the selection of a sequence $\{r_k\}$ decreasing to zero as k tends to infinity. For each value of r_k in the sequence, the function $F(\bar{x},r_k)$ is minimized using the method of steepest descent. Note that the terms $1/g_i(\bar{x})$ become infinite on the constraint boundary so that if the steepest descent process starts within the feasible region of solutions, the minimum of $F(\bar{x},r_k)$ will remain within the feasible region

also. Selections of smaller values of the parameter r_k will result in this minimum moving closer and closer to the boundaries which are binding. As r gets smaller and smaller, the contributions of the terms due to the non-binding constraints will be negligible. Those constraints which are binding force $F(\bar{x},r)$ to become infinite on each of the constraint surfaces, but the effects of each binding constraint at points just off the boundary becomes less as r decreases. It should be expected then that a binding constraint surface could be approached arbitrarily closely for r sufficiently small. Thus, the minimum of $f(\bar{x})$ subject to linear constraints $g_i(\bar{x})$ would be approached along the trajectory of minima of $F(\bar{x},r_k)$ as the sequence $\{r_k\}$ tends toward zero.

Mathematical establishment of the convergence of the created response surface techniques is included in Appendix B.

Example on Pattern Synthesis Subject to an Aperture Constraint

The preceding discussions illustrated the practical need for incorporating inequality constraints into the synthesis procedure, and indicated the required mathematical techniques for accomplishing this. It will be recalled that a wide variety of linear inequality constraints were applicable in array design, but that the mathematical form of these constraints remained invariant. It is practical, therefore, to illustrate pattern synthesis subject to constraints using a single constraint, in this case a maximum allowable aperture constraint. In order to include the unconstrained solution for comparison, it is convenient to select the example from the preceding section on the synthesis of the exponential pattern using six radiators. Figure 2.10 shows this example

where no constraints are imposed. Note that the maximum spacing from the array center is 1.9531 wavelengths.

Two specifications of maximum aperture are set forth in this example. In the first case, the maximum aperture allowed is 3.5 wavelengths which means that the maximum value for any radiator displacement from array center is 1.75 wavelengths. This constraint is stated mathematically as follows.

$$1.75 - x_i \geq 0 \quad , \quad i = 1,2,3 \tag{2.33}$$

The auxiliary function $F(\bar{a},\bar{x},r_k)$ is then given by

$$F(\bar{a},\bar{x},r_k) = \mathcal{E}(\bar{a},\bar{x}) + r_k \left[\sum_{i=1}^{3} \frac{1}{1.75-x_i} + \frac{1}{x_i} \right] \tag{2.34}$$

The sequence of $\{r_k\}$ is shown in Table II, together with the vectors which minimize $F(\bar{a},\bar{x},r_k)$ for each k. It is clearly seen that x_3 is being bound by the constraint. For $r = 10^{-9}$, the value of x_3 is 1.7499 wavelengths; convergence to a value closer to 1.7500 wavelengths could be achieved by assigning smaller values of r, but no practical purpose is served in this example by extending the process further. The desired pattern, synthesized pattern of the unconstrained array, and pattern of the constrained array are illustrated in Figure 2.14.

In the second specification, the maximum allowable aperture constraint is relaxed to allow a maximum displacement of 1.91 wavelengths from the centerline. The sequence of $\{r_k\}$ for this case is shown in Table II, while the patterns of the unconstrained array and the constrained

TABLE II TABULATION OF CONSTRAINED SOLUTIONS

d_{max} = 1.75 Wavelengths

r	$F(\bar{a},\bar{x},r)$	x_1	x_2 (in wavelengths)	x_3
10^{-2}	0.014509	0.03803	0.84828	1.43274
10^{-4}	0.004751	0.35094	1.05113	1.70808
10^{-6}	0.004030	0.36162	1.07992	1.74584
10^{-7}	0.003978	0.36233	1.08119	1.74868
10^{-8}	0.003956	0.36263	1.08278	1.7499

d_{max} = 1.91 Wavelengths

r	$F(\bar{a},\bar{x},r)$	x_1	x_2 (in wavelengths)	x_3
10^{-2}	0.012218	0.08951	0.77912	1.496
10^{-4}	0.003327	0.38514	1.15050	1.864
10^{-5}	0.002851	0.38957	1.1646	1.8936
10^{-6}	0.002718	0.39107	1.1694	1.9044
10^{-7}	0.002679	0.39160	1.1710	1.9081

Unconstrained Solution

$\mathcal{E}(\bar{a},\bar{x})$	x_1	x_2 (in wavelengths)	x_3
0.002548	0.3971	1.1887	1.9531

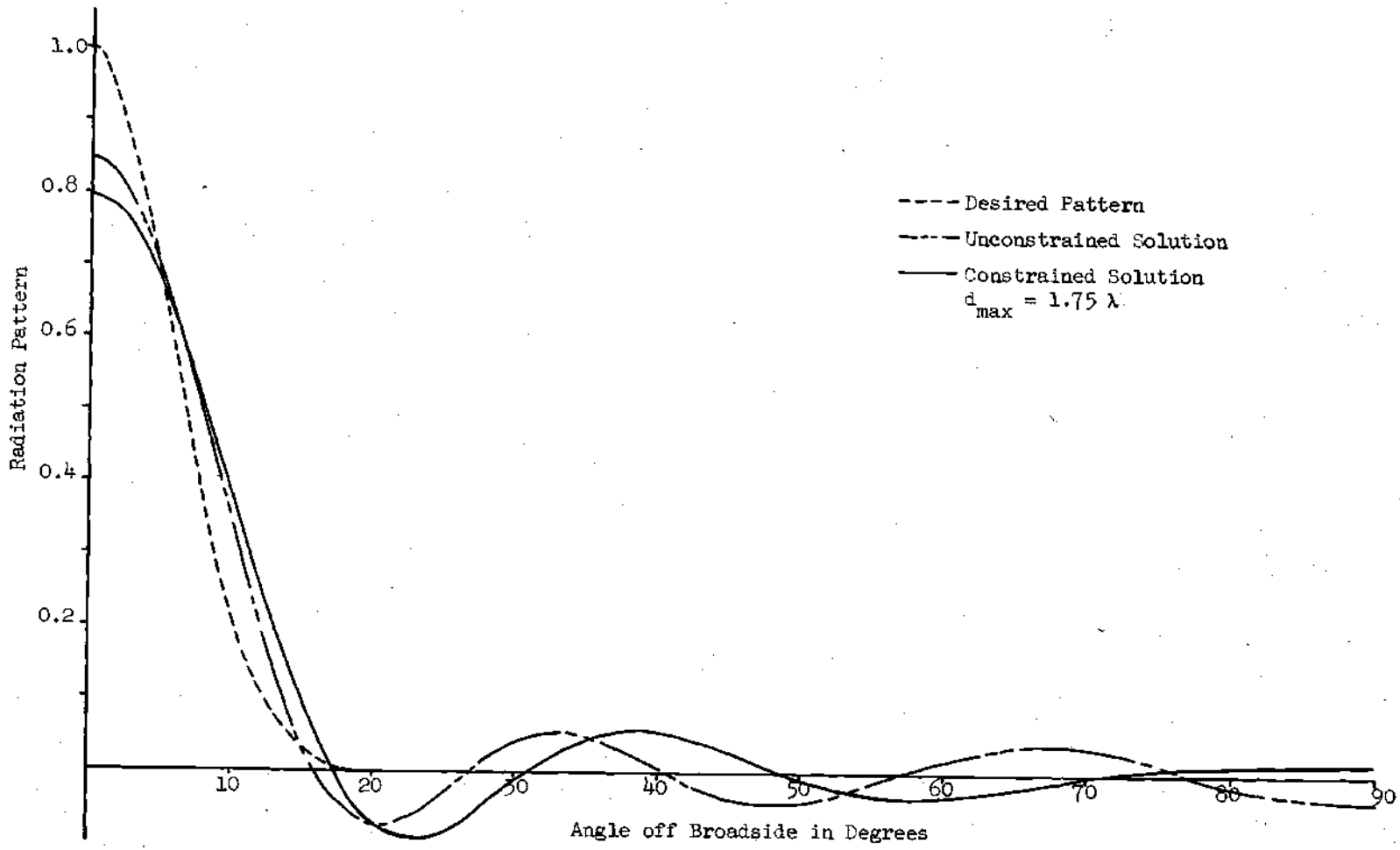

Fig. 2.14 Constrained Synthesis of Exponential Pattern for Maximum Aperture of 3.5 Wavelengths with Six Elements.

array are illustrated in Figure 2.15. The better approximation of the second array and the manner in which the constrained pattern is approaching that of the unconstrained array are the important characteristics of this illustration.

Summary

The work discussed in this chapter has illustrated that the techniques of nonlinear mathematical programming are directly applicable to the problem of array synthesis for minimum mean squared error. Insofar as ease of implementation is concerned, no increase in complexity was experienced in the use of this procedure when compared with the other iterative methods reported in the literature. Furthermore, nonlinear programming is sufficiently flexible to allow incorporation of design constraints relating the array parameters, a feature of some importance not enjoyed by any of the other known methods of array design.

Specifically, these studies have investigated the influence of the element positions as additional independent variables in the synthesis of prescribed radiation patterns. It has been demonstrated that the use of variable spacings results in a better approximation to a given pattern than the widely used Fourier synthesis method provides. The specific examples investigated did not, however, show that this improvement in performance is due to widely varying unequal interelement spacings, but rather results from the fact that for a particular number of radiators, the steepest descent procedure automatically selects the optimum aperture structure. This selection is not possible with the Fourier technique because the number of elements determines the aperture size. Furthermore, the excitations of the Fourier array do not vary as the number of

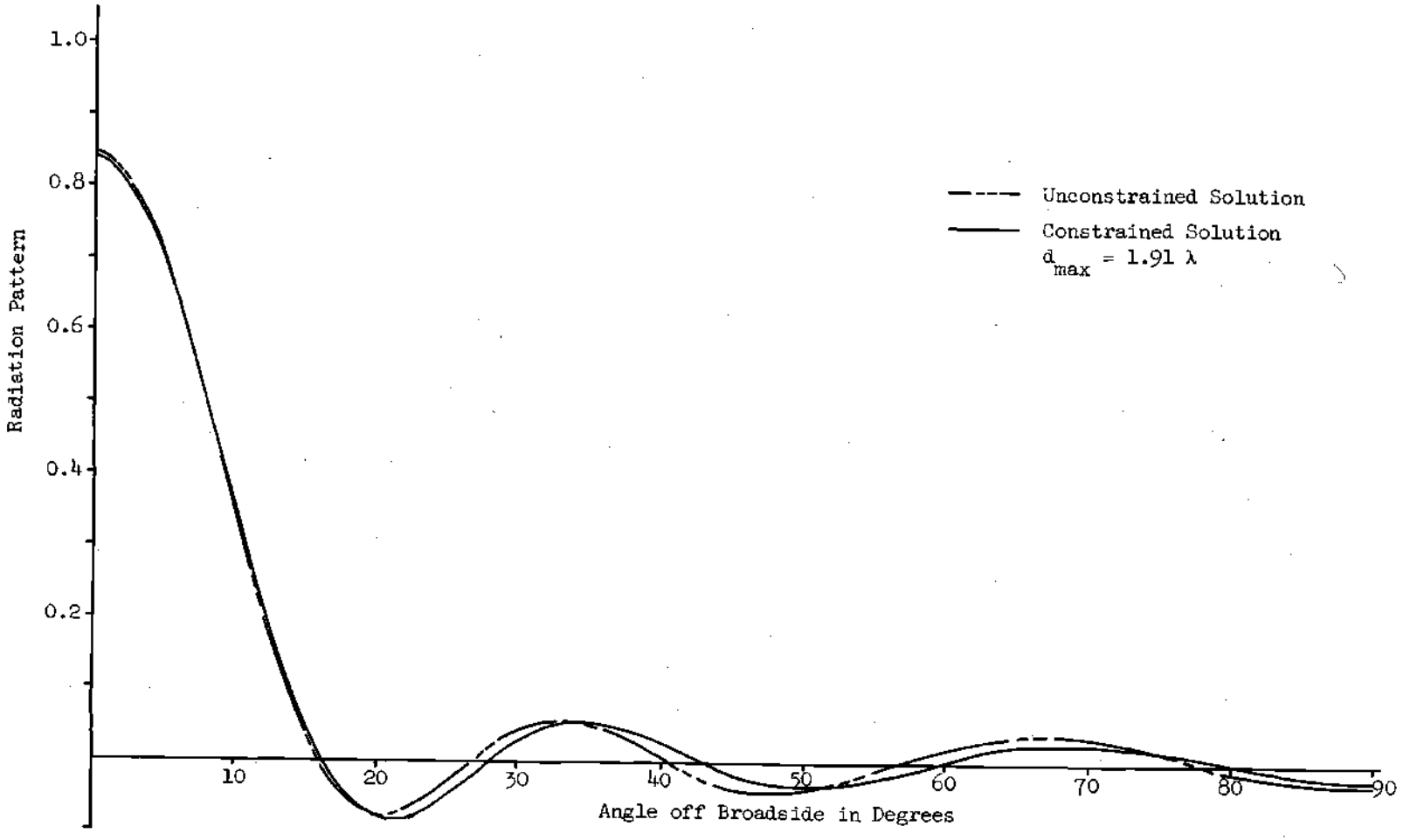

Fig. 2.15 Constrained Synthesis of Exponential Pattern for Maximum Aperture of 3.82 Wavelengths with Six Elements.

elements increases, whereas the steepest descent procedure adjusts each excitation coefficient independently as the number of radiators is increased. The specification of inequality constraints is of considerable practical interest, and in this work has been incorporated into the array synthesis procedure using the created response surface technique. Investigation of two maximum aperture constraints in the synthesis of an exponential pattern illustrated the rapid convergence of the method, and clearly showed at each iteration of the parameter r_k which variable was being bound by the constraint.

CHAPTER III

SYNTHESIS OF ARRAYS FOR OPTIMUM SIGNAL-TO-NOISE PERFORMANCE

Introduction

In this chapter, the optimization of the performance of linear arrays of isotropic point sources in an interference or noise environment whose spatial characteristics are prescribed is discussed. It is shown that when the constraint of equal spacings is imposed, the use of two linear transformations reduces the optimization problem to a conventional characteristic value, or eigenvalue problem. The cases where spacings are included as independent variables are handled using two methods. In those situations where small variations in interelement spacings are expected to improve the performance of the array a perturbational technique is developed to determine the element locations. For larger displacements, the method of steepest descent is utilized.

A brief review of the motivating factors which influenced the choice of maximum output signal-to-noise ratio, as the optimality criterion, should properly precede the discussions which follow. There are several practical instances in which the maximization of output signal-to-noise ratio is considerably more meaningful than synthesis techniques which optimize directivity or perhaps the beamwidth of the main lobe for a given sidelobe level as in Dolph-Chebyschev synthesis. One application which is suggested immediately is that of the design of radiating systems which are to operate in the vicinity of other strong radio sources where

mutual interference becomes a severe problem. The confined space of a naval vessel with its myriad of radar and communications equipment furnishes an excellent example of a complex radio frequency interference (RFI) environment. Possible interference between the electronic equipment of vessels operating in convoy further emphasizes the necessity for considering this factor in the design of antenna systems.

Another practical situation where the maximization of output signal-to-noise ratio is of paramount importance is the case of an array used for radio astronomy. The use of arrays is becoming widespread in this area, and the necessity of discriminating against interference using all possible means is obvious.

A final example of a situation where signal-to-noise ratio maximization is a paramount feature is that of a radar array mounted on an aircraft which is observing other aircraft at approximately the same altitude or higher altitudes. The clutter return will be substantial in overland operation, and use of the array's flexibility to improve the signal-to-clutter ratio should provide some relief in the overall overland airborne radar problem.

Some General Remarks

Following these introductory comments, it is necessary to carefully discuss the mathematical description of the noise, or interference environment in which the array whose performance is to be optimized is to operate. The reader should note that in the text to follow the terms noise and interference are used synonymously to describe any undesired signal.

In general, the noise power spatial distribution will be a function

of frequency as well as the angular coordinates θ and φ. The reader should refer to Figures 3.1 and 3.2 for the relation of these angular coordinates to the radiating system geometry. It is convenient, and in a large number of physical situations quite practical, to assume that the noise power input to the array is of a single frequency equal to that of the desired signal. Such an assumption is clearly justified if the overall signal processing system of which the array is to be a part is a narrowband system. Denoting the overall noise environment's mathematical description as $N(\theta,\Phi,\omega)$, this assumption allows the noise function to be simplified to

$$N(\theta,\Phi,\omega) = N(\theta,\Phi)\ \delta(\omega-\omega_o) \tag{3.1}$$

where ω_o is the angular frequency of the desired signal, and $\delta(\omega-\omega_o)$ is the delta function with the well-known characteristics

$$\delta(\omega-\omega_o) = \begin{cases} 1\ , & \omega = \omega_o \\ 0\ , & \omega \neq \omega_o \end{cases} \tag{3.2}$$

If the individual radiators in the array are isotropic, then it is clear that, for a given value of θ, the radiation pattern is invariant over the entire range of the angular coordinate Φ. Thus, no generality is lost by restricting the noise environments under consideration to be invariant with respect to Φ. For those environments whose spatial characteristics are not invariant with respect to Φ but which are separable into products of the form

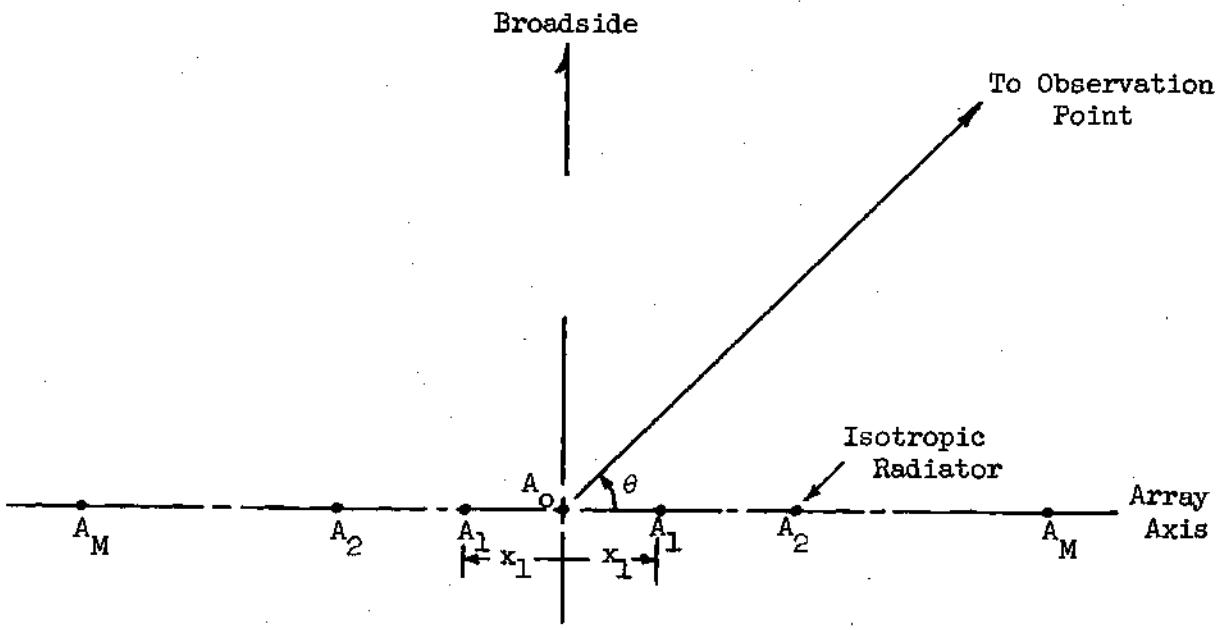

Fig. 3.1 Broadside Symmetrically Excited Array.

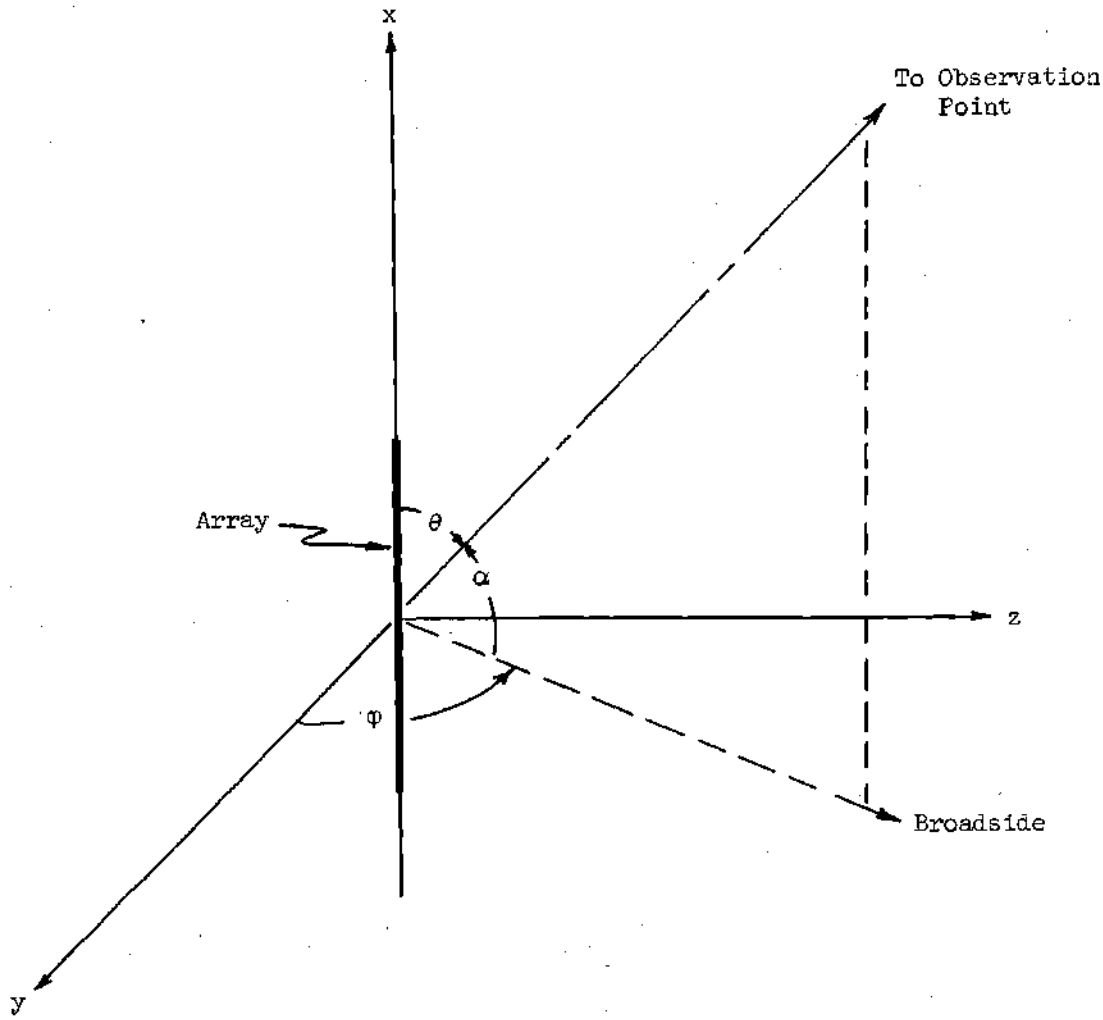

Fig. 3.2 Geometry of Radiating System.

$$N(\theta,\Phi,\omega) = N_1(\theta)\, N_2(\Phi)\, \delta(\omega-\omega_o) \tag{3.3}$$

pattern multiplication will allow the synthesis of a rectangular array of isotropic radiators. This type of noise environment is easily handled by a straightforward extension of the synthesis techniques for linear arrays, and will not be discussed further.

The synthesis of only linear arrays then allows the noise function to be written as

$$N(\theta,\Phi,\omega) = N(\theta)\, \delta(\omega-\omega_o) \tag{3.4}$$

where $N_2(\Phi)$ has been set for convenience equal to unity. This final expression is the mathematical description of the particular type of noise environment to be considered in the following development of the optimization procedure for linear arrays.

Before proceeding to the specific details of the optimization process, it is interesting to consider some of the general aspects of the problem of maximizing the output signal-to-noise ratio of a linear additive array. In many respects, this problem is similar to the matched filter problem of communication theory.

In Figure 3.3, the system composed of the array is represented schematically by a box whose tranfer function $G(\theta)$ is the power pattern factor of the array. The problem is to determine the antenna transfer function $G(\theta)$ which maximizes the signal-to-noise ratio at the output of the system for a given noise power spatial distribution $N(\theta)$. For a matched filter, the analogous functions are $|H(j\omega)|^2$ and $N(\omega)$ respectively. One could view the antenna signal-to-noise optimization problem

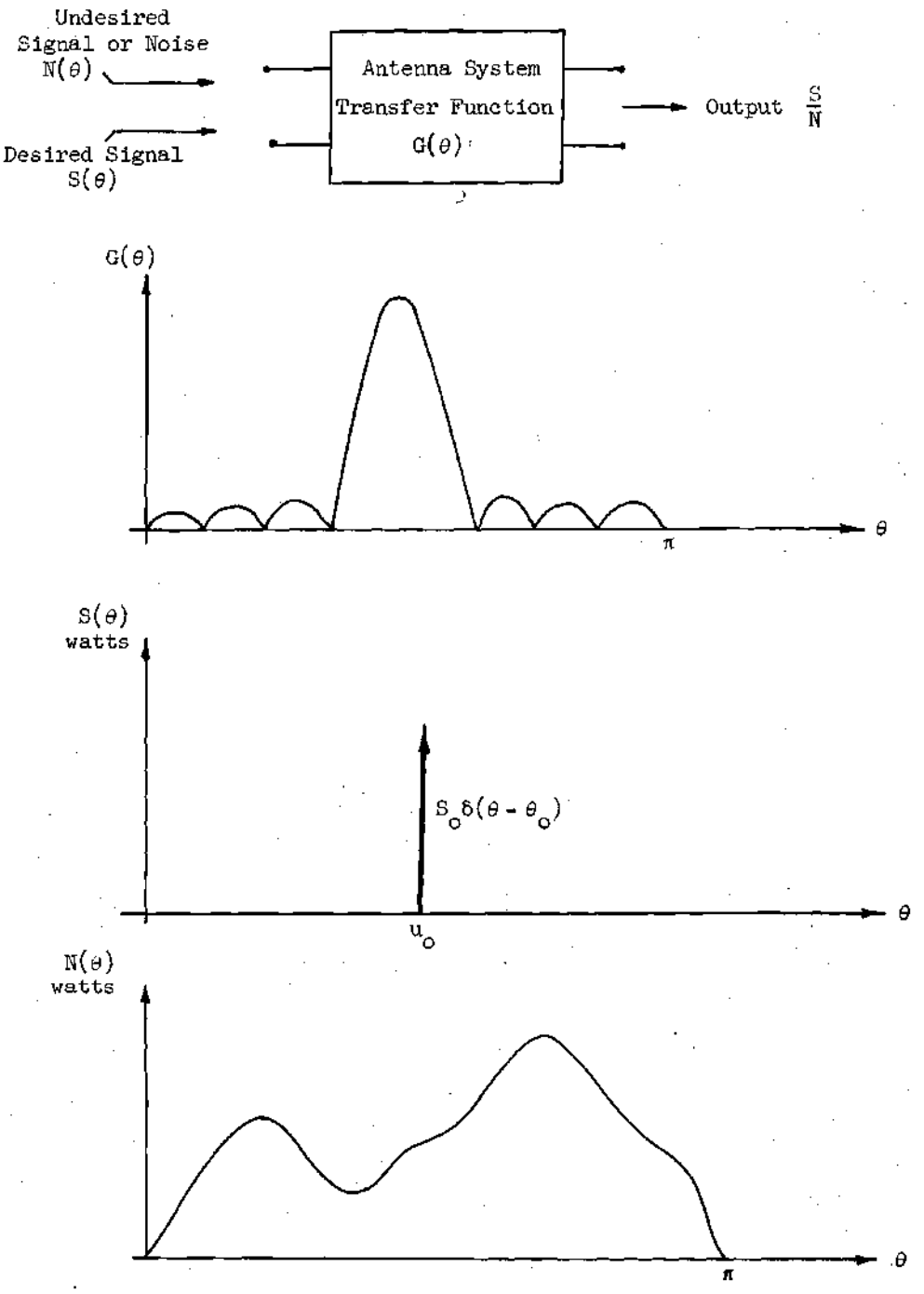

Fig. 3.3 Typical Signal and Noise Power Spatial Distributions.

as the dual of the matched filter problem where the angular coordinate θ is the dual of the frequency variable ω. The noise environment is $N(\theta)$ as illustrated, and the spatial distribution of the desired signal is given by

$$S(\theta,\Phi) = S_o \, \delta(\theta-\theta_o) \, \delta(\Phi-\Phi_o) \tag{3.5}$$

The net signal power out of the array is given by the product of the power pattern $G(\theta)$ and $S(\theta,\Phi)$, that is,

$$S = S_o \, G(\theta_o) \tag{3.6}$$

The noise power out of the array terminals will be given by

$$N = \int_{\Omega} G(\theta) \, N(\theta) \, d\Omega \tag{3.7}$$

where $d\Omega$ is the differential element of solid angle. Since $d\Omega = \sin\theta \, d\theta d\Phi$, then,

$$N = \int_0^{2\pi} \int_0^{\pi} G(\theta) \, N(\theta) \, \sin\theta \, d\theta \, d\Phi \tag{3.8}$$

The output signal-to-noise ratio will then be given by

$$\frac{S}{N} = \frac{S_o G(\theta_o)}{\int_0^{\pi} \int_0^{2\pi} G(\theta) \, N(\theta) \, \sin\theta \, d\theta \, d\Phi} \tag{3.9}$$

However, since the integrand in the denominator is independent of Φ, this expression becomes

$$\frac{S}{N} = \frac{S_o}{2\pi} \frac{G(\theta_o)}{\int_o^\pi G(\theta)\, N(\theta)\, \sin\theta\, d\theta} \tag{3.10}$$

Since the functional to be maximized is a ratio, then no generality is lost by imposing the constraint

$$G(\theta_o) = K^2 \tag{3.11}$$

where K is an arbitrary non-zero constant. Subject to this constraint, the maximization of the signal-to-noise ratio is equivalent to the minimization of the noise power out of the array, i.e. the minimization of

$$N[G(\theta)] = \int_o^\pi G(\theta)\, N(\theta)\, \sin\theta\, d\theta \tag{3.12}$$

Application of the techniques of the calculus of variations yields only the trivial result since the integrand does not involve the derivative of $G(\theta)$ with respect to θ. The obvious, though unrealizable, solution is thus

$$G(\theta) = \begin{cases} K^2 , & \theta = \theta_o \\ 0 , & \theta \neq \theta_o \end{cases} \tag{3.13}$$

It is important to realize that the "true extremal" of the variational problem outlined above does not exist as a physically realizable

solution. This should not be unexpected since the array designer does not have complete latitude with regard to admissible $G(\theta)$. One is then required to resort to the direct methods of the calculus of variations, and in particular to the Ritz Method.

The Ritz Method for direct optimization of a functional is covered in several texts (38)-(39) on the calculus of variations; the reader is referred to these texts for a complete discussion. Essentially, the application of the technique for extremizing a functional of the form

$$N[E(\theta)] = \int_0^{\pi} E^2(\theta)\, N(\theta)\, \sin\theta\, d\theta \tag{3.14}$$

involves the choice of a sequence of specific component functions. The extremizing function $E(\theta)$ is then approximated by a linear combination of members of this sequence. For illustrative purposes, the sequence of functions

$$\{ W_1(\theta), W_2(\theta), \cdots, W_N(\theta), \cdots \} \tag{3.15}$$

are linearly combined to form a comparison function

$$E_N(\theta) = \sum_{i=1}^{N} \alpha_i W_i(\theta) \tag{3.16}$$

where α_i are constants, and the individual functions $W_i(\theta)$ may also contain adjustable parameters β_i which may influence the extremization process. When a specific $E_N(\theta)$ is substituted into the functional, the integration may, in principle at least, be carried out with the result

that the functional is converted to a more conventional function of the adjustable parameters α_i and whatever additional parameters β_i are included in the component functions $W_i(\theta)$. Thus

$$N[E_N(\theta)] \Longrightarrow f(\alpha_1,\alpha_2,\cdots,\alpha_N,\ \beta_1,\cdots,\beta_N) \tag{3.17}$$

It is clear that the extrema of f lie at the vector $(\hat{\alpha}_1,\cdots,\hat{\alpha}_N,$ $\hat{\beta}_1,\cdots,\hat{\beta}_N)$ which satisfies the set of equations resulting from setting

$$\begin{aligned} \frac{\partial f}{\partial \alpha_i} &= 0 \\ & \qquad i = 1,\cdots,N \\ \frac{\partial f}{\partial \beta_i} &= 0 \end{aligned} \tag{3.18}$$

This set of equations will, unfortunately, be nonlinear in many physical situations and their solution may be a difficult matter.

In many problems, the choice of the sequence of component functions $W_i(\theta)$ is not greatly restricted. In the particular case of the optimum synthesis of linear arrays, however, one is restricted to a specific set of component functions, the mathematical form of which is dependent upon the type of array being synthesized. As an example, for a symmetrically excited broadside array, these functions are

$$\begin{aligned} W_o(\theta) &= 1 \\ W_2(\theta) &= \cos(\beta x_1 \cos\theta) \\ &\vdots \qquad\qquad \vdots \\ W_i(\theta) &= \cos(\beta x_i \cos\theta) \\ &\vdots \qquad\qquad \vdots \end{aligned} \tag{3.19}$$

These component functions combine in a sum to form the array factor of an array of (2M + 1) elements.

$$E_M(\theta) = a_o + 2\sum_{m=1}^{M} a_m \cos(\beta x_m \cos\theta) \qquad (3.20)$$

Here again, $(a_o,\cdots,a_M)$ are the excitation coefficients and $(x_1,\cdots,x_M)$ describe the radiator positions. For an array with complex excitations, the set of component functions is somewhat more complicated, as indicated by expressions (2.12) and (2.13) of the previous chapter.

Synthesis of Broadside Symmetrically Excited Arrays of Isotropic Point Sources

This section considers the synthesis of broadside arrays for optimum signal-to-noise ratio. Broadside arrays are those arrays whose excitations are such that the main beam of the radiation pattern is in the direction normal to the array axis, and the radiation pattern is symmetrical about the broadside direction. It might seem that, instead of discussing a specialized type of array initially, the analysis of the most general type of array should be undertaken. The choice of the order of discussion below was taken because the remakrs concerning these arrays lead quite logically to analysis of arrays with complex excitations and asymmetric patterns.

The radiation pattern of a broadside array is given by the expression

$$E_M(\theta) = a_o + 2\sum_{m=1}^{M} a_m \cos(\beta x_m \cos\theta) \qquad (3.21)$$

where excitation coefficients (a_o, $\cdots$, a_M) are purely real numbers. The power pattern is proportional to the square of the radiation pattern.

$$G_M(\theta) = \left\{E_M(\theta)\right\}^2 \tag{3.22}$$

The signal in this case is assumed to be incident from the broadside direction also and is given by

$$S(\theta,\varphi) = S_o\, \delta(\theta - \tfrac{\pi}{2})\, \delta(\varphi - \varphi_o) \tag{3.23}$$

The net signal power out of the array is given by

$$S = \int_{\Omega} S(\theta,\varphi)\, G(\theta,\varphi)\, d\Omega \tag{3.24}$$

which upon substitution of $d\Omega = \sin\theta\, d\theta\, d\varphi$ becomes

$$S = \int_o^{\pi} \int_o^{2\pi} S(\theta,\varphi)\, G(\theta,\varphi)\, \sin\theta\, d\varphi\, d\theta \tag{3.25}$$

Substituting the spatial characteristics of the signal results in the expression

$$S = S_o\, G(\tfrac{\pi}{2}) = S_o(a_o + 2\sum_{i=1}^{M} a_i)^2 \tag{3.26}$$

The net noise power out of the array is given by

$$N = \int_{\Omega} G(\theta,\varphi)\, N(\theta,\varphi)\, d\Omega \tag{3.27}$$

which in turn becomes

$$N = \int_0^{\pi} \int_0^{2\pi} G(\theta)\, N(\theta) \sin\theta \, d\theta \, d\varphi$$

$$= 2\pi \int_0^{\pi} G(\theta)\, N(\theta) \sin\theta \, d\theta \qquad (3.28)$$

The expression for the signal-to-noise ratio may be written as

$$\frac{S}{N} = \frac{S_o}{2\pi} \frac{\left[a_o + 2\sum_{i=1}^{M} a_i\right]^2}{\int_0^{\pi} G(\theta)\, N(\theta) \sin\theta \, d\theta} \qquad (3.29)$$

where

$$G(\theta) = \left[a_o + 2\sum_{m=1}^{M} a_m \cos\left(\beta x_m \cos\theta\right)\right]^2$$

Expression (3.29) is the general expression for the signal-to-noise ratio of a broadside symmetrically excited array with arbitrary symmetrical element placement along the array axis. It is necessary and convenient at this point in the analysis to introduce the constraint that the elements be equally spaced, that is,

$$x_i = id \qquad (3.30)$$

where d is the interelement spacing in meters. Subject to this constraint of equal spacings, the power pattern expression becomes

$$G(\theta) = \left[a_o + 2 \sum_{m=1}^{M} a_m \cos (m\beta d \cos \theta) \right]^2 \qquad (3.31)$$

With a moderate amount of algebra it is possible to expand $G(\theta)$, which results in the expression

$$G(\theta) = a_o^2 + 2 \sum_{i=1}^{M} a_i^2 + 2 \sum_{i=1}^{M} a_i^2 \cos (2i\beta d \cos \theta)$$

$$+ 4 a_o \sum_{i=1}^{M} a_i \cos (i\beta d \cos \theta) \qquad (3.32)$$

$$+ 4 \sum_{i=1}^{M} \sum_{j=i+1}^{M} a_i a_j \left[\cos ([i+j] \beta d \cos \theta) + \cos ([i-j] \beta d \cos \theta) \right]$$

Proceeding next to the evaluation of the integral in the expression for the noise power, it is possible after substitution of the above expression to write

$$N = \int_o^{\pi} G(\theta) N(\theta) \sin \theta \, d\theta$$

$$N = a_o^2 \int_o^\pi N(\theta) \sin\theta \, d\theta$$

$$+ 2 \sum_{i=1}^{M} a_i^2 \int_o^\pi [1 + \cos(2i\beta d \cos\theta)] N(\theta) \sin\theta \, d\theta$$

$$+ 4 a_o \sum_{i=1}^{M} a_i \int_o^\pi \cos(i\beta d \cos\theta) N(\theta) \sin\theta \, d\theta \qquad (3.33)$$

$$+ 4 \sum_{i=1}^{M} \sum_{j=i+1}^{M} a_i a_j \int_o^\pi \{\cos([i+j]\beta d \cos\theta) + \cos([i-j]\beta d \cos\theta)\} N(\theta) \sin\theta \, d\theta$$

This equation may be written in more convenient form using matrix notation. The equation is a quadratic form and in matrix notation is

$$N = \bar{a}^T Q \bar{a} \qquad (3.34)$$

where $\bar{a}$ is a vector composed of the excitation coefficients, and $\bar{a}^T$ denotes the transpose of $\bar{a}$

$$\bar{a}^T = [a_o \; a_1 \; \cdots \; a_M] \qquad (3.35)$$

The square matrix Q is a real symmetric matrix of order (M + 1) whose elements are given by the following expressions.

$$Q = \begin{bmatrix} q_{00} & q_{01} & \cdots & q_{0M} \\ q_{10} & q_{11} & \cdots & q_{1M} \\ \vdots & \vdots & & \vdots \\ q_{M0} & q_{M1} & & q_{MM} \end{bmatrix} \qquad (3.36)$$

The elements are clearly functions of the interelement spacings.

$$q_{oo} = \int_o^{\pi} N(\theta) \sin\theta \, d\theta$$

$$q_{ii} = 2\int_o^{\pi} [1 + \cos(2i\beta d \cos\theta)] N(\theta) \sin\theta \, d\theta \qquad (3.37)$$

$$q_{oi} = q_{io} = 2\int_o^{\pi} N(\theta) \cos(i\beta d \cos\theta) \sin\theta \, d\theta$$

$$q_{ij} = q_{ij} = 2\int_o^{\pi} N(\theta) \{\cos([i+j]\beta d \cos\theta) + \cos([i-j]\beta d \cos\theta)\} \sin\theta \, d\theta$$

$$i = 1, 2, \ldots, M \qquad j = i + 1, \ldots, M$$

The expression for the net signal power (3.26) may be similarly written

$$S = \bar{a}^T C \bar{a} \qquad (3.38)$$

where C is real symmetric and of order (M + 1). From expression (3.26), C becomes

$$C = \begin{bmatrix} 1 & 2 & 2 & \cdots & 2 \\ 2 & 4 & 4 & \cdots & 4 \\ 2 & 4 & 4 & \cdots & 4 \\ \vdots & \vdots & \vdots & & \vdots \\ 2 & 4 & 4 & \cdots & 4 \end{bmatrix} \qquad (3.39)$$

Since the signal-to-noise ratio is the quotient of two quadratic functions in the vector $\bar{a}$, it is necessary to impose an equality constraint on the components of $\bar{a}$. This is clear from equation (3.29). If the vector

$$\hat{\bar{a}}^T = [\hat{a}_o \; \hat{a}_1 \; \ldots \; \hat{a}_M] \tag{3.40}$$

optimizes the signal-to-noise ratio, then so does the vector

$$K\hat{\bar{a}}^T = [K\hat{a}_o \; K\hat{a}_1 \; \ldots \; K\hat{a}_M] \tag{3.41}$$

where K is an arbitrary non-zero multiplicative constant. This equality constraint is expression (3.11) where, for convenience, K has been set equal to unity, and is written

$$S = \bar{a}^T C \bar{a} = 1 \tag{3.42}$$

The optimization problem is now recognized as the generalized eigenvalue problem. Using the method of Lagrange multipliers, the auxiliary function

$$H(\bar{a},d,\lambda) = N(\bar{a},d) - \frac{1}{\lambda} S(\bar{a},d) \tag{3.43}$$

is formed. The stationary points of H lie at the solution of the set of equations

$$\frac{\partial H}{\partial a_i} = 0, \quad i = 0, 1, \ldots, M \tag{3.44}$$

which results in the homogeneous equation

$$C\,\bar{a} = \lambda Q\,\bar{a} \tag{3.45}$$

Apart from the trivial solution, this problem has (M + 1) solutions which satisfy the determinantal equation

$$|C - \lambda Q| = 0 \tag{3.46}$$

It is, of course, mathematically possible to determine the vectors which satisfy (3.46). Computationally, it is convenient to effect certain transformations of coordinates which reduce the solution of the generalized eigenvalue problem (3.45) to an elementary eigenvalue problem of the form

$$C''\bar{a}'' = \lambda I\,\bar{a}'' \tag{3.47}$$

The transformation sought is thus one which converts Q of (3.45) to the identity matrix I when $\bar{a}$ is transformed to $\bar{a}''$. The construction of this transformation is relatively straightforward and is adequately covered in texts by Hildebrand (40) and Braae (41).

The first step in the transformation of (3.45) into the form (3.47) is the diagonalization of matrix Q. Let the required transformation be denoted T_1, where

$$\bar{a} = T_2\,\bar{a}' \tag{3.48}$$

If T_1 is composed of columns made up of the unit normalized eigenvectors of Q, then

$$Q' = T_1^T \, Q \, T_1 \tag{3.49}$$

is a diagonal matrix whose elements are the eigenvalues of Q, that is,

$$Q' = \begin{bmatrix} \lambda_0 & & & & \\ & \lambda_1 & & & \\ & & \lambda_2 & & \\ & & & \ddots & \\ & & & & \lambda_M \end{bmatrix}$$

Having effected this transformation of coordinates in the expression (3.34), it is obviously necessary to transform the equality constraint (3.42) accordingly.

$$\begin{aligned} S &= \bar{a}'^T (T_1^T \, C \, T_1) \, \bar{a}' = 1 \\ &= \bar{a}'^T C' \, \bar{a}' = 1 \end{aligned} \tag{3.51}$$

A second linear transformation of coordinates is not performed in expression (3.50) such that the matrix Q', when modified by this transformation, becomes the identity matrix. This second transformation

$$\bar{a}' = T_2 \, \bar{a}'' \tag{3.52}$$

is obvious since Q' is a diagonal matrix.

Clearly, T_2 is constructed as below:

$$T_2 = \begin{bmatrix} \frac{1}{\sqrt{q'_{oo}}} & & & \\ & \frac{1}{\sqrt{q'_{11}}} & & \\ & & \ddots & \\ & & & \frac{1}{\sqrt{q'_{MM}}} \end{bmatrix} \tag{3.53}$$

Application of this second transformation yields

$$\begin{aligned} N &= \bar{a}''^T (T_2^T Q' T_2) \bar{a}'' \\ &= \bar{a}''^T Q'' \bar{a}'' = \bar{a}''^T I \bar{a}'' \end{aligned} \tag{3.54}$$

Transformation of the equality constraint results in the expressions

$$\begin{aligned} S &= \bar{a}''^T (T_2^T C' T_2) \bar{a}'' = 1 \\ &= \bar{a}''^T C'' \bar{a}'' = 1 \end{aligned} \tag{3.55}$$

where C" is real symmetric and of order M + 1.

To accomplish the minimization of (3.54) subject to constraint (3.55), the Lagrange multiplier method is employed. Writing the multiplier as $(-1/\lambda)$, the auxiliary function $H(\bar{a}'', \lambda)$ is formed as shown below

$$H(\bar{a}'', \lambda) = N(\bar{a}'') - \frac{1}{\lambda} S(\bar{a}'') \tag{3.56}$$

A necessary condition that $H(\bar{a}'',\lambda)$ be stationary with respect to coordinates $\bar{a}''$ is that the partial derivatives of $H(\bar{a}'',\lambda)$ with respect to individual components of $\bar{a}''$ vanish simultaneously.

Setting $\frac{\partial H}{\partial a''_i} = 0$ for $i = 0, \ldots, M$ yields the set of linear equations

$$C'' \bar{a}'' = \lambda I \bar{a}'' \tag{3.57}$$

when I denotes the identity matrix. The solution of this problem is then to determine the eigenvectors of the transformed constraint matrix C". If C" is real symmetric of rank (M + 1), then there are (M + 1) linearly independent solutions to the eigenvalue problem. Since the objective function (3.54) is quadratic, only one of these solutions corresponds to the minimum value of (3.54). This required solution is specified to within a common multiplicative constant which is determined using equality constraint (3.55).

It is then completely straightforward to obtain the actual solution $\bar{a}$ using transformed solution $\bar{a}''$ and the transformations T_1 and T_2 from the expressions

$$\bar{a}' = T_2 \bar{a}'' \tag{3.58}$$

and

$$\bar{a} = T_1 T_2 \bar{a}'' \tag{3.59}$$

Examples on the Synthesis of Broadside Arrays

In any illustration of the application of a specific synthesis method in the design of radiating systems, the choice of a set of examples

is moderately difficult. Clearly, no single example situation has all of the characteristics necessary for the proper illustration of a synthesis procedure. The requirements for conciseness are obvious; yet, it is also necessary to include a sufficient number of practically meaningful situations so that worthwhile results concerning the general behavior of the class of arrays being considered may be obtained. Specific case studies are thus required with due care being exercised in the choice of examples so that no physically important cases are omitted.

It should be noted at the outset that all of the noise distributions considered in this section are specified in closed mathematical form. This is done only as a matter of computational convenience; in an actual application involving a measured noise power distribution, a point-by-point specification is the usual case. In such a situation, it would simply be necessary to employ a proper point-by-point numerical integration procedure, because the synthesis method is not limited to the class of noise distributions which may be conveniently specified in simple mathematical form.

A second characteristic of the chosen noise distributions is that all are symmetrical about the broadside direction. It would be superfluous to examine an asymmetrical noise distribution, since a symmetrically excited broadside array may only discriminate against those distributions which are symmetrical, or even about the broadside direction.

Example I

The noise spatial distribution chosen for this example is one in which the maximum noise power is incoming from the broadside direction and tapers sinusoidally toward the ends of the array. The mathematical

specification is

$$N(\theta) = N_o \cos\left(\frac{\pi}{2}\cos\theta\right) \tag{3.60}$$

A polar plot of the distribution is shown in Figure 3.4.

As indicated in the preceding development, the procedure is somewhat involved numerically. For brevity in presentation, the matrices will be included specifically for Example I only. It is felt that this coverage will suffice since intermediate numerical steps are of secondary interest, while inclusion of them in the remaining examples would require that this section be of prohibitive length. Furthermore, in order that matrix presentation be facilitated, numerical results are included for a five element array only (M = 2), and for a spacing between elements of one half wavelength.

For the specified noise distribution,

$$Q = \begin{bmatrix} 2.0000 & 1.3333 & -0.2667 \\ 1.3333 & 3.7333 & -1.4476 \\ -0.2667 & 1.4476 & 3.9365 \end{bmatrix} \tag{3.61}$$

The first transformation T_1, is made up using the unit normalized eigenvalues of Q as columns.

$$T_1 = \begin{bmatrix} 0.77206 & 0.22933 & -0.49274 \\ -0.54217 & 0.72431 & -0.42595 \\ 0.33164 & 0.65022 & 0.68355 \end{bmatrix} \tag{3.62}$$

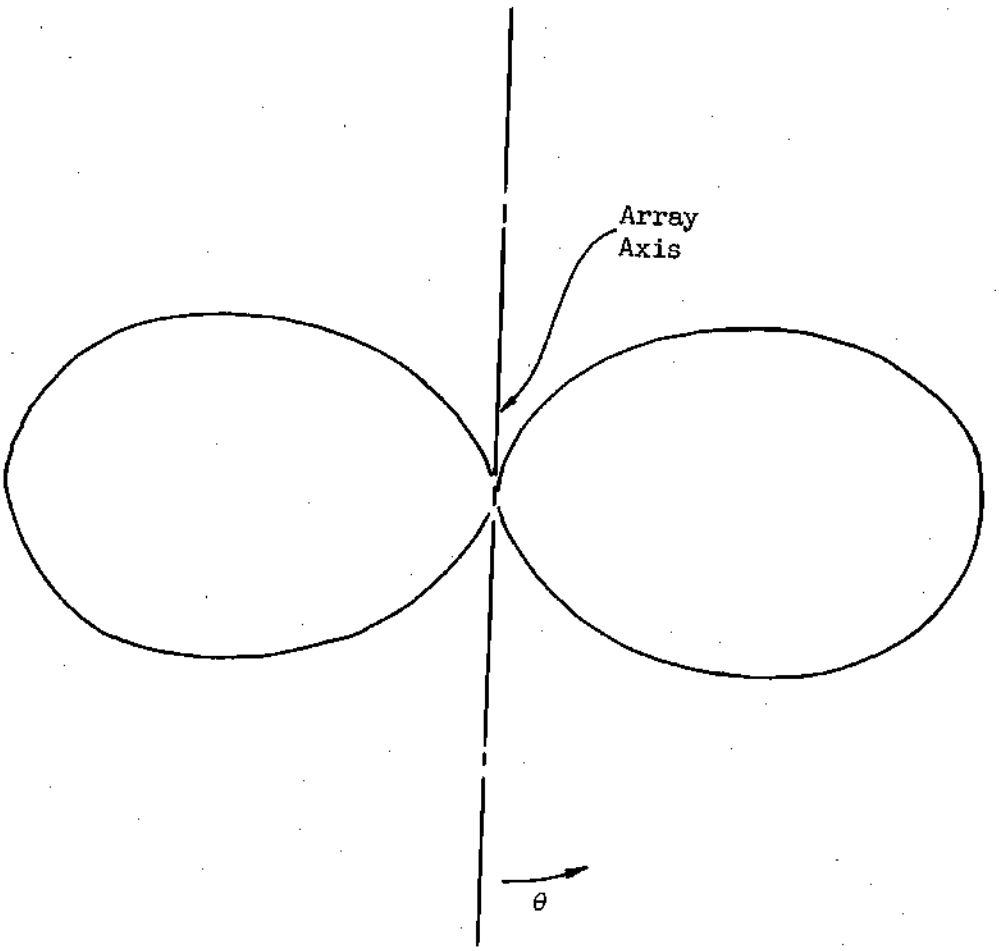

Fig. 3.4 Noise Distribution - Example I.

Application of this transformation yields

$$Q' = T_1^T \, Q \, T_1 = \begin{bmatrix} 0.94914 & 0.0000 & 0.0000 \\ 0.0000 & 5.4550 & 0.0000 \\ 0.0000 & 0.0000 & 3.2657 \end{bmatrix} \tag{3.63}$$

The second linear transformation to be employed is formed using expression (3.53).

$$T_2 = \begin{bmatrix} 1.0264 & 0.0000 & 0.0000 \\ 0.0000 & 0.42816 & 0.0000 \\ 0.0000 & 0.0000 & 0.5531 \end{bmatrix} \tag{3.64}$$

Application of this second transformation reduces Q' to the unit matrix. The constraint matrix C is given by (3.39), which is reproduced below for convenience.

$$C = \begin{bmatrix} 1 & 2 & 2 \\ 2 & 4 & 4 \\ 2 & 4 & 4 \end{bmatrix} \tag{3.65}$$

Transformation of this matrix using both T_1 and T_2 yields

$$C'' = \begin{bmatrix} 0.12981 & 0.45944 & -0.1546 \\ 0.45944 & 1.6262 & -0.05472 \\ -0.01546 & -0.05472 & 0.00184 \end{bmatrix} \tag{3.66}$$

The eignevectors of this matrix are the following vectors.

$$\begin{bmatrix} 0.96233 \\ -0.27189 \\ 0.0000 \end{bmatrix} \quad \begin{bmatrix} 0.27174 \\ 0.96182 \\ -0.032363 \end{bmatrix} \quad \begin{bmatrix} 0.008799 \\ 0.031144 \\ 0.99948 \end{bmatrix} \tag{3.67}$$

Of these three eigenvectors, the first and third yield nulls in the power pattern at the broadside direction, and consequently do not represent the required solution. After applying the appropriate transformation to the second eigenvector using

$$\hat{\hat{a}} = T_1 T_2 \hat{\hat{a}}'' \quad , \tag{3.68}$$

the vector of excitations for the optimum array is obtained.

$$\hat{\hat{a}} = \begin{bmatrix} 0.24167 \\ 0.11667 \\ 0.26250 \end{bmatrix} \tag{3.70}$$

The constraint

$$\hat{\underline{a}}^T C \hat{\underline{a}} = 1 \qquad (3.71)$$

is satisfied by (3.70). The power pattern for an array with this excitation is illustrated in Figure 3.5. For convenience of the reader, the noise distribution is illustrated on the same diagram.

Continuing with the five element example, it is interesting to examine the effect of varying the constant interelement spacing d upon the signal-to-noise ratio. Figure 3.6 illustrates graphically the results of letting d range from 0.2λ up to 2.0λ. The increase in signal-to-noise ratio is monotonic to a spacing of approximately 0.95λ after which a marked decrease is to be noted. The improvement may be attributed directly to the increase in aperture, while the decrease in signal-to-noise ratio beyond a spacing of 1.0λ is caused by the formation of secondary beams. The effects of the secondary maxima are not as pronounced as in the following two examples since the noise distribution has small values in the angular sector around the endfire ($\theta = 0$ and $\theta = \pi$) directions. Figure 3.7 illustrates the power pattern for the optimum array with an interelement spacing of 0.95 wavelengths.

A complete specification of the excitation vector for each of the spacing values of Figure 3.6 is shown in Figure 3.8. These curves indicate the individual element amplitudes as a fraction of the center element's excitation. The tendency of the array to be uniformly excited for larger values of interelement spacings is a consequence of the broadside oriented noise distribution. It is well known that a uniformly excited array yields a narrower beam than one with a decreasing amplitude taper toward the outer elements. For the noise distribution of

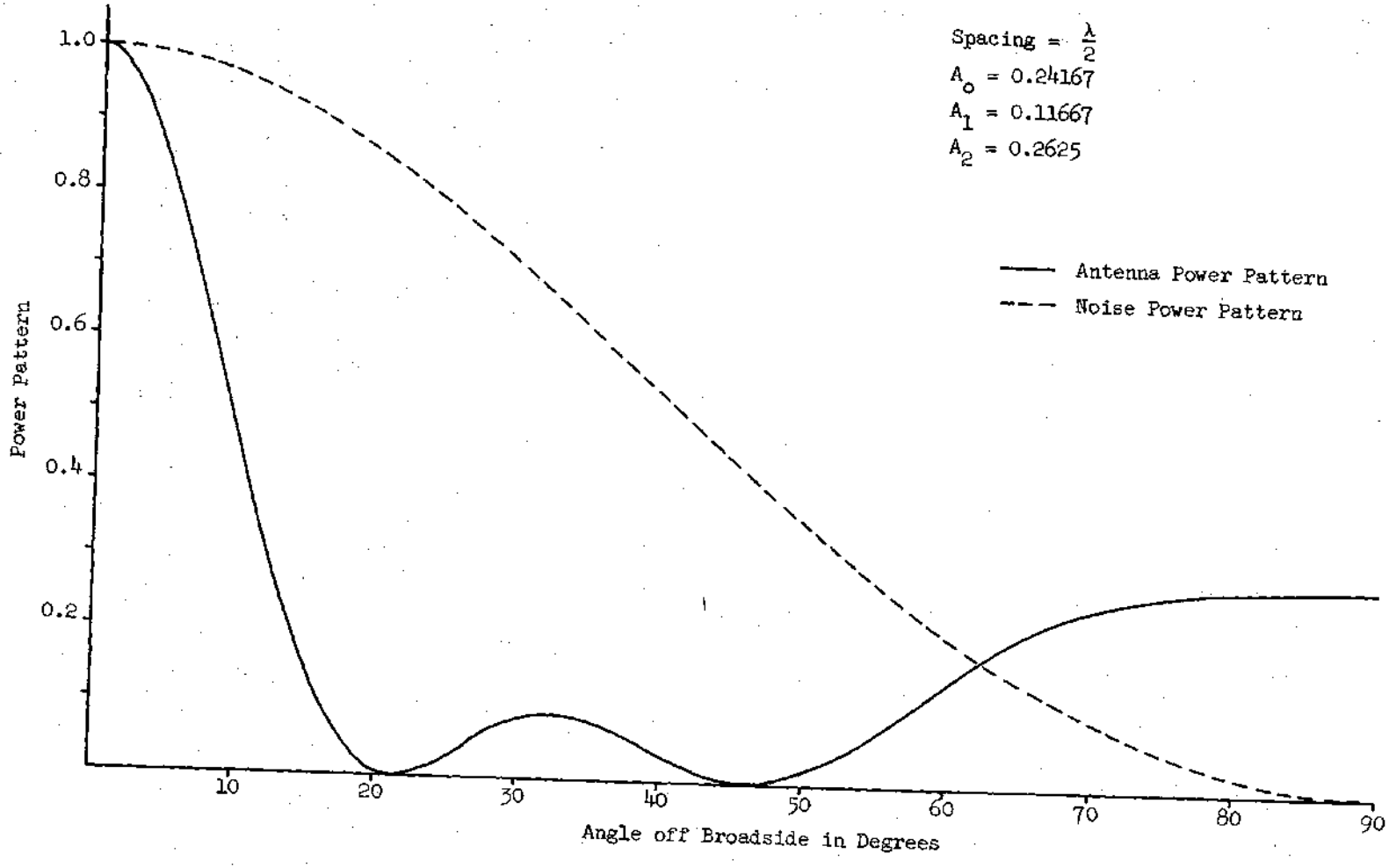

Fig. 3.5 Power Pattern for Five Element Optimum Array in Noise Environment - Example I.

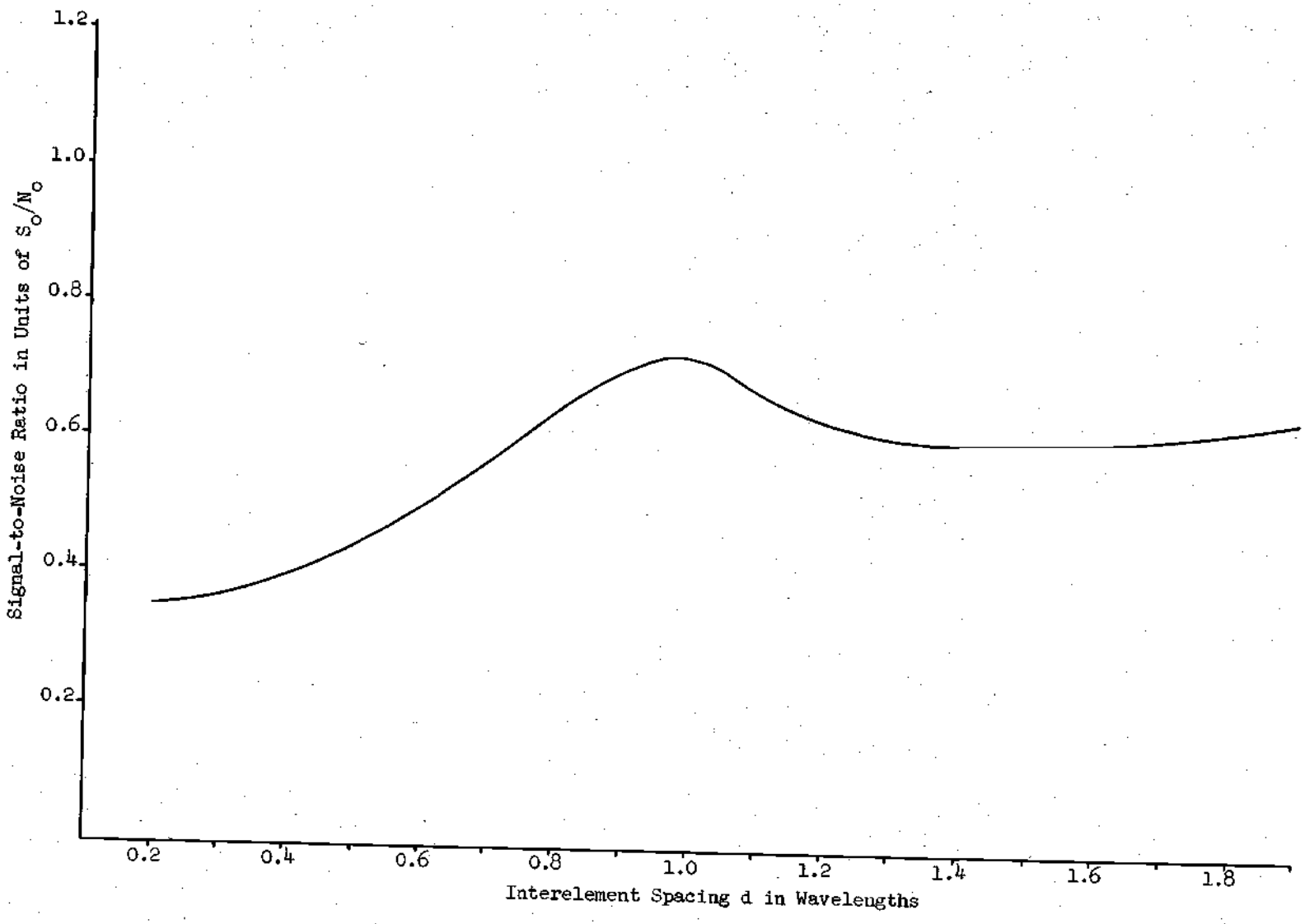

Fig. 3.6 Performance of Five Element Array in Noise Environment - Example I.

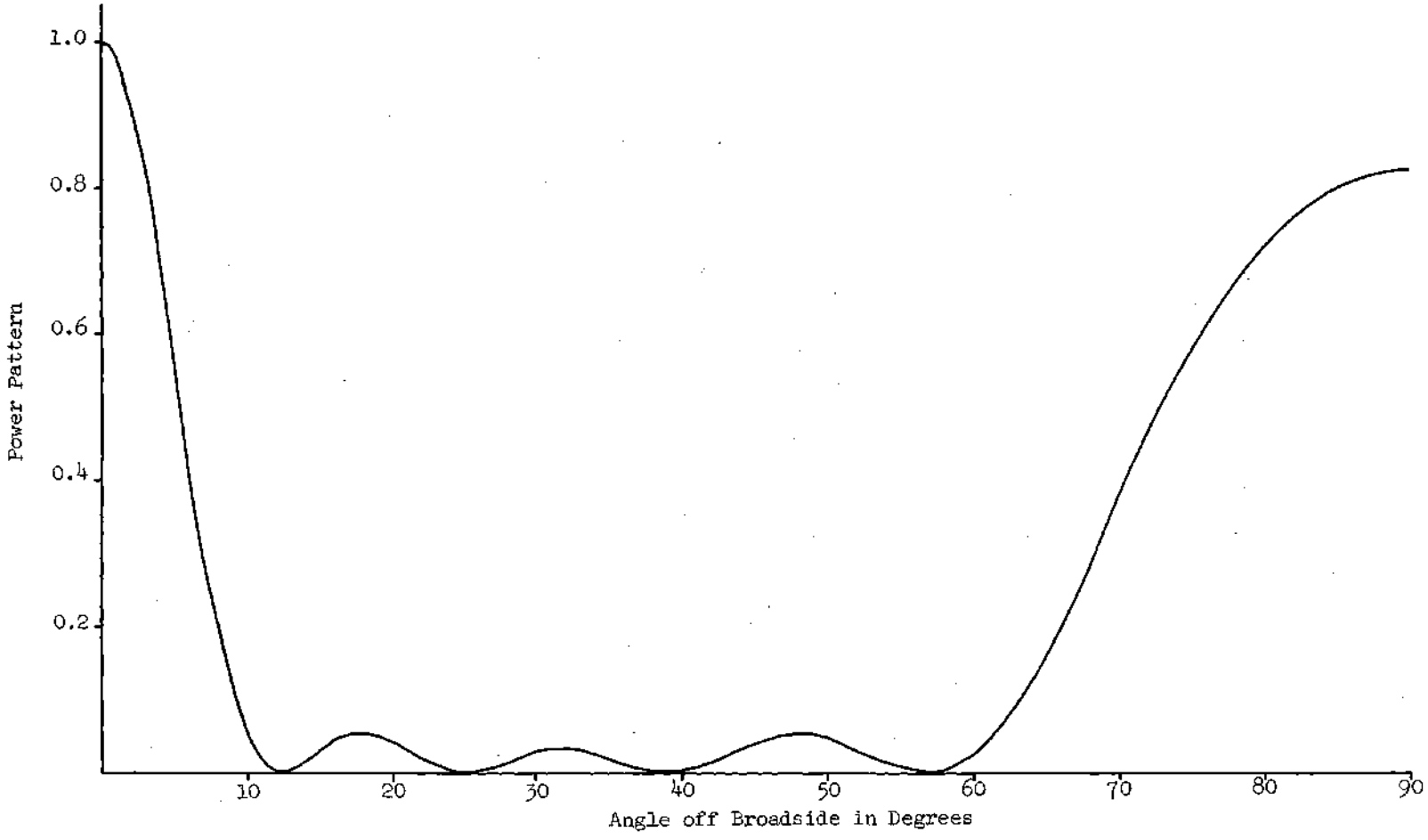

Fig. 3.7 Power Pattern of Optimum Five Element Equally Spaced Array for Spacing of 0.95 λ - Example I.

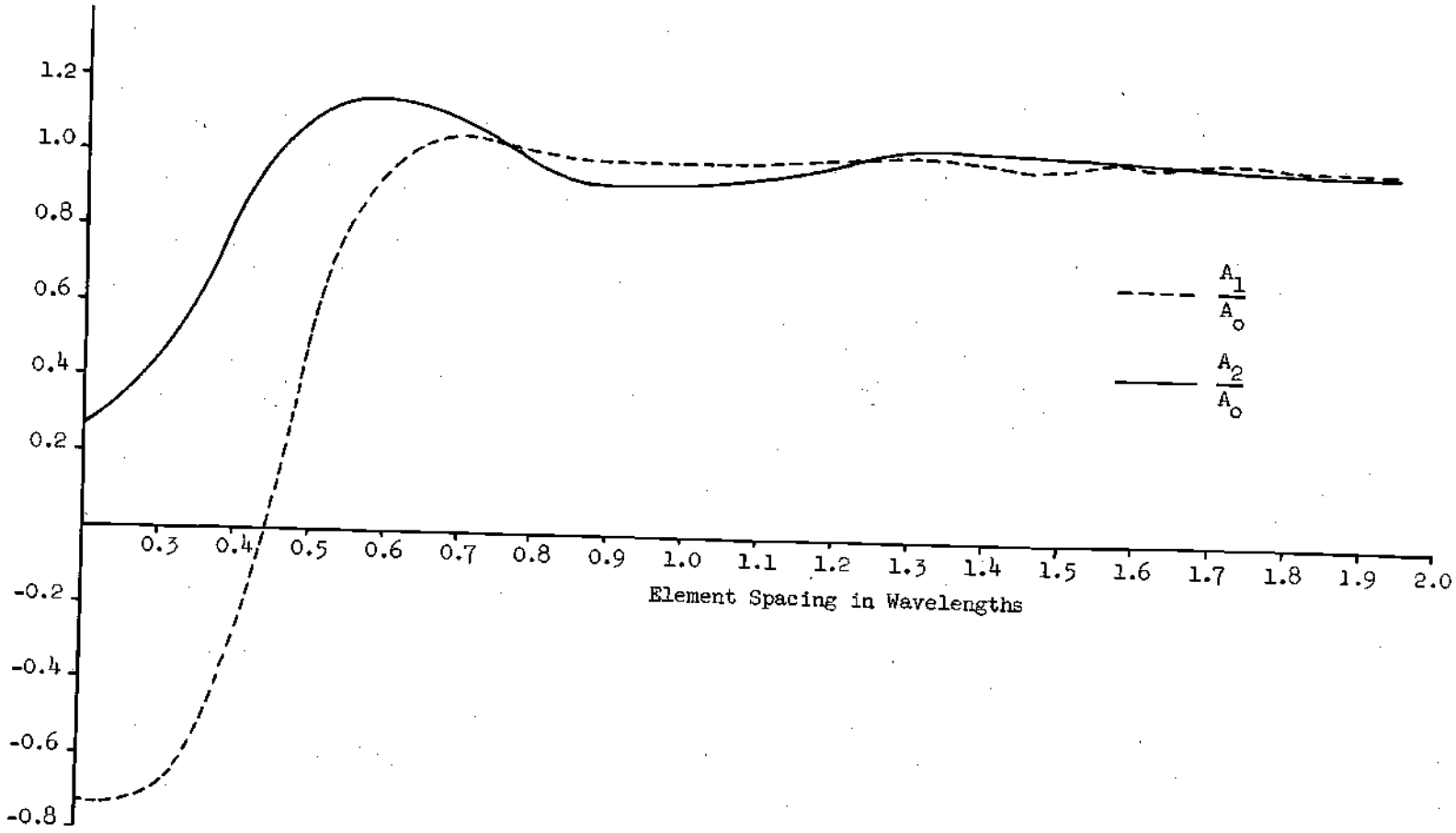

Fig. 3.8 Amplitude Distribution for Optimum Five Element Equally Spaced Array in Noise Environment - Example I.

this example, a narrow main beam is of more importance than low sidelobes since the majority of the noise power input to the array is in the angular sector near broadside.

A final characteristic of this example which is of fundamental importance is the behavior of the signal-to-noise ratio for a given spacing as a function of the number of elements in the array. Clearly, this is a prohibitive task if an attempt is made to include all spacings; however, adequate results are obtained in this example by choosing two representative spacing values. The reason for choosing a spacing of one half wavelength as one value is for purposes of comparison of array performance with that of Dolph-Chebyschev arrays. The choice of second value is taken as that spacing for which the signal-to-noise ratio for the five element array is maximum, in this case $d = 0.95\lambda$. The results of these calculations are shown in Figure 3.9.

The fact that the synthesis procedure in this example is optimum is demonstrated mathematically in the previous theoretical discussions. It is, however, instructive to compare results obtained using this synthesis technique with those where an array of equal size is designed by use of the Dolph-Chebyschev method. This comparison is illustrated graphically in Figure 3.10 where the signal-to-noise ratio for a five element Chebyschev array is plotted versus the design sidelobe level. The superiority of the developed synthesis technique is clearly indicated, although the lower values of sidelobe levels around -10 db yield close results for the Chebyschev array.

Example II

The noise spatial distribution for this example is specified

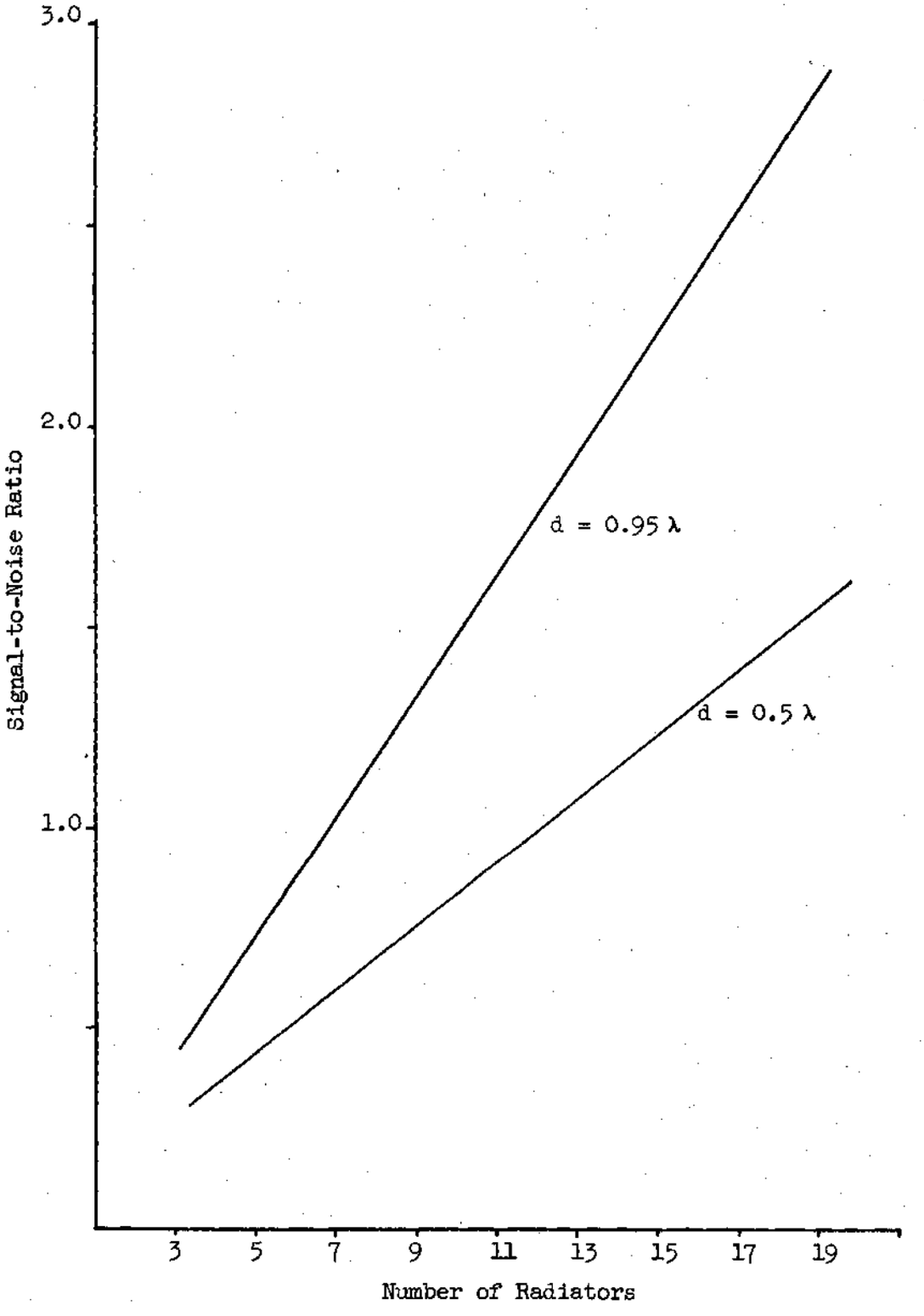

Fig. 3.9 Signal-To-Noise Ratio of Broadside Arrays as a Function of the Number of Radiators - Example I .

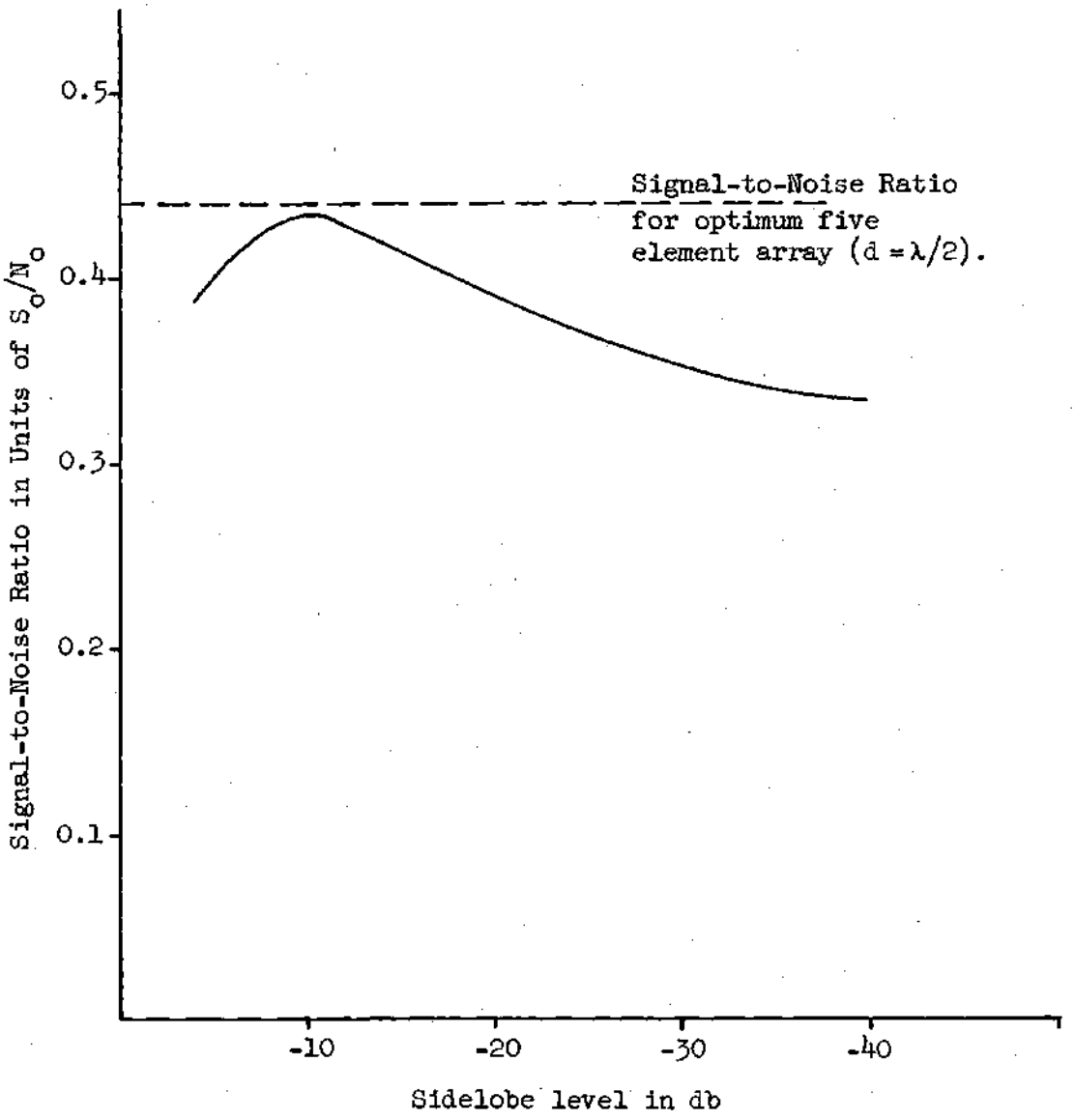

Fig. 3.10 Signal-to-Noise Ratio for Five Element Chebyschev Array - Example I.

mathematically by the expression

$$N(\theta) = N_o \left| \sin \left(\frac{\pi}{2} \cos \theta \right) \right| \qquad (3.72)$$

where N_o is a positive non-zero constant. This distribution represents a spatial characteristic which is maximum at the endfire directions ($\theta = 0$ and $\theta = \pi$) and tapers sinusoidally to a zero value at broadside ($\theta = \pi/2$). A polar plot is illustrated in Figure 3.11.

The power pattern for the optimum half wavelength spaced five element array is illustrated in Figure 3.12. Comparison of this pattern with Figure 3.5, the pattern of the optimum five element array for Example I shows the marked change in the sidelobe structure in the pattern of Figure 3.12, a change which is due to the fact that the largest noise input is from the endfire direction rather than broadside as in Example I. The excitation vector for this array is

$$\hat{\underline{a}}^T = [0.23438 \quad 0.21875 \quad 0.16406] \qquad (3.73)$$

which yields a signal-to-noise ratio of 1.94 S_o/N_o.

Examination of the effects of varying the interelement spacing of the five element array yields the information shown graphically in Figure 3.13. The effect of secondary maxima at spacings beyond approximately 0.9λ is quite pronounced, as should be expected, since the initial formation of the secondary beam occurs at the endfire bearing, the direction of maximum noise input. The maximum value of signal-to-noise ratio for the five element array is 4.06 S_o/N_o which occurs at a spacing of 0.8 wavelengths. The power pattern of this array is shown in Figure 3.14.

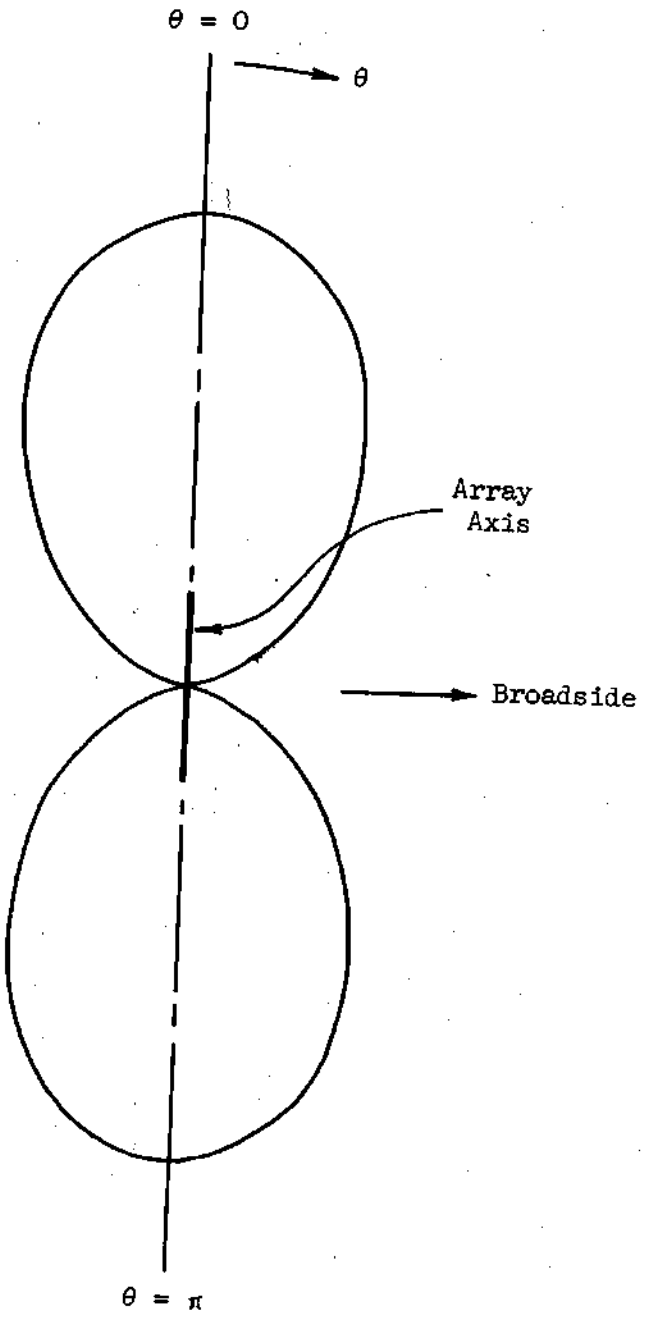

Fig. 3.11 Normalized Noise Distribution - Example II.

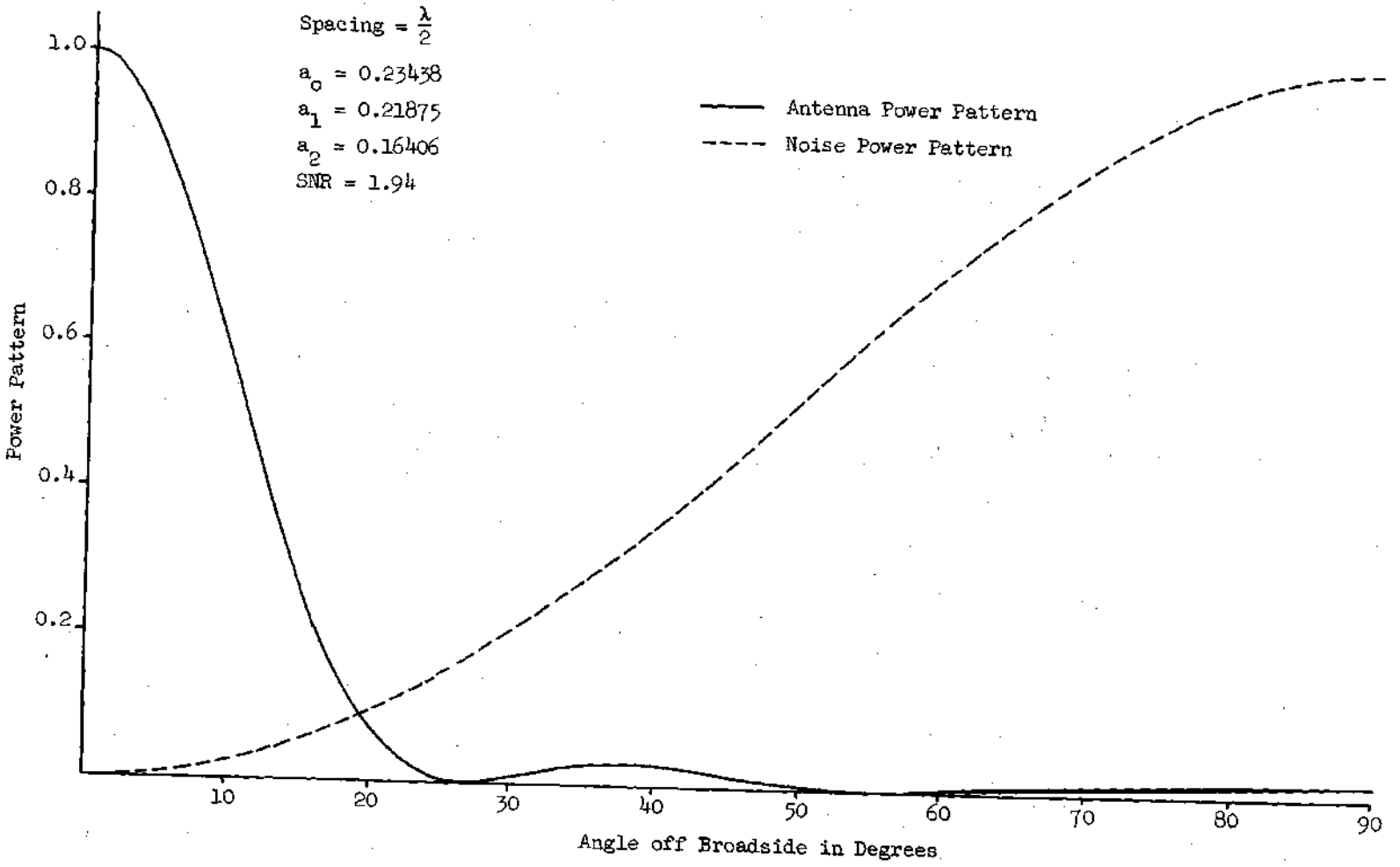

Fig. 3.12 Power Pattern for Optimum Five Element Array Noise Environment - Example II.

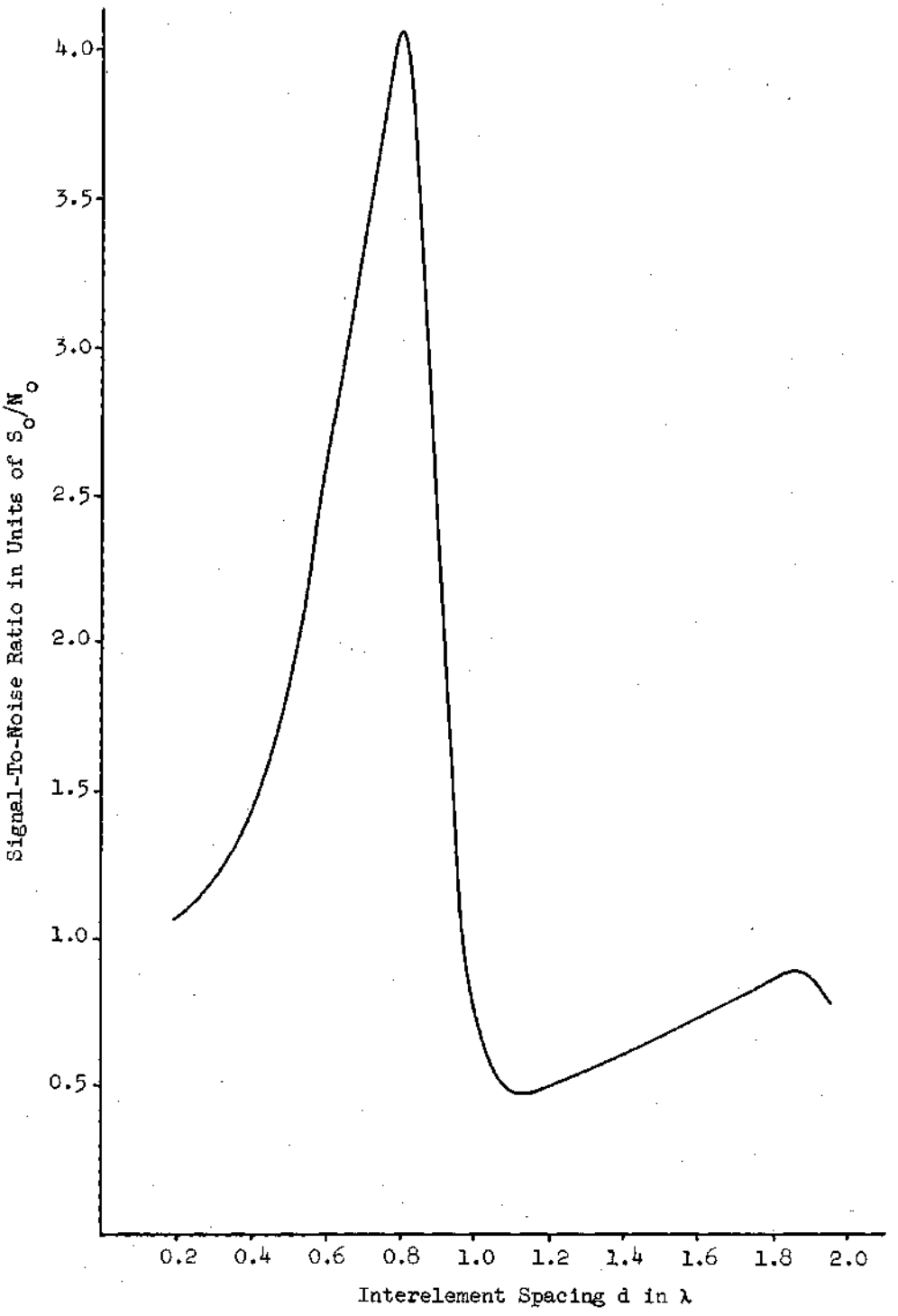

Fig. 3.13 Performance of Five Element Array in Noise Environment - Example II.

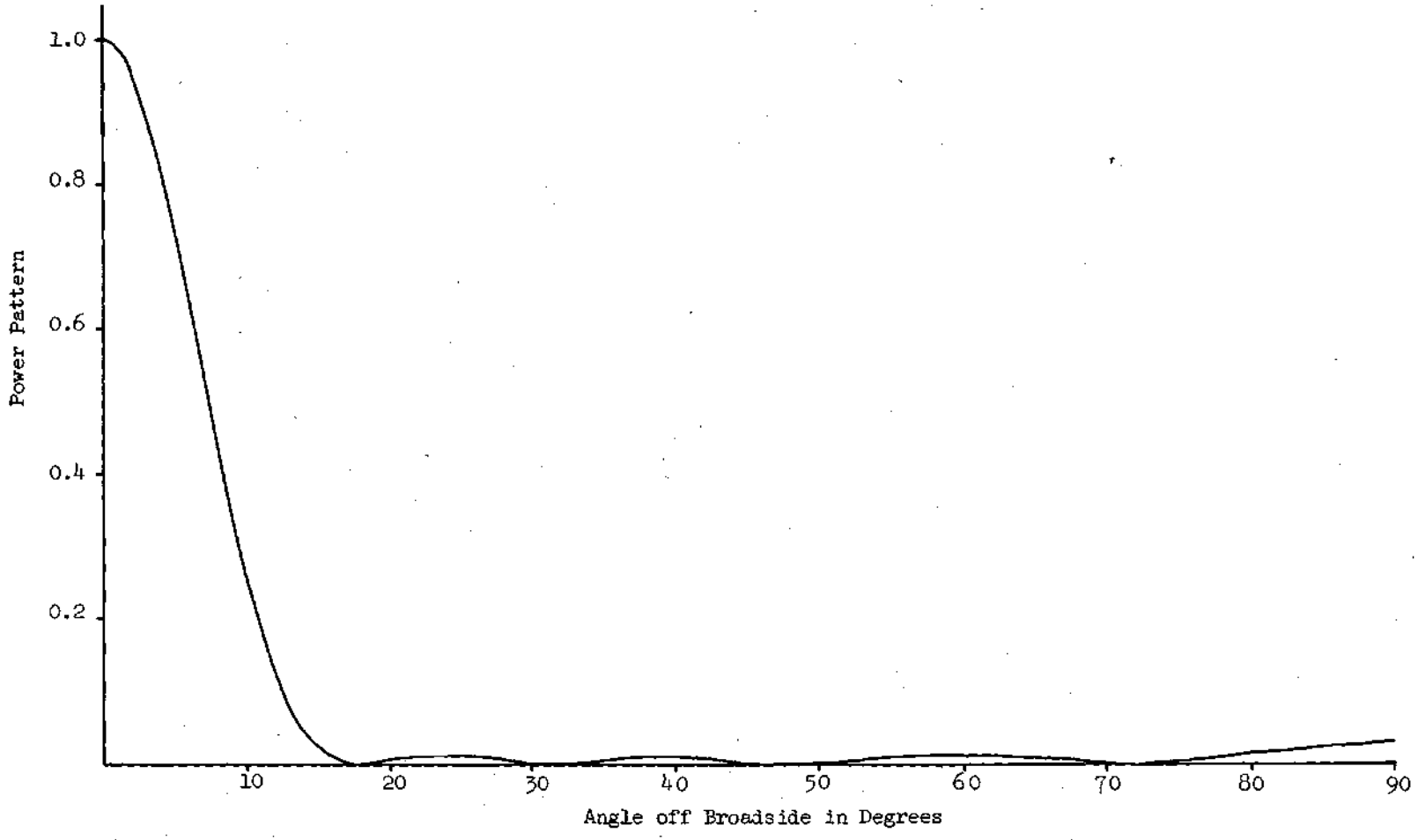

Fig. 3.14 Power Pattern of Optimum Five Element Equally Spaced Array for 0.8 Wavelength Interelement Spacing - Example II.

The specification of the excitation of the five element array as a function of the interelement spacing is shown in Figure 3.15. Variation of the element amplitudes is more marked and is due primarily to the nature of the noise distribution.

An increase in the number of elements results in a rapid increase in signal-to-noise ratio as indicated in Figure 3.16. In this example, as in the previous one, results are shown for spacings of one-half wavelength and that spacing for which the signal-to-noise ratio is maximum for the five element array.

A final comparison of the signal-to-noise ratio of the synthesized array and that of a Dolph-Chevyschev array is shown in Figure 3.17.

Example III

To complete the case studies of representative noise spatial distributions, the following example is considered. Whereas the noise distributions in Example I and II had maxima in the broadside and endfire directions respectively, the function

$$N(\theta) = N_o \left| \sin (\pi \cos \theta) \right| \tag{3.74}$$

has nulls in these directions. Figure 3.18 illustrates graphically this noise distribution.

Figure 3.19 shows the power pattern of an optimized five element array with an interelement spacing of one-half wavelength. The excitation vector for this array is

$$\hat{\underline{a}}^T = [0.2500 \quad 0.16667 \quad 0.20833] \tag{3.75}$$

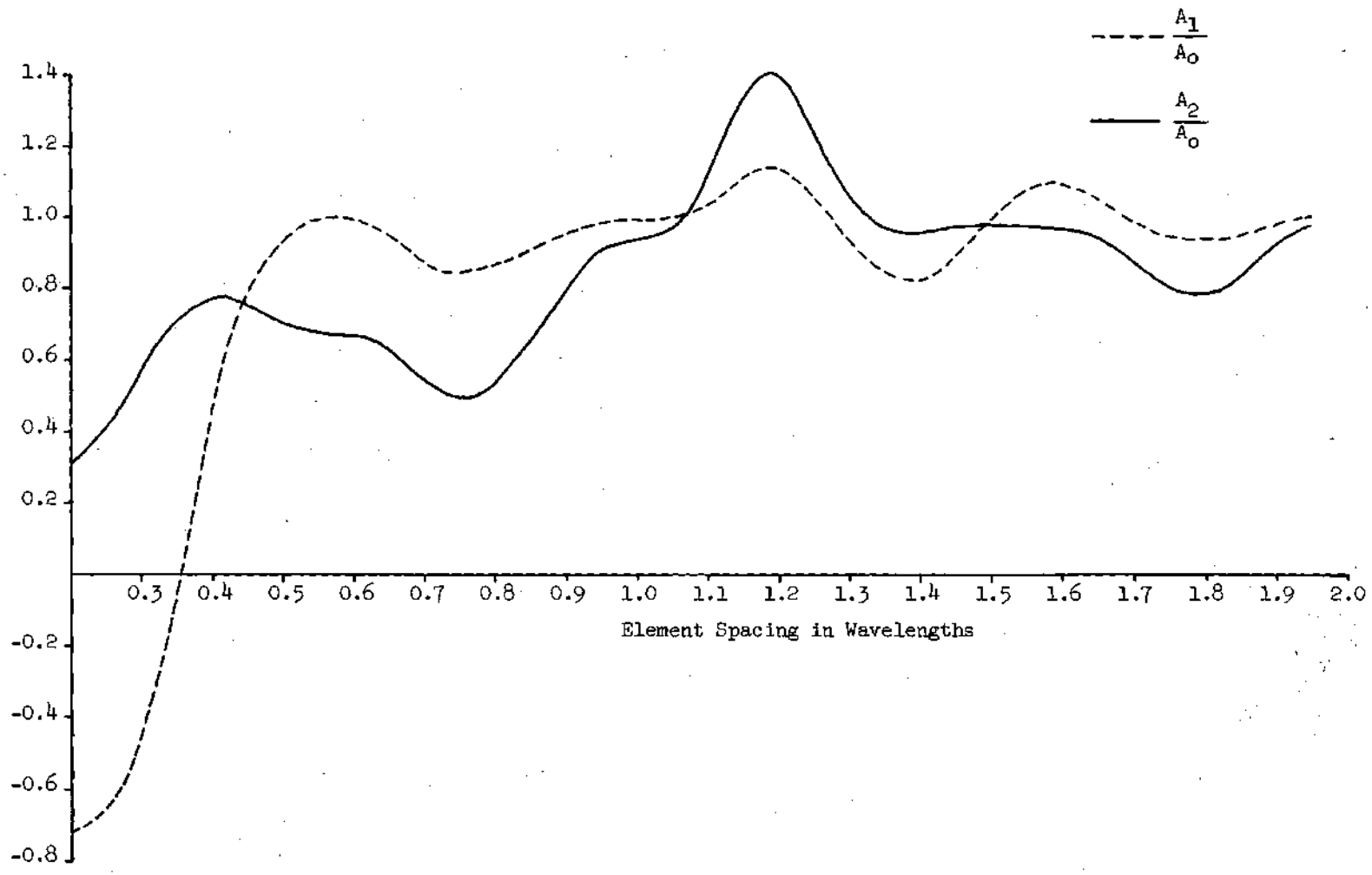

Fig. 3.15 Amplitude Distribution for Optimum Five Element Equally Spaced Array in Noise Environment - Example II.

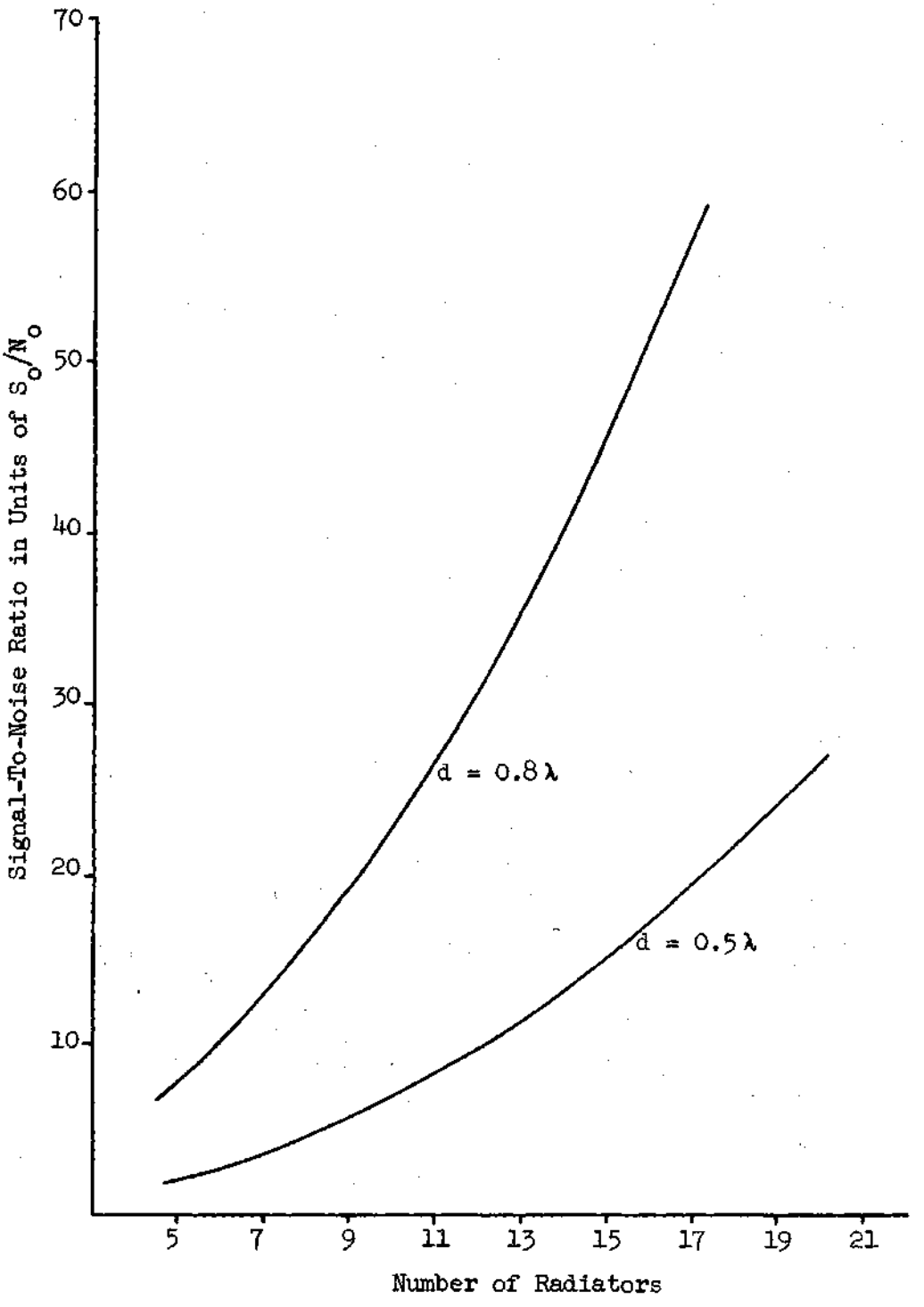

Fig. 3.16 Signal-to-Noise Ratio of Broadside Arrays as a Function of Number of Radiators - Example II.

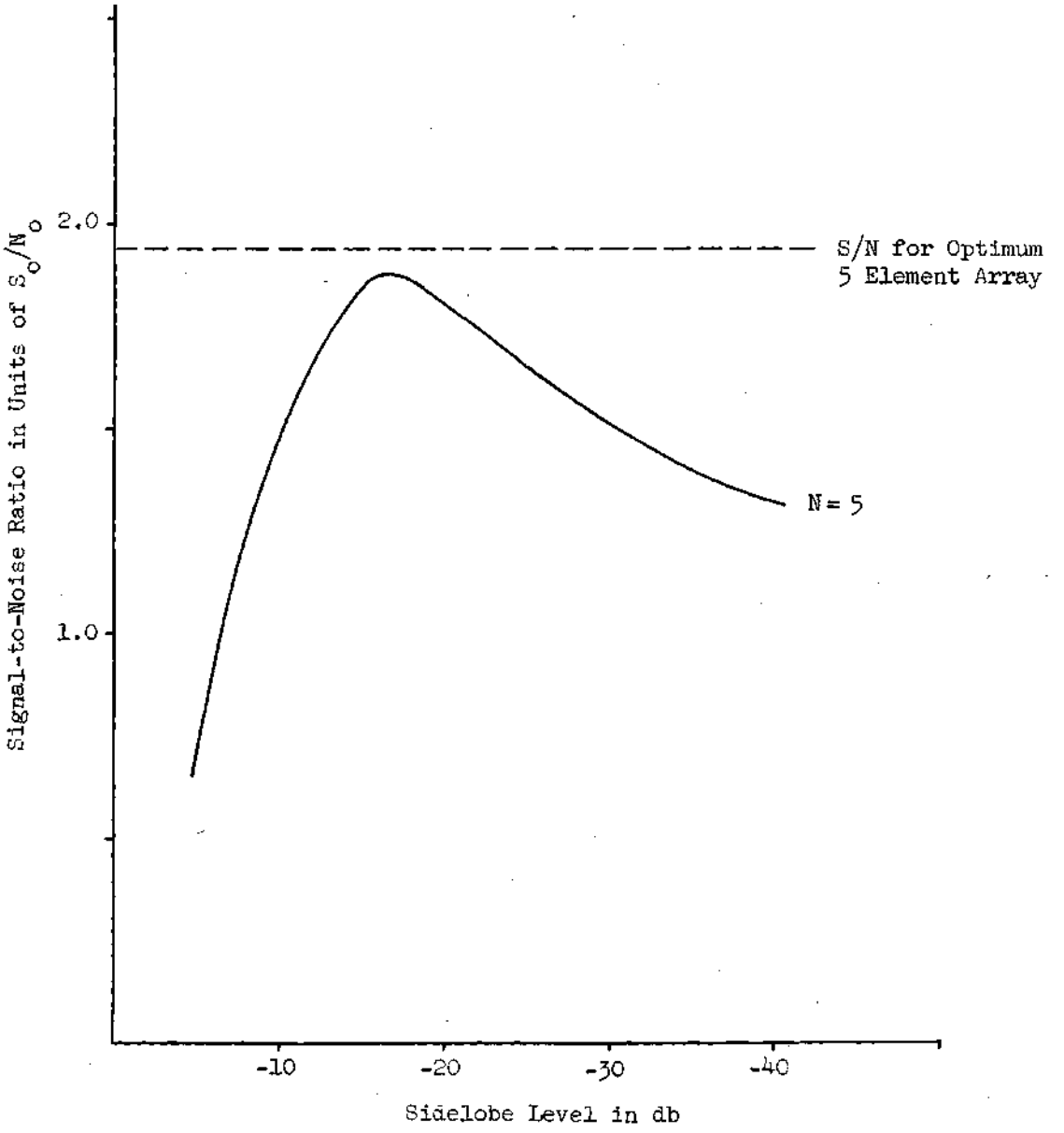

Fig. 3.17 Signal-to-Noise Ratio for Five Element Chebyschev Array in Noise Environment - Example II.

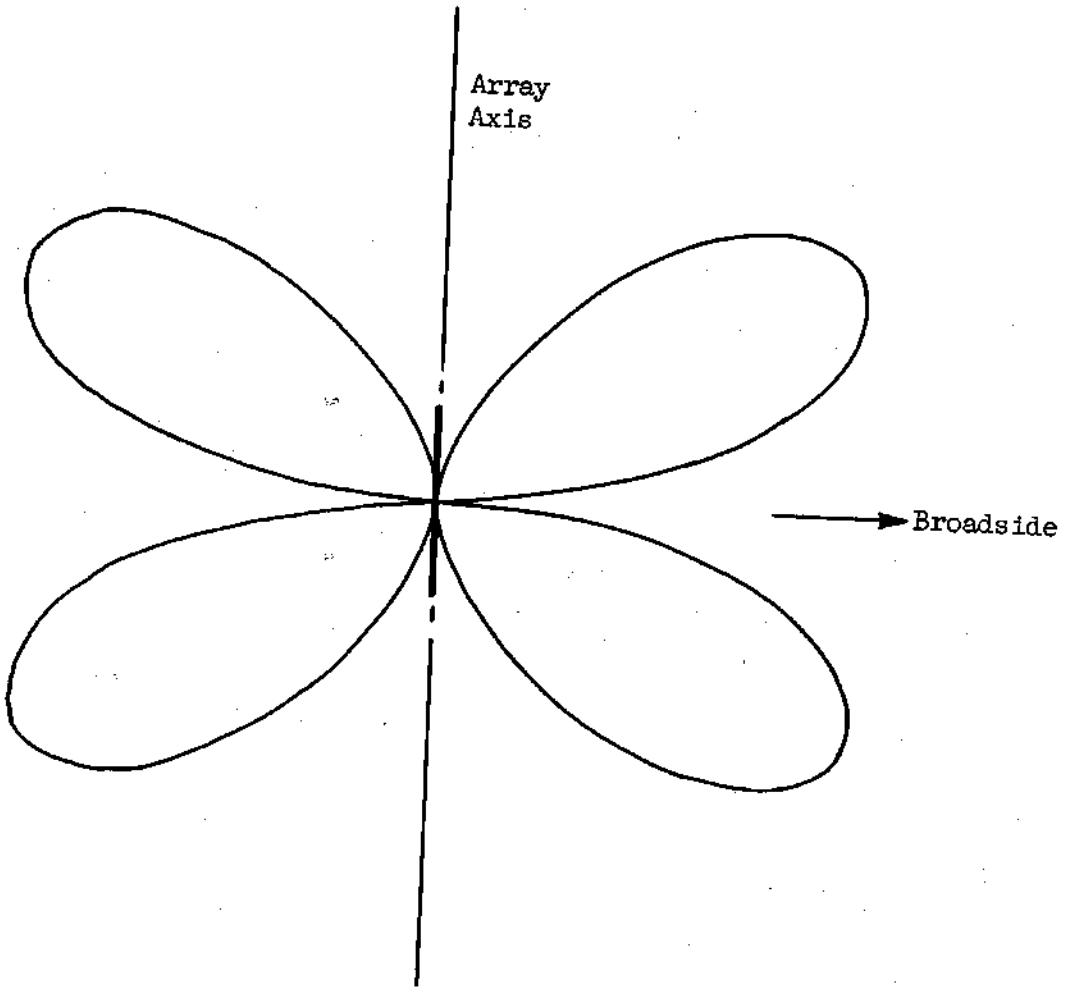

Fig. 3.18 Normalized Noise Distribution - Example III.

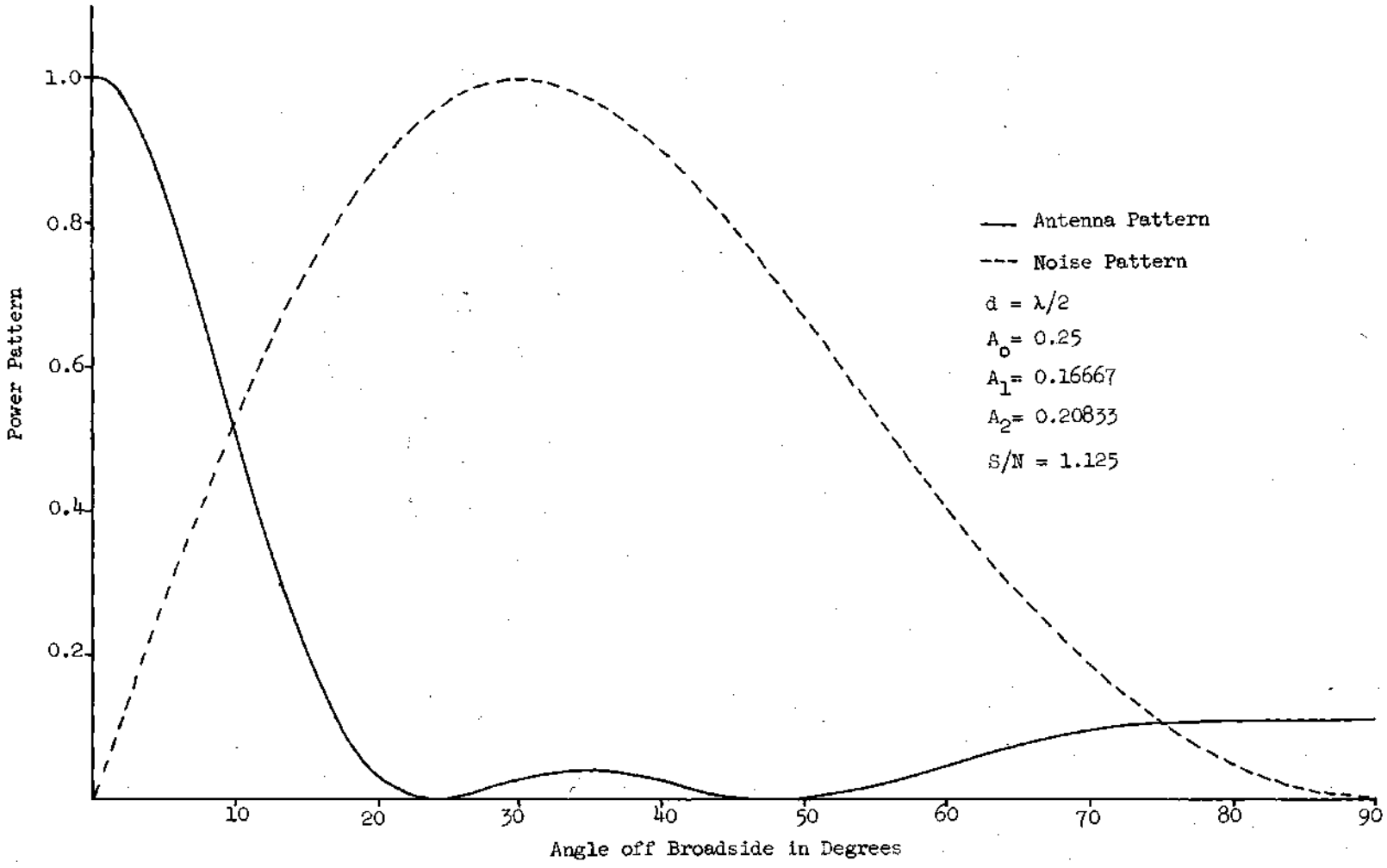

Fig. 3.19 Power Pattern for Optimum Five Element Array Noise Environment - Example III.

which results in a signal-to-noise ratio of 1.125 S_o/N_o. Variation of the signal-to-noise ratio with interelement spacing is illustrated in Figure 3.20. The maximum value occurs at a spacing of 0.9 wavelengths. The power pattern of this array is shown in Figure 3.21. As in the previous examples, the excitations of the elements for various spacings are shown in Figure 3.22.

The results of increasing the number of radiators for a spacings one-half wavelength are shown in Figure 3.23.

Finally, comparisons of the five element array with a Dolph-Chebyschev array are illustrated graphically in Figure 3.24.

Variable Spacings in the Optimization of Signal-to-Noise Ratio

The preceding developments have illustrated methods for the optimization of the performance of equally spaced arrays in a prescribed noise environment. Results of the examples show that arrays designed using the developed procedure offer substantial increases in performance over arrays designed using the Dolph-Chebyschev procedure. All arrays were constrained to be equally spaced, but the effects of varying this constant interelement spacing were studied with the result that for a five element array, substantial peaks in the signal-to-noise ratio were noted for spacings ranging from 0.8 wavelengths up to 0.95 wavelengths. One is tempted, therefore, to include element positions as independent variables in the signal-to-noise ratio optimization process, as was done in pattern synthesis for minimum mean squared error in the previous chapter.

Two methods are studied in this research for accomplishing this

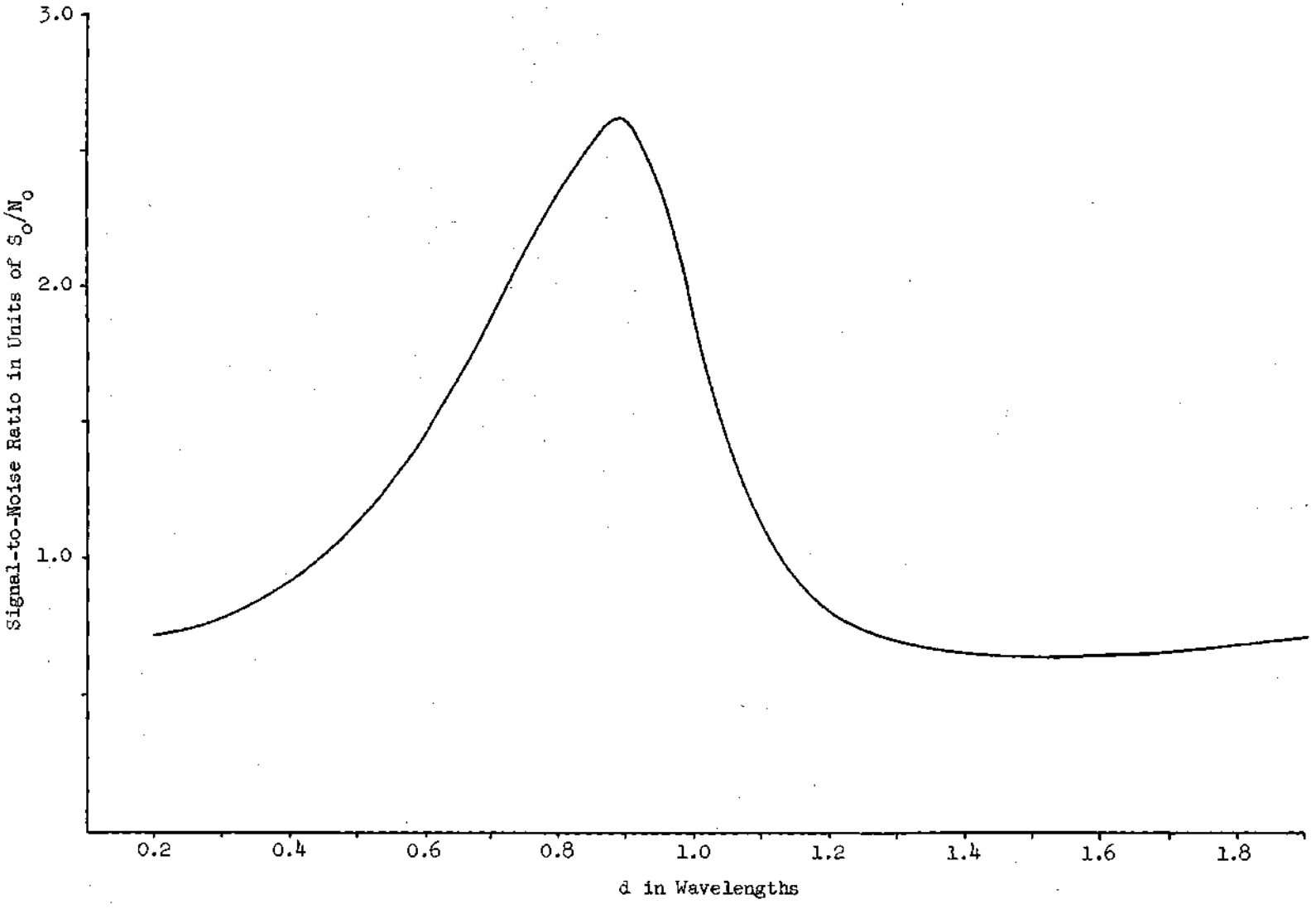

Fig. 3.20 Performance of Equally Spaced Five Element Array in Noise Environment - Example III.

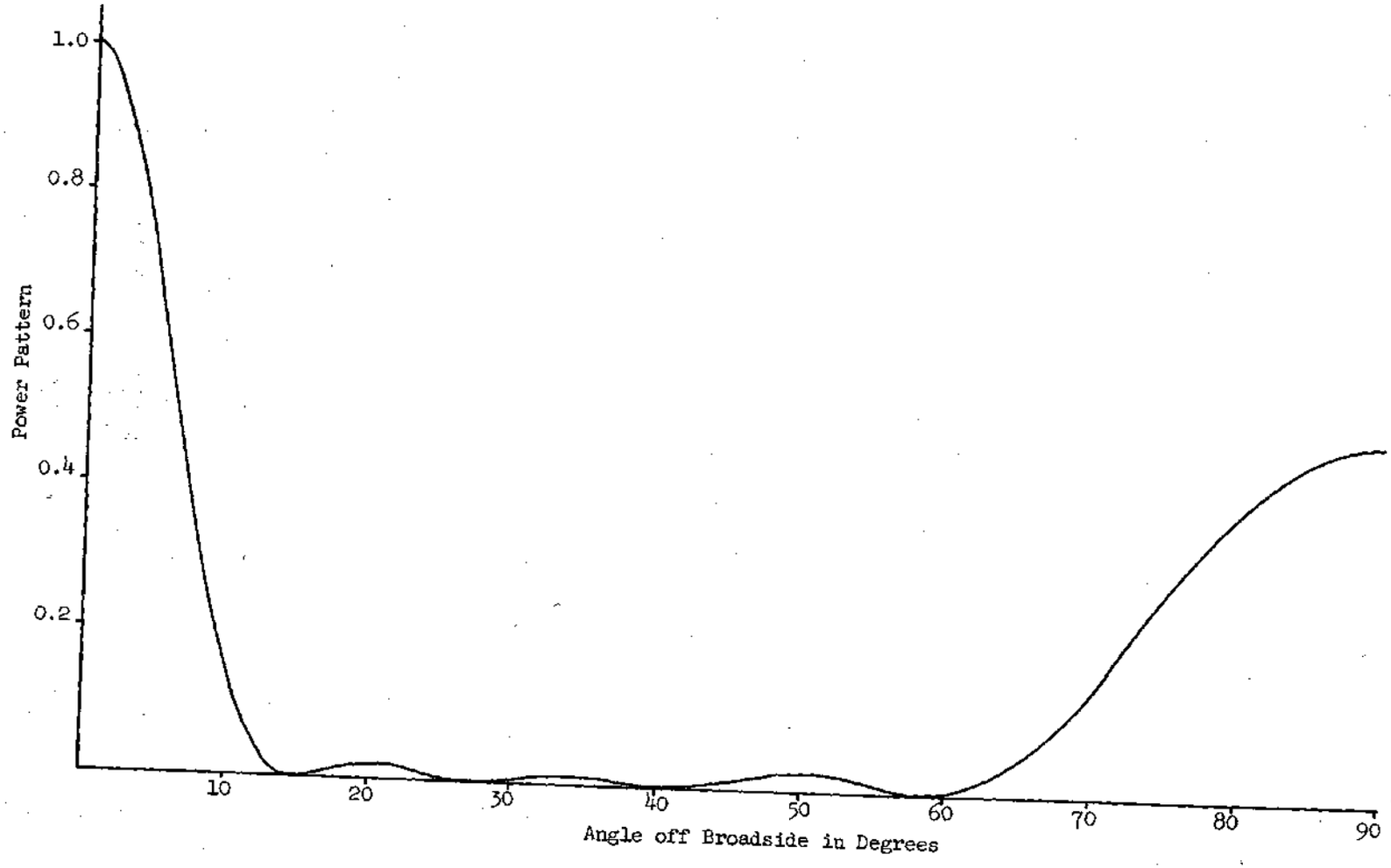

Fig. 3.21 Power Pattern of Optimum Five Element Equally Spaced Array for Spacing of 0.9 Wavelengths - Example III.

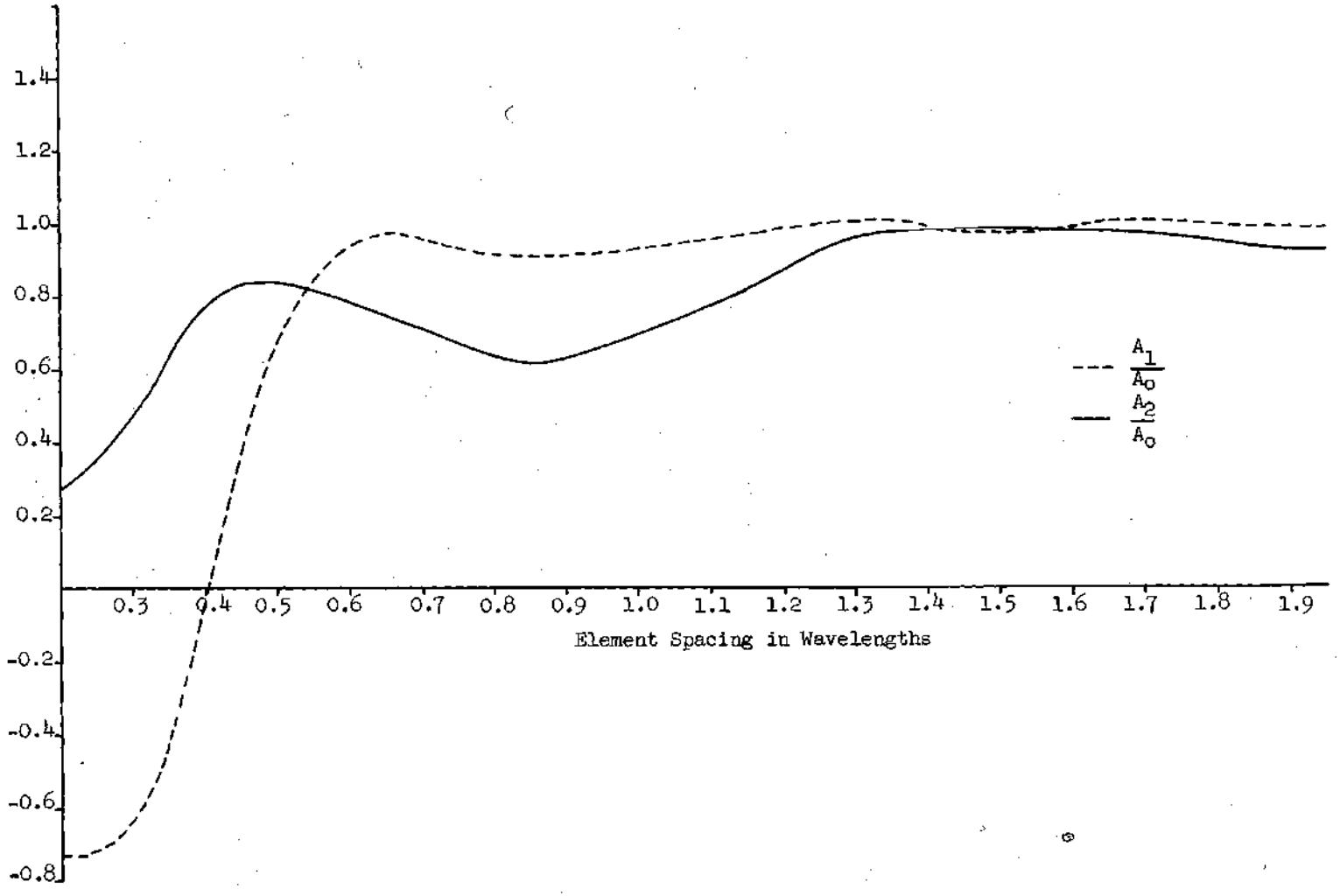

Fig. 3.22 Amplitude Distribution for Five Element Equally Spaced Array in Noise Environment - Example III.

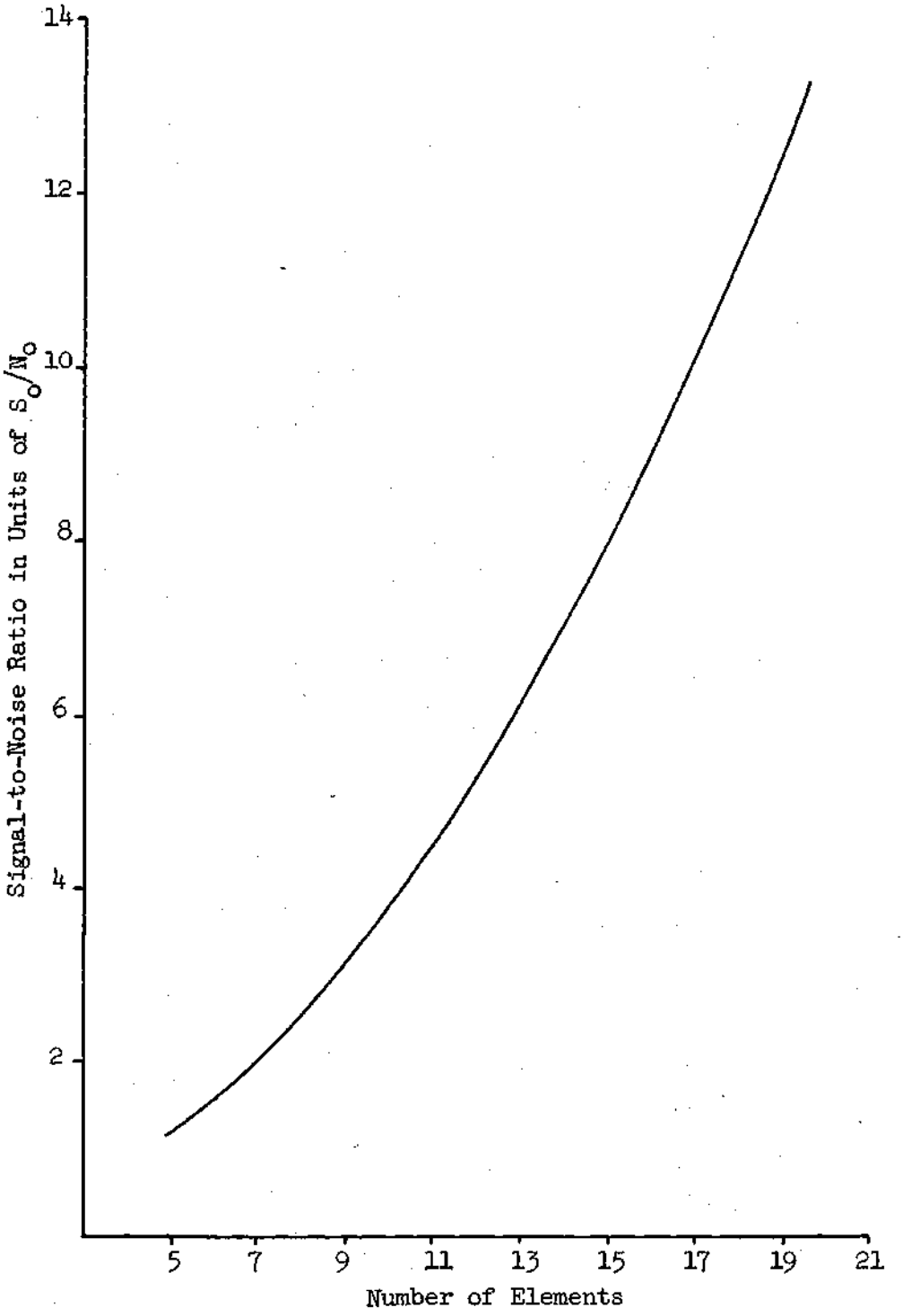

Fig. 3.23 Performance of $\frac{\lambda}{2}$ Spaced Array in Noise Environment - Example III.

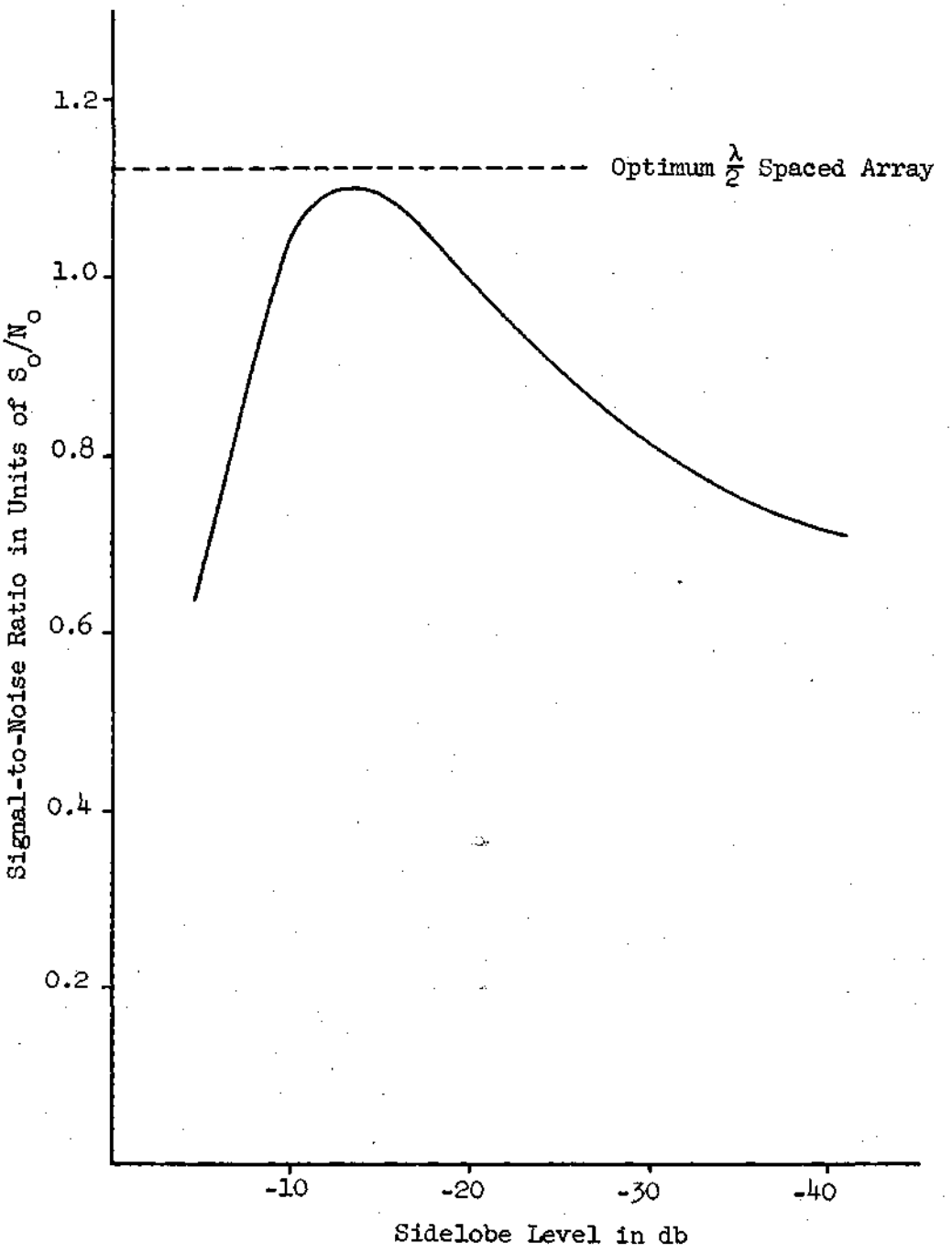

Fig. 3.24 Signal-to-Noise Ratio for Five Element Chebyschev Array in Noise Environment - Example III.

inclusion of radiator locations as independent parameters in the optimization procedure. When the displacement of the radiators is expected to be small about some average spacing, a perturbational analysis is derived. Larger displacements require use of the method of steepest descent.

Optimization of the signal-to-noise performance of an array is essentially the problem of finding the optimum balance between beamwidth of the radiation pattern and the sidelobes of the pattern. The beamwidth is primarily a function of the total aperture width, while sidelobe level is predominantly determined by the amplitude distribution across this aperture. The influence of the amplitude distribution is dominant, however, over that of aperture because of the effects of the grating lobes which appear at wide values of interelement spacing in arrays. The examples of the previous section illustrated the degradation in signal-to-noise performance caused by these secondary beams as the spacing between radiators approached one wavelength. The amount of degradation was, of course, dependent upon the spatial characteristics of the noise distribution, but was significant in each of the example distributions, as shown in Figures 3.6, 3.12, and 3.19. It should be expected, therefore, that the use of spacings as independent variables would not result in arrays characterized by widely varying separations between elements; in fact, one would predict from the foregoing qualitative discussion that the solution would not represent a marked deviation from the optimum equally spaced array. This prediction is borne out by the examples included in this section.

The specific approach taken in this research to the inclusion of element positions as independent variables recognizes the dominance of

the amplitudes of excitation of the radiators. It is an iterative method which combines the synthesis procedure developed for arrays with known element locations with either the method of steepest descent or a perturbational technique for handling small variations in spacings about some average value. Implementation of the procedure is a two step undertaking for each iteration. A "trial" solution is selected by choosing the equally spaced array which resulted in optimum performance using the methods of the previous section. The amplitudes resulting from this solution are then held constant, and spacings are allowed to vary independently using either the method of steepest descent or the perturbational technique. The process is then repeated until the optimum array is synthesized. Because of the dominance of the amplitude terms, only one iteration was performed for the example noise distributions included in this report. The improvement in signal-to-noise ratio was very small in each case, justifying the termination of the process. This small increase in signal-to-noise ratio does not preclude the possibility of a strong extremem to which the process might be converging extremely slowly. Physical insight, however, makes the existence of such a strong extremum improbable, primarily because of the degradations due to secondary beams as the average spacing approaches one wavelength. Smaller values of spacings are ruled out because of necessity for a narrow main beam.

The development of the perturbational technique for handling small variations in spacings is deferred to Appendix A because of algebraic complexity. This method of presentation is additionally justified because of the dominant role played by the amplitude distribution in the optimization process. The method of steepest descent proved adequate in the

investigation of the influence of the spacing parameter as the following examples will illustrate.

Figures 3.25, 3.26, and 3.27 show the power patterns of arrays derived using the excitation vectors of the examples of the previous section which yielded optimum signal-to-noise for the equally spaced arrays. Holding the amplitudes fixed in each case, the spacings were allowed to vary using the method of steepest descent to seek the minimum value of the integral

$$I(\hat{\bar{a}},\bar{x}) = \int_0^{\pi} G(\hat{\bar{a}},\bar{x},\theta)\, N(\theta)\, \sin\theta\, d\theta \qquad (3.76)$$

which represents the net noise power out of the array. Note that the solution vectors in all three cases deviate negligibly from the equal spacings for which the amplitudes are optimum. Subsequent iterations using the combination of the optimization technique for known spacings and steepest descent procedures would not appreciably improve the signal-to-noise ratio. The apparent conclusion to be drawn from these results is that unequal spacings are secondary in influence to the amplitudes of radiator excitations, and that the optimization technique for equal spacings will be adequate for most practical situations.

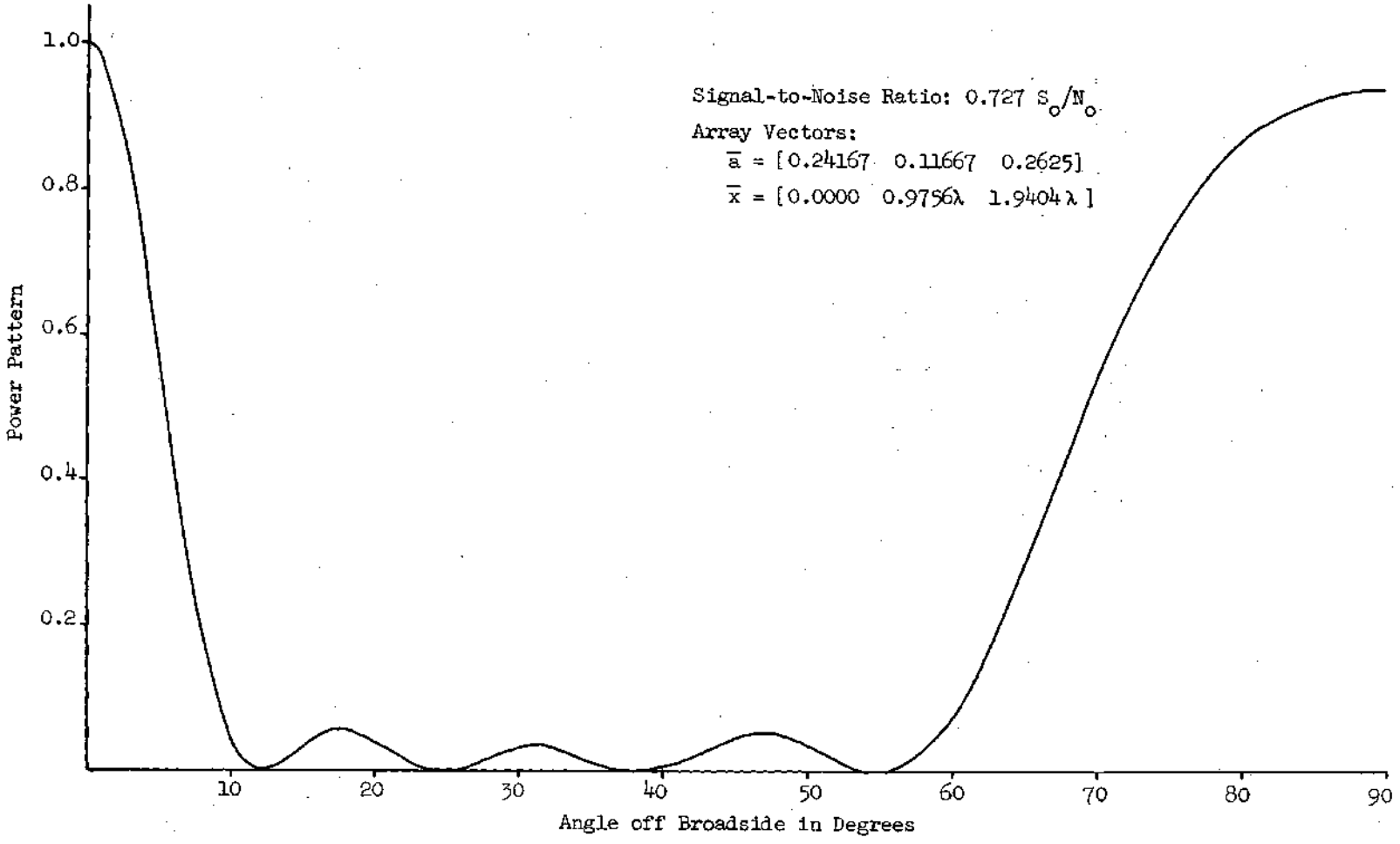

Fig. 3.25 Power Pattern of Array Obtained by Steepest Descent for Noise Pattern - Example I.

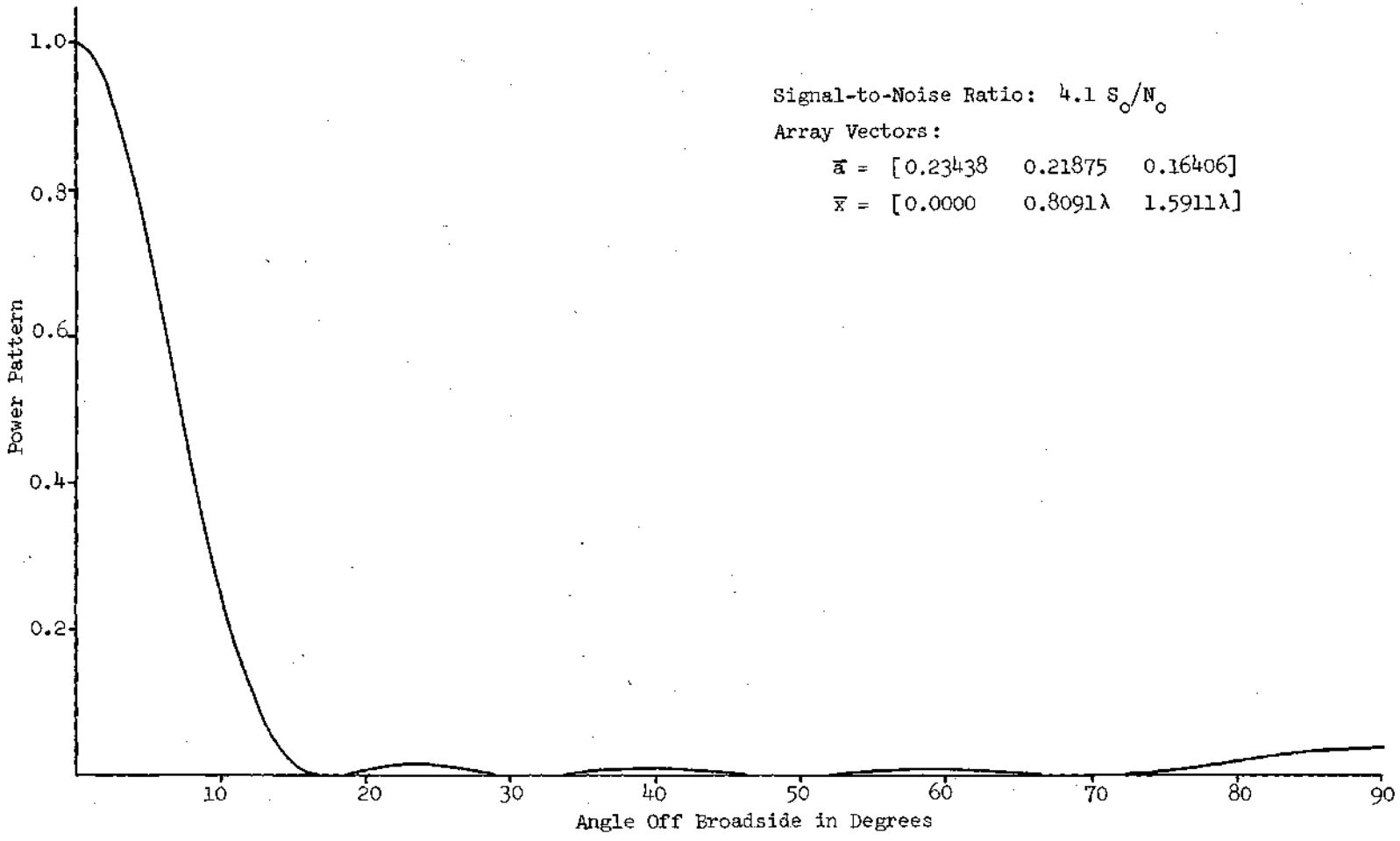

Fig. 3.26 Power Pattern of Array Obtained Using Steepest Descent for Noise Pattern - Example II.

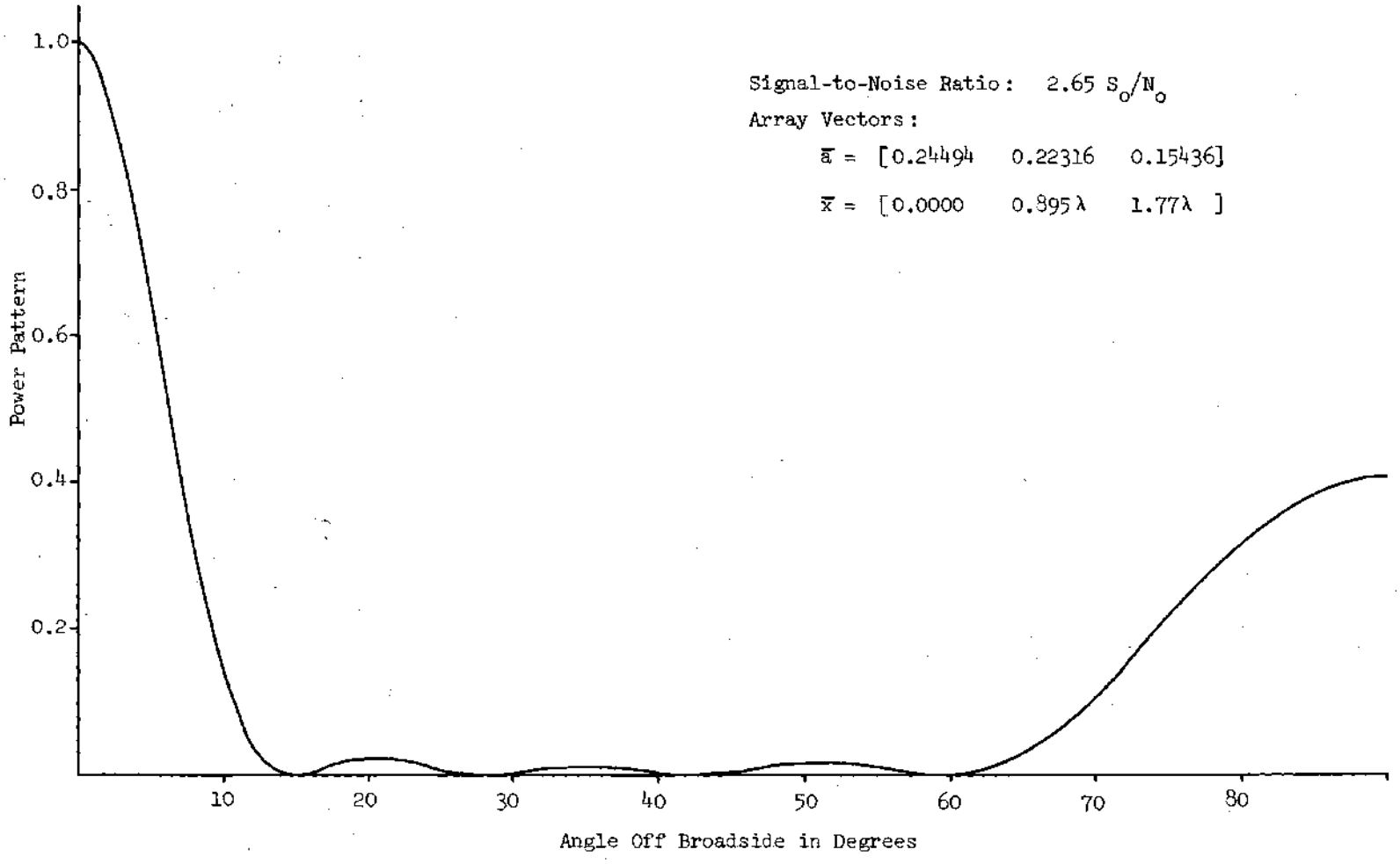

Fig. 3.27 Power Pattern of Array Obtained Using Steepest Descent for Noise Pattern - Example III.

CHAPTER IV

CONCLUSIONS

This research has investigated the optimization of the performance of linear arrays of isotropic radiators. The particular optimality criteria considered were pattern synthesis for minimum mean squared error and synthesis for maximum signal-to-noise ratio when the array is to be operated in a known or measurable noise environment. In each of these cases, specific efforts were devoted to investigation of the role of variable element spacings in improvement of array performance.

In the area of radiation pattern synthesis, the inclusion of variable spacings in synthesis procedures has been the object of increasing attention in the current literature. Mathematical complexity has limited the development of compact synthesis procedures. This research has demonstrated that the methods of nonlinear programming provide a useful means of overcoming this complexity, in addition to furnishing other advantages such as the incorporation of design constraints, a feature not exhibited by the methods currently in use.

While all degrees of freedom readily usable by the array designer were included in the synthesis procedure, specific attention was devoted to study of unequally spaced arrays. The examples included in Chapter II showed that use of variable spacings was a key factor in improved array performance when compared with the performance of arrays synthesized by the widely used Fourier technique. This improvement, however, did not

appear to result from widely varying interelement spacings, but from a more efficient utilization of aperture structure.

Incorporation of linear inequality constraints among the design variables was accomplished by the use of the created response surface technique. The effects of a maximum aperture constraint were studied in the synthesis of a broadside exponential pattern. Two particular constraints were imposed, and illustrated the pattern deformation due to reduced aperture. Convergence of the created response surface method was rapid in both cases. The ability to handle inequality constraints was shown to be one of the most useful features of the nonlinear programming approach to optimum pattern synthesis.

A comparison of the synthesis procedure of this research and current methods reported in the literature shows no increase in complexity of implementation for the procedure studied. The use of the digital computer is dictated in all current methods of array design where element locations are considered as independent variables.

The synthesis of arrays for maximum signal-to-noise ratio is a topic of contemporary interest in antenna research. Prior to this work, little has been published in this area. Initial attention was, therefore, directed toward optimization of equally spaced arrays. The optimization problem was shown to reduce to the generalized characteristic value problem when an equality constraint was imposed on input signal power from a particular direction. Two linear transformations which converted the generalized problem to a more conventional eigenvalue problem were derived. The results of the optimization procedure were studied for three representative noise distributions. In every case, a substantial increase in

performance was noted when the arrays designed by the developed procedure were compared with arrays designed by the Dolph-Chebyschev process.

Variable spacings were included in the signal-to-noise ratio optimization procedure using the steepest descent technique. Indications are from the example noise distributions considered that the dominant role was played by the array excitation vectors. Unequal spacings were of less importance.

Several interesting extensions of the signal-to-noise ratio optimization procedure are suggested by this work. One of the most practical would be the modification of the technizue to allow specification of non-separable noise spatial distributions. This extension will be marked by a probable substantial increase in mathematical complexity. A second extension might include the specification of a noise power spectrum in the frequency domain as well as having a spatial distribution. In this case the array would operate in conjunction with a conventional filter, with the characteristics of both array and filter being derived from the synthesis procedure.

APPENDICES

APPENDIX A

CONVERGENCE OF THE METHOD OF STEEPEST DESCENT

The proof of the convergence of the steepest descent method is readily carried out following Saaty and Bram (29). While this and similar proofs on convergence are readily accessible in several references, the following must be included for completeness.

Let the objective function to be minimized be denoted $f(\bar{x})$, where $\bar{x}$ is an n-dimensional vector. Assume that $f(\bar{x})$ is continuous with continuous second derivatives, and define the set

$$S = \{ \bar{x} \mid f(\bar{x}) \leq f(\bar{x}) \} \tag{A.1}$$

for some $\bar{x}_o$. Assume S is bounded (an obviously necessary assumption if a solution to the minimization problem is to exist). Further assume that the inequality below holds

$$| \bar{u}^T H(\bar{x}) \bar{u} | \leq M \bar{u}^T \bar{u} \tag{A.2}$$

where $\bar{u}$ is any vector, $\bar{x} \in S$, and $H(\bar{x})$ is the nxn matrix of second partial derivatives of f evaluated at point $\bar{x}$. Let the values of $\bar{x}$ in the steepest descent be given by the iterative equation

$$\bar{x}_{k+1} = \bar{x}_k \nabla f(x_k) \tag{A.3}$$

where λ_k is a scalar satisfying

$$f\left(\bar{x}_k - \lambda_k \nabla f(\bar{x}_k)\right) \leq f\left(\bar{x}_k - \lambda \nabla f(\bar{x}_k)\right) \qquad (A.4)$$

for all $\lambda \geq 0$.

The proof of convergence must establish two results which are: (a) a subsequence $\bar{x}_{km}$ converges to a point $\bar{x} \in S$ for which $\nabla f(\bar{x}) = 0$, and, (b) $f(\bar{x}_{km})$ decreases monotonically to $f(\bar{x})$. It must first be established that if $\bar{x}_k \in S$, then $\bar{x}_{k+1} \in S$. To show this, let $\bar{x}_k \in S$, and assume $\nabla f(\bar{x}_k) \neq 0$. Denote the line segment connecting $\bar{x}_{k+1}$ and $\bar{x}_k$ by the set

$$L = \left\{ \bar{x} \mid \bar{x} = \bar{x}_k - \lambda \nabla f(\bar{x}_k),\ \lambda \geq 0 \right\}, \qquad (A.5)$$

and denote

$$g(\lambda) = f\left(\bar{x}_k - \lambda \nabla f(\bar{x}_k)\right) - f(\bar{x}_k) \qquad (A.6)$$

The illustrations of Figure A.1 will be of assistance in these and following developments. Using Taylor's formula, $g(\lambda)$ may be written

$$g(\lambda) = -\lambda \bar{u}_k^T \bar{u}_k + \frac{\lambda^2}{2!} \bar{u}_k^T H(\bar{z}) \bar{u}_k \qquad (A.7)$$

where $\bar{z} \in \bar{L}$, $H(\bar{z})$ is the nxn Hessian evaluated at $\bar{z}$, and for notational convenience $\bar{u}_k = \nabla f(\bar{x}_k)$. By hypothesis, both $\bar{u}_k$ and $H(\bar{z})$ are continuous; thus $g'(\lambda)/\lambda = 0$ is continuous and is given by

$$g'(0) = -\bar{u}_k^T \bar{u}_k < 0 \qquad (A.8)$$

Consequently, there exists some interval $(0,\lambda')$ where $g(\lambda) < 0$ for every

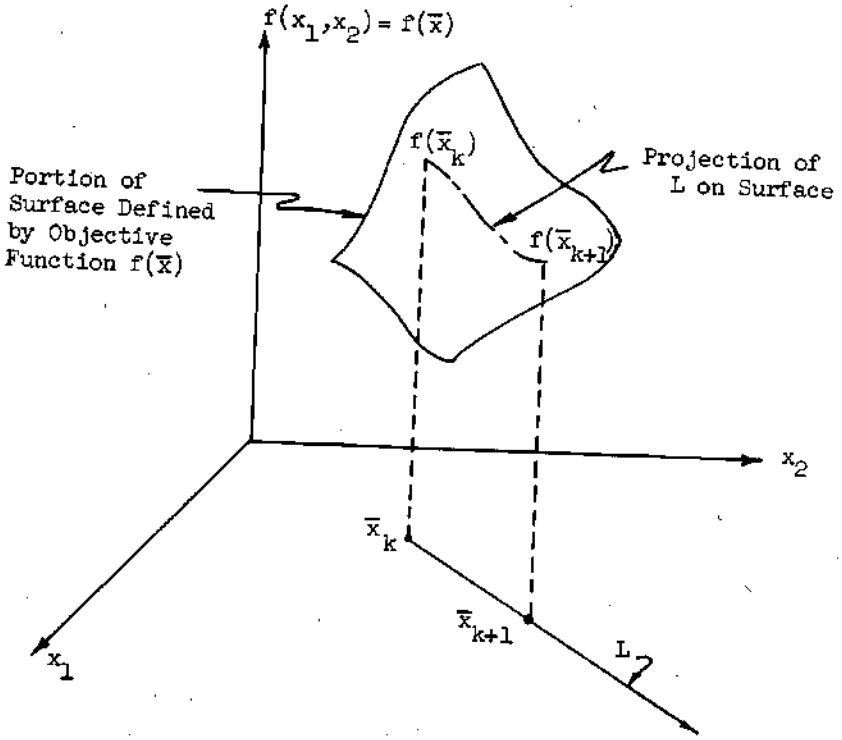

(a) Section of Typical Three Dimensional Surface

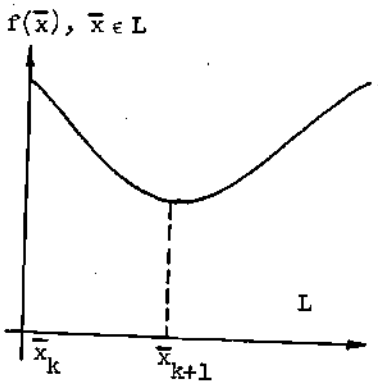

(b) Plot of $f(\bar{x})$ for $\bar{x} \in L$

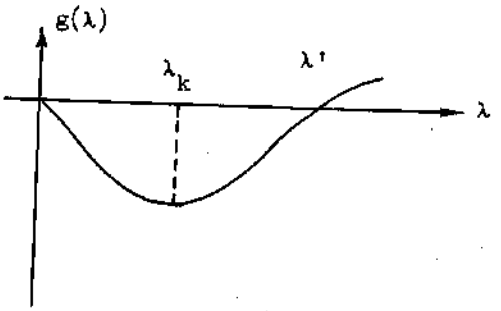

(c) Plot of $g(\lambda)$

Fig. A.1 Geometrical Constructions Relative To Steepest Descent Procedure.

$\lambda \in (0,\lambda')$, and thus

$$f(\bar{x}_k - \lambda \bar{u}_k) < f(\bar{x}_k)$$

for $\lambda \in (0,\lambda')$. Let λ_k denote the point at which $g(\lambda)$ is minimum. Then $\lambda_k > 0$ and

$$f(\bar{x}_k - \lambda_k \bar{u}_k) \leq f(\bar{x}_k) \tag{A.10}$$

which establishes $\bar{x}_{k+1} = \bar{x}_k - \lambda_k \bar{u}_k$ as a member of set S.

It is necessary to confirm the fact than $\bar{u}_k^T \cdot \bar{u}_k \to 0$ as $k \to \infty$. If $g(\lambda) < 0$ for every λ, then the hypothesis that S was compact would be violated; hence, there exists some $\lambda' > 0$ so that $g(\lambda') = 0$. Let λ' be the least positive λ such that $g(\lambda')$ vanishes. Then,

$$\lambda' = \frac{2\, \bar{u}_k^T \bar{u}_k}{\bar{u}_k^T\, H(\bar{z})\, \bar{u}_k} \tag{A.11}$$

Using the hypothesis on the boundedness of $|\bar{u}^T H \bar{u}|$, then

$$\lambda' \geq \frac{2}{M} \tag{A.12}$$

and

$$g(\lambda) \leq -\lambda \bar{u}_k^T u_k + \frac{\lambda^2}{2} M\, \bar{u}_k^T \bar{u}_k \tag{A.13}$$

From this expression, it may be readily seen that the only stationary point in the interval $(0,\lambda')$ is the minimum at $\lambda = \lambda_k$; consequently $g(\lambda)$ reaches its maximum at the end points of intervals $(\delta,\ 2/M - \delta)$,

$\delta > 0$. It is easily shown by direct substitution that

$$g(\delta) = g(\tfrac{2}{M} - \delta) = -\delta(1 - \tfrac{M}{2}\delta)\,\bar{u}_k^T \bar{u}_k \qquad (A.14)$$

This bounds $g(\lambda)$ as follows

$$g(\lambda_k) \leq g(\lambda) \leq -\delta(1 - \tfrac{M}{2}\delta)\,\bar{u}_k^T \bar{u}_k \qquad (A.15)$$

for every value of k. Since $-g(\lambda_k) > 0$,

$$\sum_{k=1} -g(\lambda_k) < \infty \qquad (A.16)$$

which is easily shown by direct substitution of $g(\lambda_k) = f(\bar{x} - \lambda_k \bar{u}_k) - f(\bar{x}_k)$ into this sum, observing that a telescoping series results, and then applying the hypothesis that S is bounded. Since $\delta > 0$, and $\delta < 2/M - \delta$, then $\delta < 1/M$ and $(1 - M\delta/2) > 1/2$. Consequently, if

$$\sum_{k=1} -g(\lambda_k) < \infty \quad ,$$

this requires that $\bar{u}_k^T \bar{u}_k \to 0$ as $k \to \infty$ which in turn requires that $\nabla f(\bar{x}_k) \to 0$ as $k \to \infty$.

Since S is compact and since $\bar{x}_k \in S$ for every k, then the sequence $\bar{x}_k$ has an accumulation point in S, and consequently a subsequence $\bar{x}_{kM} \to \bar{x}$ and $\nabla f(\bar{x}_{kM}) \to \nabla f(\bar{x}) = 0$. The fact that for every λ_k, $g(\lambda_k) <$) ensures that $f(\bar{x}_{kM})$ decreases monotonically to $f(\bar{x})$ which completes the convergence proof.

It should be noted that in most developments on steepest descent techniques, the necessity of a unimodal objective function is imposed. As pointed out in earlier discussions, unimodality is not a property of functions resulting from physical problems such as the antenna optimization problem considered in this research. To circumvent this difficulty, several techniques are applicable. A most important factor is the use of prior knowledge of the physical nature of the problem in the choice of the initial point for the procedure. In a large number of problems, this will prove sufficient to ensure convergence if the surface described by the objective function is not too irregular. Secondly, a series of checks on the behavior of the value of the objective function at the points of iteration, interpolating where required, will result in a decreasing sequence $\{f(\bar{x}_k)\}$ and will in turn provide for convergence to a point where $\bar{x}$ where $\nabla f(\bar{x}) = 0$.

APPENDIX B

CONVERGENCE OF THE CREATED RESPONSE SURFACE METHOD

Rigorous establishment of the convergence of the minimization of $f(\bar{x})$ subject to constraints $g_i(\bar{x})$ may be accomplished as follows: Let $f(\bar{x})$ be a real valued twice continuously differentiable function where $\bar{x}$ is a n-vector. There are n non-negativity constraints $x_i \geq 0$ and m other linear inequalities in the set of inequalities $g_i(\bar{x})$. Then for a sequence $\{ r_k \}$ decreasing to zero as k tends to infinity,

$$\lim_{\substack{r_k \to 0 \\ k \to \infty}} \min_{\bar{x}} F(\bar{x}, r_k) = \min_{\bar{x}} f(\bar{x}) \tag{B.1}$$

where

$$F(\bar{x}, r_k) \triangleq f(\bar{x}) + r_k \sum_{i=1}^{m+n} \frac{1}{g_i(\bar{x})} \tag{B.2}$$

To establish that $F(\bar{x}, r_k)$ converges to the minimum of $f(\bar{x})$ subject to constraints $g_i(\bar{x})$, it must be shown that given any $\epsilon > 0$, there exists a K such that for every $k > K$,

$$\left| \min_{\bar{x}} F(\bar{x}, r_k) - f(\hat{\bar{x}}) \right| < \epsilon \tag{B.3}$$

Where $f(\hat{\bar{x}})$ is the actual constrained minimum of $f(\bar{x})$.

Note that because the constraints are linear, for $r_2 < r_1$

$$\min_{\bar{x}} F(\bar{x},r_2) < \min_{\bar{x}} F(\bar{x},r_1) \tag{B.4}$$

Because $f(\bar{x})$ is continuous, there will exist a neighborhood $N(\hat{x})$ such that for $\epsilon > 0$ and for every $\bar{x}$ in $N(\hat{x})$,

$$f(\bar{x}) < f(\hat{x}) + \frac{\epsilon}{2} \tag{B.5}$$

For $\bar{x} \in N(\hat{x})$, choose K such that

$$\frac{r_k}{\min_i g_i(\bar{x})} < \frac{\epsilon}{2(m+n)} \tag{B.6}$$

Then for $k > K$,

$$\min_{\bar{x}} F(\bar{x},r_k) < \min_{\bar{x}} F(\bar{x},r_k) \leq f(\hat{x}) + \epsilon \tag{B.7}$$

which proves the desired convergence property of the auxiliary function $F(\bar{x},r)$.

APPENDIX C

EXTENSION OF OPTIMIZATION PROCEDURE TO ARRAYS WITH COMPLEX EXCITATIONS

The method for optimizing the signal-to-noise ratio of a broadside array may be simply extended to include arrays with complex excitation coefficients. Since the details of the optimization procedure are identical with that for broadside arrays once the quadratic forms representing signal power and noise power out of the array are obtained, this appendix is concerned only with the derivation of these forms.

The power pattern of an array with complex excitation but a purely real radiation pattern is given by the square of equation (2.13).

$$G(\theta) = a_o + 2\sum_{m=1}^{M} a_m \cos(\beta m d \cos\theta) + b_m \sin(m\beta d \cos\theta)^2 \qquad (C.1)$$

After a moderate amount of algebraic manipulation, the expansion of (C.1) yields

$$\begin{aligned} G(\theta) = {} & a_o^2 + 4a_o \sum_{m=1}^{M} \{a_m \cos(m\beta d \cos\theta) + b_m \sin(m\beta d \cos\theta)\} \\ & + 4\sum_{m=1}^{M}\sum_{n=1}^{M} \{a_m a_n \cos(m\beta d \cos\theta)\cos(n\beta d \cos\theta) \\ & + b_m b_n \sin(m\beta d \cos\theta)\sin(n\beta d \cos\theta) \\ & + a_m b_n \cos(m\beta d \cos\theta)\sin(n\beta d \cos\theta) \\ & + a_n b_m \cos(n\beta d \cos\theta)\sin(m\beta d \cos\theta)\} \end{aligned} \qquad (C.2)$$

Imposing the constraint that the power pattern in some angular direction, say θ_o, will be prescribed value

$$G(\theta_o) = K^2 \tag{C.3}$$

then the optimization of the signal-to-noise ratio consists of minimizing the integral

$$I = \int_o^\pi G(\theta)\, N(\theta) \sin\theta \, d\theta \tag{C.4}$$

The integral I is a quadratic form similar to expression (3.34) for the case of the broadside array. Expansion of I yields

$$\begin{aligned} I = {} & a_o^2 \int_o^\pi N(\theta) \sin\theta \, d\theta + 4 a_o \sum_{m=1}^{M} a_m \int_o^\pi N(\theta) \cos(m\beta d \cos\theta) \sin\theta \, d\theta \\ & + 4 a_o \sum_{m=1}^{M} b_m \int_o^\pi N(\theta) \sin(m\beta d \cos\theta) \sin\theta \, d\theta \\ & + 4 \sum_{m=1}^{M} \sum_{n=1}^{M} \Big\{ a_m a_n \int_o^\pi N(\theta) \cos(m\beta d \cos\theta) \cos(n\beta d \cos\theta) \sin\theta \, d\theta \\ & \quad + b_m b_n \int_o^\pi N(\theta) \sin(m\beta d \cos\theta) \sin(n\beta d \cos\theta) \sin\theta \, d\theta \\ & \quad + a_m b_n \int_o^\pi N(\theta) \cos(m\beta d \cos\theta) \sin(n\beta d \cos\theta) \sin\theta \, d\theta \\ & \quad + a_n b_m \int_o^\pi N(\theta) \cos(n\beta d \cos\theta) \sin(m\beta d \cos\theta) \sin\theta \, d\theta \Big\} \end{aligned} \tag{C.5}$$

In matrix notation, I may be written

$$I = \bar{e}^T F \bar{e} \tag{C.6}$$

where $\bar{e}^T = [a_o\ a_1 \ldots a_M\ b_1 \ldots b_M]$ is a vector of order 2M + 1. The square matrix F is real symmetric of order 2M + 1 also and may be denoted as follows:

$$F = \begin{bmatrix} f_{00} & f_{01} & f_{02} & \cdots & f_{0,2M} \\ f_{01} & f_{11} & f_{12} & \cdots & f_{1,2M} \\ f_{02} & f_{12} & F_{22} & \cdots & f_{2,2M} \\ \vdots & & & \ddots & \vdots \\ f_{0,2M} & f_{1,2M} & f_{2,2M} & \cdots & f_{2M,2M} \end{bmatrix} \tag{C.7}$$

The elements of F are specified by the following expressions

$$f_{oo} = \int_o^\pi N(\theta) \sin\theta \, d\theta$$

for i = 1, ..., M:

$$\begin{aligned} f_{oi} &= 2\int_o^\pi N(\theta) \cos(i\beta d \cos\theta) \sin\theta \, d\theta \\ f_{o,i+M} &= 2\int_o^\pi N(\theta) \sin(i\beta d \cos\theta) \sin\theta \, d\theta \\ f_{ii} &= 4\int_o^\pi N(\theta) \cos^2(i\beta d \cos\theta) \sin\theta \, d\theta \end{aligned} \tag{C.8}$$

$$f_{i+M,i+M} = 4\int_0^{\pi} N(\theta) \sin^2 (i\beta d \cos\theta) \sin\theta \, d\theta$$

for i = 1, ... , M:

$$f_{ij} = 4\int_0^{\pi} N(\theta) \cos (i\beta d \cos\theta) \cos (j\beta d \cos\theta) \sin\theta \, d\theta$$

$$f_{i,j+M} = 4\int_0^{\pi} N(\theta) \cos (i\beta d \cos\theta) \sin (j\beta d \cos\theta) \sin\theta \, d\theta \qquad (C.8)$$

$$f_{i+M,j+M} = 4\int_0^{\pi} N(\theta) \sin (i\beta d \cos\theta) \sin (j\beta d \cos\theta) \sin\theta \, d\theta$$

Similarly the equality constraint may be written as a quadratic form

$$\bar{e}^T C \bar{e} = K^2 \qquad (C.9)$$

where C is of order 2M + 1, real, and symmetric.

$$C = \begin{bmatrix} c_{00} & c_{01} & \cdots & c_{0,2M} \\ c_{01} & c_{11} & \cdots & c_{1,2M} \\ \cdot & \cdot & & \cdot \\ \cdot & \cdot & & \cdot \\ \cdot & \cdot & & \cdot \\ c_{0,2M} & c_{1,2M} & \cdots & c_{2M,2M} \end{bmatrix} \qquad (C.10)$$

The elements of C are given by the following expressions.

$$C_{oo} = 1$$

for $i = 1, \ldots, M$:

$$C_{oi} = 2 \cos (i\beta d \cos \theta_o)$$

$$C_{o,i+M} = 2 \sin (i\beta d \cos \theta_o)$$

$$C_{ii} = 4 \cos^2 (i\beta d \cos \theta_o)$$

$$C_{i+M,i+M} = 4 \sin^2 (i\beta d \cos \theta_o) \qquad (C.11)$$

for $i = 1, \ldots, M$:

$$C_{ij} = 4 \cos (i\beta d \cos \theta_o) \cos (j\beta d \cos \theta_o)$$

$$C_{i,j+M} = 4 \cos (i\beta d \cos \theta_o) \sin (j\beta d \cos \theta_o)$$

$$C_{i+M,j+M} = 4 \sin (i\beta d \cos \theta_o) \sin (j\beta d \cos \theta_o)$$

From this point, the optimization procedure is identical to that developed for broadside arrays in Chapter III.

APPENDIX D

A PERTURBATIONAL TECHNIQUE FOR SIGNAL-TO-NOISE RATIO OPTIMIZATION

In this appendix, small variations in interelement spacings are considered in the optimization of the signal-to-noise ratio of a linear array. The developed procedure may be used in conjunction with the procedure derived in Chapter III of this thesis to synthesize arrays which differ slightly in geometrical arrangement from the optimum equally spaced array. An example is included to illustrate application of the method.

The point of departure in this development is the excitation vector of an equally spaced array which has been optimized for a particular value of constant interelement spacing. If this vector of radiator excitations is denoted

$$\bar{a}^T = [a_o \quad a_1 \quad \dots \quad a_M] \tag{D.1}$$

then the power pattern of such an array will be given by

$$G(\theta) = \left\{ a_o + 2 \sum_{m=1}^{M} a_m \cos (x_m \cos \theta) \right\}^2 \tag{D.2}$$

In this expression, θ is the angle measured from the array axis, and β has been incorporated into x_m as follows.

$$x_m = \beta d_m \tag{D.3}$$

Let the spacing of the radiator from the center of the array d_m be composed of a "base interelement separation," say d, which will be corrected by a perturbation denoted as Δ_m. This may be written mathematically as

$$d_m = md + \Delta_m \tag{D.4}$$

in which case the expression for the power pattern of the array may be written as

$$G(\theta) = \left\{ a_o + 2 \sum_{m=1}^{M} \cos (m\beta d \cos \theta + \beta \Delta_m \cos \theta) \right\}^2 \tag{D.5}$$

An appropriate trigonometric identity allows (D.5) to be written as

$$G(\theta) = \left\{ a_o + 2 \sum_{m=1}^{M} a_m \cos (m\beta d \cos \theta) \cos (\beta \Delta_m \cos \theta) - 2 \sum_{m=1}^{M} a_m \sin (m\beta d \cos \theta) \sin (\beta \Delta_m \cos \theta) \right\}^2 \tag{D.6}$$

For small arguments, the following approximations are valid.

$$\begin{aligned} \sin (\beta \Delta_m \cos \theta) &\approx \beta \Delta_m \cos \theta \\ \cos (\beta \Delta_m \cos \theta) &\approx 1 - \frac{\beta^2 \Delta_m^2}{2} \cos^2 \theta \end{aligned} \tag{D.7}$$

It is convenient to effect the change of variable

$$\psi = \beta d \cos \theta \tag{D.8}$$

in which case

$$\sin\left(\beta\Delta_m \cos\theta\right) \approx \frac{\Delta_m \psi}{d}$$

$$\cos\left(\beta\Delta_m \cos\theta\right) \approx 1 - \frac{1}{2}\left(\frac{\Delta_m \psi}{d}\right)^2 \tag{D.9}$$

A change in variables in the expression for $G(\theta)$ results in

$$G(\psi) \approx \left\{ a_o + 2\sum_{m=1}^{M} a_m \left(\left[1 - \frac{1}{2}\left(\frac{\Delta_m \psi}{d}\right)^2\right] \cos m\psi - \frac{\Delta_m \psi}{d} \sin m\psi \right) \right\}^2 \tag{D.10}$$

Upon expansion of this expression and subsequent dropping of terms which involve powers of Δ_m and higher, the approximate expression for $G(\psi)$ becomes

$$\begin{aligned} G(\psi) \approx & \sum_{m=1}^{2M} f_m(\bar{a}) \cos m\psi \\ & + \sum_{m=1}^{M} \left\{ 4 a_m^2 \left(\frac{\Delta_m}{d}\right)^2 \psi^2 \sin^2 m\psi - 2 a_o a_m \left(\frac{\Delta_m}{d}\right)^2 \psi^2 \cos^2 m\psi \right. \\ & \qquad \left. - 4 a_o a_m \frac{\Delta_m}{d} \psi \sin m\psi \right\} \\ & + 8 \sum_{m=1}^{M} \sum_{n=m+1}^{M} a_m a_n \frac{\Delta_m \Delta_n}{d^2} \psi^2 \sin m\psi \sin n\psi \\ & - 4 \sum_{m=1}^{M} \sum_{n=1}^{M} a_m a_n \left\{ \left(\frac{\Delta_n}{d}\right)^2 \psi^2 \cos m\psi \cos n\psi \right. \\ & \qquad \left. + 2 \frac{\Delta_n}{d} \psi \cos m\psi \sin n\psi \right\} \end{aligned} \tag{D.11}$$

where the $f_m(\bar{a})$ are functions of the excitation vector $\bar{a}$ only. This compact notation is used in this term because it does not enter into the end result to follow.

The integral to be minimized is (3.28), which after a change of variable becomes

$$I = \frac{1}{\beta d} \int_{-\beta d}^{\beta d} G(\psi)\, N(\psi)\, d\psi \tag{D.12}$$

The integral may be written after substitution for $G(\psi)$ as follows.

$$\begin{aligned}
\beta d\, I = {} & \sum_{m=o}^{2M} f_m(\bar{a}) \int_{-\beta d}^{\beta d} N(\psi) \cos m\psi\, d\psi \\
& + 2 \sum_{m=1}^{M} \left\{ 2a_m^2 \left(\frac{\Delta_m}{d}\right)^2 \int_{-\beta d}^{\beta d} \psi^2 N(\psi) \sin^2 m\psi\, d\psi \right. \\
& \qquad - a_o a_m \left(\frac{\Delta_m}{d}\right)^2 \int_{-\beta d}^{\beta d} \psi^2 N(\psi) \cos^2 m\psi\, d\psi \\
& \qquad \left. - 2a_o a_m \frac{\Delta_m}{d} \int_{-\beta d}^{\beta d} \psi\, N(\psi) \sin m\psi\, d\psi \right\} \qquad \text{(D.13)} \\
& + 8 \sum_{m=1}^{M} \sum_{n=m+1}^{M} a_m a_n \frac{\Delta_m \Delta_n}{d^2} \int_{-\beta d}^{\beta d} \psi^2 N(\psi) \sin m\psi \sin n\psi\, d\psi \\
& - 4 \sum_{m=1}^{M} \sum_{n=1}^{M} a_m a_n \frac{\Delta_n}{d} \left\{ \frac{\Delta_n}{d} \int_{-\beta d}^{\beta d} \psi^2 N(\psi) \cos m\psi \cos n\psi\, d\psi \right. \\
& \qquad \left. + 2 \int_{-\beta d}^{\beta d} \psi\, N(\psi) \cos m\psi \sin n\psi\, d\psi \right\}
\end{aligned}$$

The identifications listed below will ease the notational problem.

$$
\begin{aligned}
q_m &= \int_{-\beta d}^{\beta d} N(\psi) \cos m\psi \, d\psi \\
b_m &= \int_{-\beta d}^{\beta d} \psi^2 N(\psi) \sin^2 m\psi \, d\psi \\
c_{mn} &= \int_{-\beta d}^{\beta d} \psi^2 N(\psi) \sin m\psi \sin n\psi \, d\psi \\
f_{mn} &= \int_{-\beta d}^{\beta d} N(\psi) \psi^2 \cos m\psi \cos n\psi \, d\psi \\
g_m &= \int_{-\beta d}^{\beta d} \psi N(\psi) \sin m\psi \, d\psi \\
h_{mn} &= \int_{-\beta d}^{\beta d} \psi N(\psi) \cos m\psi \sin n\psi \, d\psi
\end{aligned}
\qquad (D.14)
$$

Substitution of these quantities in (D.13) yields

$$
\begin{aligned}
\beta_d I &= \sum_{m=o}^{2M} q_m f_m(\bar{a}) \\
&\quad + \sum_{m=1}^{M} \left\{ 4 b_m \frac{a_m^2}{d^2} \Delta_m^2 - 2 e_m \frac{a_o a_m}{d^2} \Delta_m^2 \right. \\
&\quad \left. - 4 g_m \frac{a_o a_m}{d} \Delta_m \right\}
\end{aligned}
$$

$$+ 8 \sum_{m=1}^{M} \sum_{n=m+1}^{M} c_{mn} \frac{a_m a_n}{d^2} \Delta_m \Delta_n$$

$$- \sum_{m=1}^{M} \sum_{n=1}^{M} \left\{ 4 f_{mn} \frac{a_m a_n}{d^2} \Delta_n^2 + 8 h_{mn} \frac{a_m a_n}{d} \Delta_n \right\} \qquad \text{(D.15)}$$

Minimization of I implies that

$$\frac{\partial I}{\partial \Delta_i} = 0 \quad , \quad i = 1, \ldots, M \qquad \text{(D.16)}$$

Carrying out this operation yields the set of linear equations below where $i = 1, 2, \ldots, M$.

$$2 \sum_{m=1}^{i-1} c_{mi} a_m \Delta_m + \left(2 b_i a_i - e_i a_o - 2 \sum_{m=1}^{M} f_{mi} a_m \right) \Delta_i$$

$$+ 2 \sum_{m=i+1}^{M} c_{im} a_m \Delta_m = d \left(g_i a_o + 2 \sum_{m=1}^{M} h_{mi} a_m \right) \qquad \text{(D.17)}$$

The set of Δ_i which satisfy these linear equations are added to the base values in (D.4) to determine the new element locations.

The application of this method is a matter of some algebraic complexity, and a step by step numerical example is beyond the scope of this appendix. Figure D.1 summarizes the results of such an application. This illustration shows the moderate increase in aperture resulting from the use of this procedure. For convenience of the reader, the sidelobe structure of the power pattern is plotted on an expanded scale.

As with any approximate method, the usefulness of this perturbational technique is limited. As pointed out in Chapter IV, the spacing parameter proved to be secondary in importance to the amplitudes of radiator excitation in signal-to-noise optimization. The steepest descent process proved completely adequate for incorporation of spacings into the optimization process, with the perturbational method outlined here being of reduced importance.

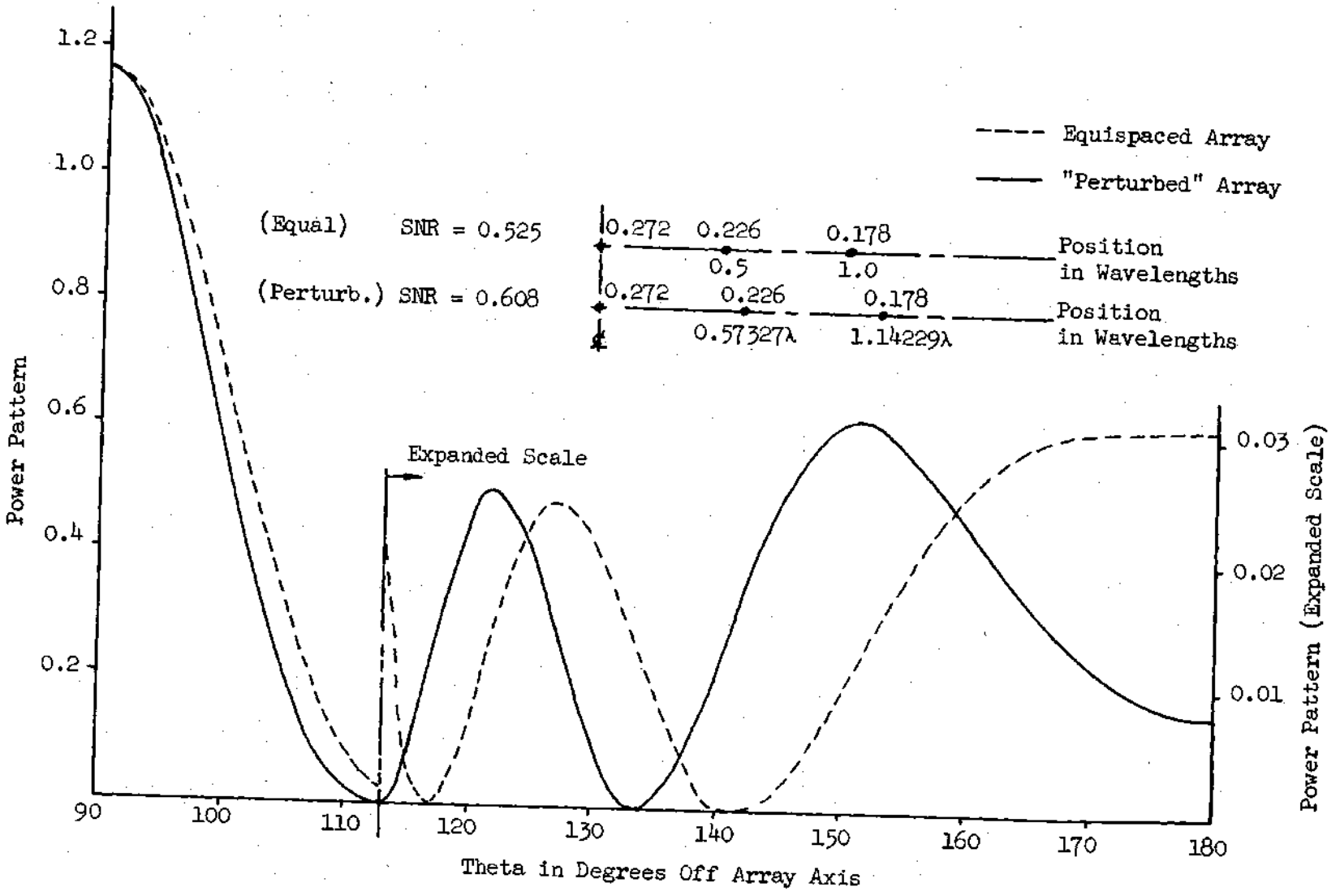

Fig. D.1 Example of Synthesis Using Perturbational Method.

BIBLIOGRAPHY

1. S. Silver, Microwave Antenna Theory and Design, McGraw-Hill Book Company, Inc., New York, N. Y., 1949.

2. J. D. Krawus, Antennas, McGraw-Hill Company, Inc., New York, N. Y., 1950.

3. E. C. Jordan, Electromagnetic Waves and Radiating Systems, Chapter 12, Prentice-Hall, Inc., Englewood Cliffs, N. J., 1950.

4. S. A. Schelkunoff, "A Mathematical Theory of Linear Arrays," Bell System Tech. J., vol. 22, p. 80-107, 1943.

5. M. Hoffman, "The Utility of the Pattern Matrix for Linear Array Computations," IRE Trans. on Antennas and Propagation, vol. AP-9, p. 97-100, January 1961.

6. P. M. Woodward, "A Method of Calculating the Field Over a Plane Aperture Required to Produce a Given Polar Diagram," Journal of the Institution of Electrical Engineers, vol. 93, pt. III-A, p. 1554-1558, 1947.

7. C. L. Dolph, "A Current Distribution for Broadside Arrays Which Optimizes the Relationship Between Beamwidth and Sidelobe Levels," Proc. IRE, vol. 34, p. 335-448, June 1946.

8. R. H. DuHamel, "Optimum Patterns for Endfire Arrays," Proc. IRE, vol. 41, p. 652-659, May 1953.

9. L. B. Brown and G. A. Scharp, Tchebyscheff Antenna Distribution, Beamwidth, and Gain Tables, Nav Ord Rept. 4629, Naval Ordnance Laboratory, Corona, 28 February 1958.

10. T. T. Taylor, "Design of Line Source Antennas for Narrow Beamwidth and Low Sidelobes," IRE Trans. on Antennas and Propagation, vol. AP-3, p. 16-28, January 1955.

11. T. T. Taylor, "Design of Circular Apertures for Narrow Beamwidth and Low Sidelobes," IRE Trans. on Antennas and Propagation, vol. AP-8, p. 17-22, January 1960.

12. G. J. Van der Maas, "A Simplified Calculation for Dolph-Tchebyscheff Arrays," J. Appl. Phys., vol. 25, p. 121-124, January 1954.

13. W. H. Von Aulock, "Properties of Phased Arrays," Proc. IRE, vol. 48, p. 1715-1727, October 1960.

14. H. Unz, "Linear Arrays With Arbitrarily Distributed Elements," IRE Trans. on Antennas and Propagation, vol. AP-8, p. 222-223, March 1960.

15. D. D. King, R. F. Packard, and R. K. Thomas, "Unequally Spaced Broadband Antenna Arrays," IRE Trans. on Antennas and Propagation, vol. AP-8, p. 380-385, July 1960.

16. R. F. Harrington, "Sidelobe Reduction by Non-Uniform Element Spacing," IRE Trans. on Antennas and Propagation, vol. AP-9, p. 187-192, March 1961.

17. A. L. Maffett, "Array Factors with Non-Uniform Spacing Parameter," IRE Trans. on Antennas and Propagation, vol. AP-10, p. 131-136, March 1962.

18. M. G. Andreasen, "Linear Arrays with Variable Interelement Spacing," IRE Trans. on Antennas and Propagation, vol. AP-10, p. 137-145, March 1962.

19. A. Ishimaru, "Theory of Unequally Spaced Arrays," IRE Trans. on Antennas and Propagation, vol. AP-10, p. 691-701, November 1962.

20. C. H. Tang, "An Approximate Method of Designing Non-Uniformly Spaced Arrays," IEEE Trans. on Antennas and Propagation, vol. AP-13, p. 177-179, January 1965.

21. A. I. Uzkov, "An Approach to the Problem of Optimum Directive Antenna Design," Compt. Rend. (Dokl.) Acad. Sci. URSS, vol. LIII, no. 1, 1946.

22. P. M. Woodward and J. D. Lawson, "The Theoretical Precision with Which an Arbitrary Radiation Pattern May Be Obtained from a Source of Finite Size," Journal of the Institution of Electrical Engineers vol. 94, pt III-A, p. 363-369, 1948.

23. C. J. Bouwkamp and N. G. deBruijn, "The Problem of Optimum Antenna Current Distributions," Phillips Res. Rept., vol. 1, p. 135-138, January 1946.

24. H. J. Riblet, "Note on the Maximum Directivity of an Antenna," Proc. IRE, vol. 36, p. 620-623, May 1948.

25. T. T. Taylor, "A Discussion of the Maximum Directivity of an Antenna," Proc. IRE, vol. 36, p. 1135, September 1948.

26. C. T. Tai, "The Optimum Directivity of Uniformly Spaced Arrays of Dipoles," IEEE Trans. on Antennas and Propagation, vol. AP-12, p. 447-454, July 1964.

27. L. Solymar, "Maximum Gain of a Line Source Antenna if the Distribution Function is a Finite Fourier Series," IRE Trans. on Antennas and Propagation, vol. AP-6, p. 215-219, July 1958.

28. H. N. Kritikos, "Optimal Signal-to-Noise Ratio for Linear Arrays by the Schwartz Inequality," Journal of the Franklin Institute, p. 295-304, October 1963.

29. T. L. Saaty and J. Bram, Nonlinear Mathematics, McGraw-Hill Book Company, New York, New York, 1964.

30. G. Hadley, Nonlinear and Dynamic Programming, Addison-Wesley Publishing Company, Reading, Mass., 1964.

31. G. Leitmann (Editor), Optimization Techniques with Applications to Aerospace Systems, Academic Press, New York, New York, 1962.

32. R. A. Michelson and W. Schomer, "A Three Parameter Antenna Pattern Synthesis Technique," Microwave J., vol. 8, no. 9, p. 88-94, September 1965.

33. W. C. Davidon, Variable Metric Method for Minimization, Argonne National Laboratory, Rept. ANL-5990 (Rev.), Nov. 1959.

34. J. B. Rosen, "The Gradient Projection Method, Part I: Linear Constraints," J. Soc. Ind. Appl. Math., vol. 8, no. 1, p. 181-217, March 1960.

35. C. W. Carroll, "The Created Response Surface for Optimizing Nonlinear Restrained Systems," Operations Res., vol. 9, no. 2, p. 169-184, March-April 1961.

36. C. H. Walter, Traveling Wave Antennas, McGraw-Hill Book Company, New York, New York, 1965.

37. R. Fletcher and M. J. D. Powell, "A Rapidly Convergent Descent Method for Minimization."

38. L. E. Elsgolc, Calculus of Variations, Addison-Wesley Publishing Company, Reading, Mass., p. 153-165.

39. R. Weinstock, Calculus of Variations with Applications to Physics and Engineering, McGraw-Hill Book Company, New York, New York, p. 240-249, 1952.

40. F. B. Hildebrand, Methods of Applied Mathematics, Second Edition, Prentice-Hall, Inc., Englewood Cliffs, New Jersey, 1965.

41. R. Brase, Matrix Algebra for Electrical Engineers, Addison-Wesley Publishing Company, Reading, Mass., 1963.

VITA

Gordon Worley Breland was born in Section, Alabama, on August 6, 1937. He is the son of Virgil and Lucy Bell Breland.

He was educated in public schools in Ashland, Kentucky, Petersburg, Virginia, and Atlanta, Georgia. In June 1957, he received the B.E.E. degree from Auburn University, Auburn, Alabama. He received the M.S.E.E. degree in June 1963 from the Georgia Institute of Technology.

Following a short employment as Junior Engineer with ITT Federal Laboratories, he entered the United States Air Force in 1957. From 1957-1960, he served as Communications Officer. Subsequent to this assignment, he was associated with the ICBM Site Activation Effort at Mountain Home AFB, Idaho. Following his Air Force service, he was employed as Senior Electronic Systems Engineer by Lockheed-Georgia Company from 1961 to 1963. This employment was briefly interrupted by recall to active duty during the Cuban Crisis of 1962. In 1963 he accepted employment as a Teaching Assistant at Georgia Institute of Technology, followed by an appointment as Instructor in 1964. He resigned this position to accept a National Science Foundation Traineeship in September 1965.